SPACE SYSTEMS

Document No. 69SD4372
January 15, 1970

GRAVITY GRADIENT STABILIZATION SYSTEM

for the

APPLICATIONS TECHNOLOGY SATELLITE

FINAL TECHNICAL REPORT
Hardware Development and Test
VOLUME II
Book 1

GENERAL ELECTRIC

DOCUMENT NO. 69SD4372
JANUARY 15, 1970

FINAL REPORT
FOR THE
APPLICATIONS TECHNOLOGY SATELLITE
GRAVITY GRADIENT
STABILIZATION SYSTEM

VOLUME II
HARDWARE DEVELOPMENT AND TEST

CONTRACT NO. NAS 5—9042

NATIONAL AERONAUTICS AND SPACE ADMINISTRATION
R.W. WIRTH
ATS TECHNICAL OFFICER

APPROVED BY: R.E. Clayton
R.E. CLAYTON
ATS-E PROGRAM MANAGER

GENERAL ELECTRIC
SPACE SYSTEMS ORGANIZATION
Valley Forge Space Center
P. O. Box 8555 • Philadelphia, Penna. 19101

TABLE OF CONTENTS

Section			Page
1	GRAVITY GRADIENT STABILIZATION SYSTEMS DESIGN AND DEVELOPMENT		1-1
	1.1	Volume II Contents	1-1
	1.2	Hardware Summary	1-1
	1.3	Deliverable Hardware End Items	1-12
		1.3.1 Thermal Model	1-12
		1.3.2 Dynamic Model	1-13
		1.3.3 Engineering Units	1-14
		1.3.4 Prototype Units	1-14
		1.3.5 Flight System	1-14
	1.4	Field and Flight Support	1-15
2	BOOM SUBSYSTEM		2-1
	2.1	Introduction	2-1
	2.2	Engineering Development	2-5
		2.2.1 Major Subcontract	2-5
		2.2.2 Interface Considerations	2-5
		2.2.3 150-Foot Rod Considerations	2-8
		2.2.4 Motor Selection	2-9
		2.2.5 Potentiometer Boom Length Indicater	2-9
		2.2.6 Boom Electrical Isolation	2-10
		2.2.7 Tip Target Configuration	2-10
		2.2.8 Release Monitor	2-10
		2.2.9 Design Details	2-11
		2.2.10 Test Program	2-17
		2.2.11 Damper Boom Digitation Program	2-43
		2.2.12 Summary and Conclusion of Development Program	2-48
	2.3	Qualification Tests Primary Boom	2-51
		2.3.1 Component Qualification Primary Boom	2-51
		2.3.2 System Qualification, Primary Boom	2-51
	2.4	Flight Acceptance, Primary Boom	2-53
		2.4.1 ATS-A	2-53
		2.4.2 ATS-D	2-54
		2.4.3 ATS-E	2-55
	2.5	Qualification Tests, Damper Boom	2-56
		2.5.1 Component Qualification, Damper Boom	2-57
		2.5.2 System Qualification, Damper Boom	2-57

Section			Page
	2.6	Flight Acceptance, Damper Boom	2-58
	2.6.1	ATS-A	2-58
	2.6.2	ATS-D	2-58
	2.6.3	ATS-E	2-59
3	COMBINATION PASSIVE DAMPER		3-1
	3.1	Purpose of the CPD	3-1
	3.2	Engineering Development	3-2
	3.2.1	CPD Unit Nomenclature	3-2
	3.2.2	CPD Description	3-2
	3.2.3	Details of Major Subsystems	3-13
	3.2.4	Test Equipment	3-71
	3.2.5	Test Results	3-75
	3.2.6	Other Significant Test Results	3-79
	3.2.7	Testing General	3-81
	3.2.8	Conclusions and Recommendations of Engineering Development	3-85
	3.2.9	Chronological Summary of CPD Design	3-86
	3.2.10	Drawings and Specifications	3-91
	3.3	Qualification Tests	3-93
	3.3.1	Component Qualification	3-94
	3.3.2	System Qualification	3-94
	3.4	Flight Acceptance	3-95
	3.4.1	ATS-A	3-95
	3.4.2	ATS-D	3-95
	3.4.3	ATS-E	3-96
	3.5	Reference List	3-96
	3.5.1	Component History Documents	3-96
	3.5.2	Quarterly Progress Reports	3-97
	3.5.3	Other Pertinent Documents	3-97
4	TV CAMERA SYSTEM		4-1
	4.1	Introduction	4-1
	4.2	Engineering Development	4-1
	4.2.1	General	4-1
	4.2.2	Electrical	4-4
	4.2.3	Mechanical	4-14
	4.2.4	Engineering Test Program	4-18
	4.2.5	Summary and Conclusions of TV Camera Development	4-26

TABLE OF CONTENTS (CONT'D)

Section			Page
	4.3	Qualification Tests, TV Camera	4-27
	4.3.1	Component Qualification	4-27
	4.3.2	System Qualification	4-28
	4.4	Flight Acceptance Tests, TV Camera	4-28
	4.4.1	ATS-A	4-29
	4.4.2	ATS-D	4-29
	4.4.3	ATS-E	4-30
5		SOLAR ASPECT SENSOR	5-1
	5.1	Introduction	5-1
	5.1.1	Purpose	5-1
	5.1.2	Description	5-1
	5.1.3	Principle of Operation	5-2
	5.2	Engineering Development	5-8
	5.2.1	Source Selection	5-8
	5.2.2	Operating Characteristics	5-8
	5.2.3	Mechanical Considerations	5-12
	5.2.4	Electrical Considerations	5-13
	5.2.5	Engineering Test Program	5-14
	5.2.6	Conclusions	5-29
	5.3	Qualification	5-29
	5.3.1	Component Qualification	5-30
	5.4	Flight Acceptance	5-30
	5.5	Applicable Documents	5-33
	5.6	List of Reference	5-35
6		Power Control Unit	6-1
	6.1	Purpose and Function	6-1
	6.2	Engineering Development	6-2
	6.2.1	Mechanical Considerations	6-2
	6.2.2	Electrical Considerations	6-5
	6.2.3	Optimization Program	6-14
	6.2.4	Engineering Tests and Results	6-17
	6.3	Qualification	6-44
	6.3.1	Component Qualification	6-45
	6.3.2	System Qualification	6-45
	6.4	Flight Acceptance	6-45

TABLE OF CONTENTS (CONT'D)

Section			Page
7	RF ATTITUDE SENSOR		7-1
	7.1	Introduction	7-1
	7.2	Electrical Design	7-2
		7.2.1 75.76 MHz IF Amplifier	7-4
		7.2.2 IF Filter	7-6
		7.2.3 IF Amplifier - Detector	7-7
		7.2.4 Video Filter	7-8
		7.2.5 Limiters	7-10
		7.2.6 Acquisition Control	7-10
		7.2.7 Sweep Circuit	7-12
		7.2.8 Frequency Multiplier	7-14
		7.2.9 2.56 MHz Oscillator	7-22
		7.2.10 Digital Processing	7-24
		7.2.11 256 Divider and Phase Detector	7-26
		7.2.12 Video Telemetry Circuit	7-31
		7.2.13 Power Supply	7-35
	7.3	Mechanical Design	7-37
		7.3.1 RF Assembly	7-41
		7.3.2 RF Support	7-41
		7.3.3 Varactor Chain	7-41
		7.3.4 Base plate	7-42
		7.3.5 Cover	7-42
		7.3.6 Modules	7-42
		7.3.7 Equipment Plates	7-44
		7.3.8 Equipment Plate Subassembliers	7-44
8	QUALITY CONTROL AND TEST		8-1
9	RELIABILITY		9-1
	9-1	Introduction and Summary	9-1
	9.2	Summary of Significant Activities and Accomplishments	9-2
	9.3	Systems Reliability Assessment	9-5
	9.4	Discussion of Test Failure History	9-6
10	MATERIALS AND PROCESSES		10-1

TABLE OF CONTENTS (CONT'D)

Section		Page
11	MANUFACTURING	11-1
	11.1 Controlled Environmental Area	11-1
	11.2 Materials Laboratory	11-1
	11.3 Electronics Shop	11-1
	11.4 Machine Shop	11-2
12	PARTS PROGRAM	12-1
13	NEW TECHNOLOGIES	13-1
	13.1 Angle Indicator	13-2
	13.2 Angle Indicator Readout Device	13-3
	13.3 CPD Clutch Mechanism	13-3

LIST OF ILLUSTRATIONS

Figure		Page
1-1	ATS Gravity Gradient Hardware.	1-4
1-2	Packaging Arrangement for the ATS-A System.	1-5
2-1	STEM Principle	2-2
2-2	Primary Boom Assembly (1/2 system)	2-4
2-3	Damper Boom with Linear Actuator at Right	2-4
2-4	Gravity Gradient Rod Sample.	2-11
2-5	Primary Boom Assembly Schematic (1/2 system).	2-12
2-6	Primary Boom Package Locations Showing Scissoring Pivots	2-14
2-7	Scissoring Linkage Seal, Primary Boom System	2-16
2-8	Damper Boom Schematic	2-21
2-9	Damper Boom Ball Lock Release Scheme	2-22
2-10	Boom Straightness Measuring Tank (left), Boom Deployment Track (right)	2-28
2A-1	Damper Boom Straightness Profile	2-66
3-1	Combination Passive Damper Schematic	3-3
3-2	Combination Passive Damper for ATS.	3-3
3-3	Combination Passive Damper Package Elevation View	3-4
3-4	Combination Passive Damper Package Plan View	3-5
3-5	CPD Engineering Unit Assembled (Cover Removed) and T-1 Damper Boom Package in Place	3-11
3-6	Details of CPD Engineering Unit 1	3-11
3-7	Baseplate and Caging Mechanism of CPD Engineering Unit 1 with Damper Boom Package in Place	3-12
3-8	Caging Cable and Baseplate (with Pyrotechnic Device 2) After Uncaging Operation, CPD Engineering Unit 1	3-13
3-9	Flux Density Measurements	3-15
3-10	Flux Density Measurements Effect of Pole Pieces.	3-15
3-11	Magnetic Arrangement of Single and Double Penetration.	3-17
3-12	Force on Diamagnetic Specimen in Non-Uniform Field	3-22
3-13	Eddy Current Damper Suspension System Schematic	3-22
3-14	Diamagnetic Suspension Characteristic	3-25
3-15	Suspension Load Capacity vs. Initial Air Gap Setting.	3-27
3-16	Torque Angle Characteristics for Bismuth and Various Thicknesses of Pyrolytic Graphite	3-28
3-17	Definition of Magnet Side	3-29
3-18	Energy Dissipation by Eddy Current and Hysteresis in Torsional Restraint vs. Amplitude of Oscillation (ATS-A Eddy Current Damper)	3-35

Figure		Page
3-19	Passive Hysteresis Damper for ATS-D/E Configuration (Engineering Unit No. 2).	3-38
3-20	Passive Hysteresis Damper Details.	3-39
3-21	Passive Hysteresis Damper Suspension System, ATS-D/E Configuration	3-40
3-22	Wire Attachment to End Flexure.	3-40
3-23	Idealized Damping Curves for Original PHD and VTHD (Torsional Restrain Omitted)	3-41
3-24	CPD Clutch Mechanism.	3-49
3-25	Force vs. Displacement for Square Flutted Diaphragm (0.014 in. beryllium copper)	3-51
3-26	Two-Way Clutch Solenoid Specification Sheet.	3-52
3-27	CPD Solenoid Section	3-53
3-28	Force vs. Travel Test Results for Engineering Solenoid Unit	3-54
3-29	Deep Indentation at Edge of V-Groove Caused by Detent Ball in ECD Mode	3-56
3-30	Encoder Disc for Angle Indicator	3-58
3-31	Angle Indicator Head Assembly	3-60
3-32	Typical Angle Indicator Bit Circuit	3-60
3-33	Angle Indicator Assembly in Test Fixture.	3-61
3-34	Angle Indicator Assembly Exploded View	3-61
3-35	Angle Indicator Thermal Test Results (Average of Two Modules)	3-64
3-36	Original Encoder Disc Design.	3-66
3-37	New Encoder Disc Design	3-66
3-38	Caging Cable Calibration Results	3-69
3-39	Eddy Current Caging Torque Test Results	3-69
3-40	Advanced Damping Test Fixture (ADTF)	3-73
3-41	Low Order Force Fixture (LOFF)	3-74
4-1	TV Camera System (l to r) Electronics, Camera and Mounting Bracket (Engineering Unit 5101)	4-3
4-2	Electronics Unit Details	4-2
4-3	Camera (Engineering Unit 5101).	4-4
4-4	Vidicon Heater Current vs. Telemetry Output Voltage	4-7
4-5	Vidicon Target Supply Voltage vs. Telemetry Output Voltage	4-7
4-6	Temperature vs. Telemetry Output Voltage	4-8
4-7	TV Camera Model 0431F Block Diagram	4-8
4-8	TV Camera Schematic (Lear Siegler Dwg. 124901).	4-9
4-9	TV Camera Assembly (GE Dwg. 47D209695).	4-15
4-10	Control Unit Assembly (GE Dwg. 47D207485)	4-19

LIST OF ILLUSTRATIONS (CONT'D)

Figure		Page
5-1	Solar Aspect Sensor Electronics (r) and Typical Detector	5-1
5-2	SAS Detector Orientation	5-2
5-3	Sensor Pictorial Representation	5-3
5-4	Solar Aspect Sensor Logic Diagram	5-5
5-5	SAS Detector Alignment Geometry	5-9
5-6	Crosscoupling Effects on Bit Output	5-10
5-7	SAS Termination Circuit	5-13
5-8	Optical Alignment Setup	5-15
5-9	Nulling Circuit	5-16
5-10	Reticle 1 AGC and B1 Test Results	5-17
5-11	Reticle 1, Bit 2 Test Results	5-17
5-12	Reticle 1, Bits 4 and 5 Test Results	5-18
5-13	Reticle 1, Bits 6, 7, and 8 Test Results	5-18
5-14	Transition Edge Error vs. True Transition Position (Reticle 1, Bit 1)	5-19
5-15	Transition Edge Error vs. Transition Position (Reticle 1, Bit 2)	5-19
5-16	Transition Edge Error vs. True Transition Position (Reticle 1, Bits 3 and 4)	5-20
5-17	Translation Edge Error vs. True Translation Position (Reticle 1, Bits 5, 6, 7, and 8)	5-20
5-18	SAS Detector and Test Fixture	5-24
5-19	Sensed Angle Geometry	5-25
5-20	Theoretical Value vs. Actual Readout	5-26
5-21	SAS Solar-Vacuum Test in 5- by 6-foot Chamber	5-28
5-22	Test Profile Temperature Excursion	5-28
5B-1	GE 5000-watt Xenon Compact Arc Lamp	A2-2
5B-2	Solar Cell Relative Spectral Response	A2-2
5B-3	Fused Quartz Index of Refraction	A2-3
5B-4	Product of Solar Spectrum and Silicon Solar Cell Response	A2-4
5B-5	Product of Xenon Spectrum	A2-4
5C-1	SAS Test Console	A3-2
5C-2	Detector Simulation Circuit	A3-3
5C-3	AGC Cell Output Simulation	A3-3
5C-4	Diode Leakage Measuring Circuit	A3-4
5C-5	Output Current Measuring Circuit	A3-5
5C-6	Detector Monitoring Circuit	A3-5

LIST OF ILLUSTRATIONS (CONT'D)

Figure		Page
6-1	Power Control Unit, Prototype Hardware	6-3
6-2	PCU Wiring Boards for the First Flight Unit Shown During Assembly.	6-4
6-3	Power Control Unit Schematic (GE Dwg. 47J207904)	6-7
6-4	Thermal Test Chamber Temperature.	6-18
6-5	Thermal Test Power Supply Module Temperature	6-19
6-6	Thermal Test, R53 Temperature	6-19
6-7	Thermal Test, R20 Heat Sink Temperature	6-20
6-8	Thermal Test, Field Driver Scissor B Temperature	6-20
6-9	Thermal Test, Q22 Heat Sink Temperature (Armature Scissor B)	6-21
6-10	Thermal Test, R24 Heat Sink Temperature.	6-21
6-11	PCU Mounting Surface Temperature vs. Time.	6-23
6-12	Squib Driver A9 Output Transistor Temperature vs. Time	6-23
6-13	Hysteresis Driver Transistor Q2 Temperature vs. Time	6-24
6-14	Hysteresis Driver Q1 Transistor Temperature vs. Time	6-24
6-15	A18 Field Driver Scissor B Temperature vs. Time	6-25
6-16	Temperature of Heat Sink Beside Q22 (Output of Mod A19) vs. Time	6-25
6-17	A19 Scissor B Armature Driver Transistor Temperature vs. Time	6-26
6-18	R53 (Detector Lamp Circuit) Resistor Temperature vs. Time	6-26
6-19	Solenoid Driver Transistor Satuartion Voltage vs. Input Voltage Hysteresis Damper	6-29
6-20	Solenoid Driver Transistor Saturation Voltage vs. Input Voltage, Rod B Emergency	6-29
6-21	Hysteresis Damper Solenoid Driver Test Circuit.	6-32
6-22	Motor Field Driver Transistor Saturation Voltage vs. Input Voltage, Rod B Field Driver.	6-35
6-23	Field Driver Test Circuit	6-36
6-24	Line Voltage Drop Determining Circuit	6-37
6-25	Motor Armature Driver Saturation Voltage vs. Input Voltage Rod A Motor Armature Driver	6-39
6-26	-5 Volt Power Supply vs. Load at Nominal Voltage	6-41
6-27	-5 Volt Power Supply Output vs. Input Voltage (650-ohm Load)	6-41
6-28	Squib Driver Pulse Width vs. Input Voltage	6-43
6-29	Squib Driver Load Current vs. Input Voltage	6-43
6-30	Squib Driver Delay Time vs. Input Voltage.	6-44

LIST OF ILLUSTRATIONS (CONT'D)

Figure		Page
7-1	RF Attitude Sensor Mockup	7-3
7-2	RF Attitude Sensor Block Diagram	7-3
7-3	75.76 MHz IF Schematic	7-5
7-4	Receiver IF Filter	7-6
7-5	Last IF Amplifier-Detector	7-7
7-6	10 kHz Filter	7-9
7-7	Limiters Schematic	7-11
7-8	Acquistion Control	7-12
7-9	Sweep Circuit	7-13
7-10	Multiplier Block Diagram	7-15
7-11	X2 Circuit Schematic	7-16
7-12	X4 Circuit Schematic	7-18
7-13	X6 Circuit Schematic	7-19
7-14	227.8 Mc Amplifier Circuit Schematic	7-21
7-15	2.56 Mc Oscillator and Buffer	7-23
7-16	Digital Data Collection	7-25
7-17	Data Timing Diagram	7-25
7-18	8-Bit Counter Schematic	7-27
7-19	8-Bit Counter Logic	7-29
7-20	256 Dividers and Phase Detectors	7-32
7-21	3-Channel Summer	7-33
7-22	Chopper Amplifier	7-34
7-23	Power Supply	7-38
7-24	RF Attitude Sensor Packaging	7-39
9-1	Mathematical Model - Basic Gravity Gradient Stabilization Mission	9-7
9-2	Mathematical Model - Gravity Gradient Experiment (ATS-A), Initial Stabilization Assumed	9-8
11-1	Typical Dynamic Units	11-3
11-2	Thermal Model Units	11-4
11-3	Assembly of Flight 2 CPD in Clean Area	11-5
11-4	Typical PCU Wiring Board Featuring Cordwood Modular Construction	11-6
11-5	Working Model of CPD Caging Arrangement	11-6
13-1	Boom Angle Indicator	13-5
13-2	Encoder Disc	13-5
13-3	CPD Clutch Mechanism	13-6

SECTION 1

GRAVITY GRADIENT STABILIZATION

SYSTEMS DESIGN AND DEVELOPMENT

SECTION 1

GRAVITY GRADIENT STABILIZATION SYSTEM DESIGN AND DEVELOPMENT

1.1 VOLUME II CONTENTS

A comprehensive discussion of the ATS gravity gradient stabilization system hardware development and test effort is contained in this volume. Sections 2 through 7 are devoted to each of the principal subsystems. Beginning with the requirements and assumptions, the engineering efforts directed at the implementation of each subsystem are discussed. Results of investigations and engineering tests having a significant influence on the final design are included, but in the interest of a concise presentation, many of the detailed reports have been omitted. In most cases, these details are contained in a collection of "Component History Documents" or in the periodic monthly and quarterly progress reports and PIR's that were published during the life of the contract. This documentation can be made available for review upon request through the cognizant GE Contract Administrator assigned to NASA programs. Discussions in Sections 2 through 7 are preceeded by a "facts sheet" which forms a ready reference to the requirements, controlling documents, and principal subcontractor for each subsystem. Sections 8 through 12 present discussions of the Manufacturing, Quality Control, Materials and Processes, Reliability and Parts Program activities directed at the implementation and test of the subsystem engineering designs.

The last section summarizes the new technologies that were uncovered and reported by GE as a result of gravity gradient system developments under contract NAS 5-9042. Table 1-1 shows the principal subdivisions of the contract and the approximate time these activities took place.

1.2 HARDWARE SUMMARY

Under the contract with NASA/Goddard, General Electric furnished flight qualified gravity anchored passive stabilization systems for three ATS vehicles (designated ATS-A, -D and -E). One of the systems was designed to orbit the earth at an altitude of 6000 miles (ATS-A), and the other two systems were designed to orbit the earth at synchronous altitude, approximately 23,000 miles (ATS-D and -E).

Table 1-1. NAS 5-9042 Composite Schedule

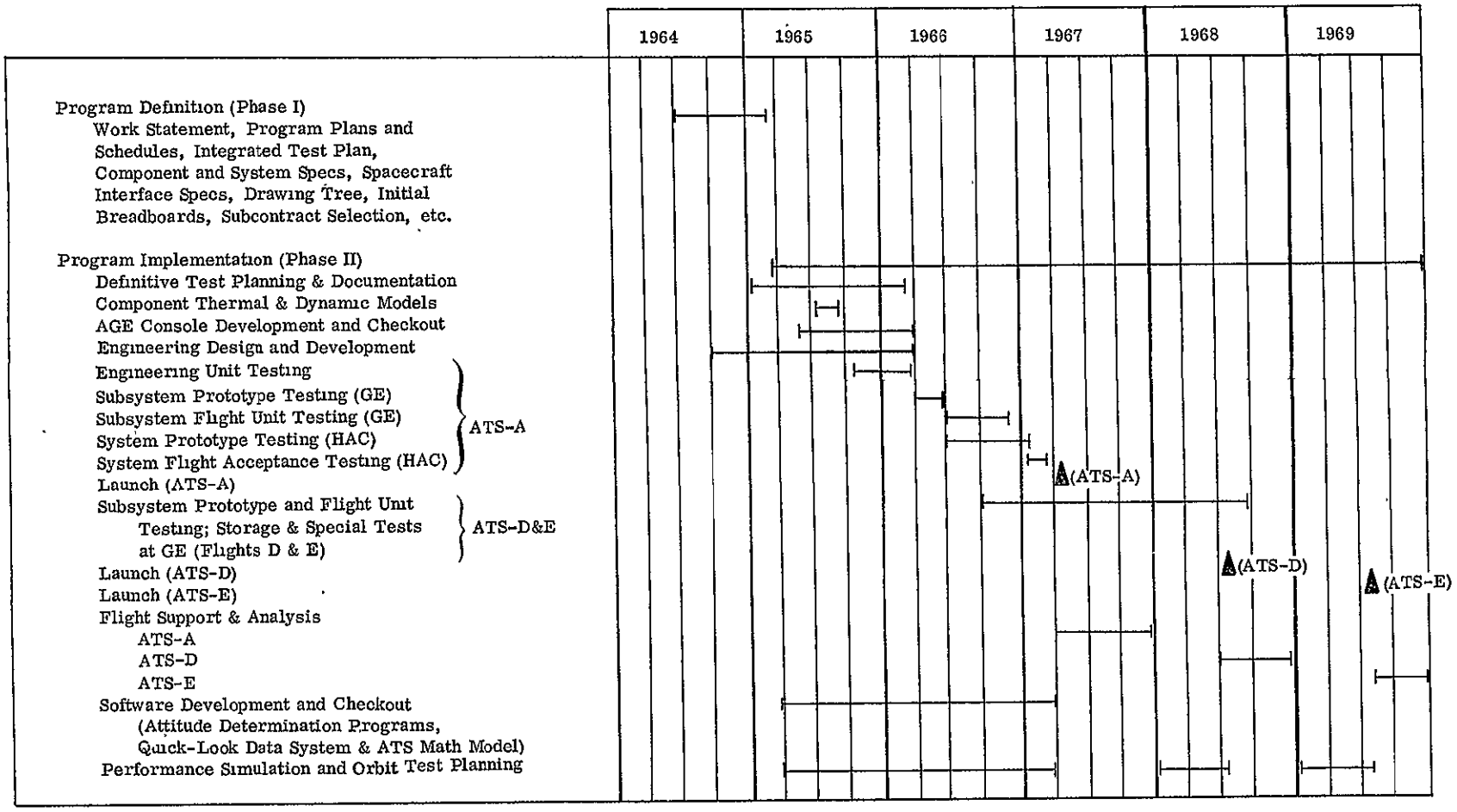

The essential elements of the ATS gravity gradient system are a pair of long booms that are extended from the spacecraft's center body to establish predetermined inertial levels and insure spacecraft orientation, and a gravity sensitive damper that insures spacecraft stability by dissipating oscillatory energy.

Each system was designed to allow important stabilization parameters, such as inertial ratios and damping characteristics, to be varied in orbit to assess their effect on performance of the system. The major subdivisions of each ATS gravity gradient stabilization system are shown in Figure 1-1; they include two primary boom packages, a Combination Passive Damper, a Damper Boom assembly, TV Camera, a Solar Aspect Sensor and a Power Control Unit. The packaging arrangement in the ATS spacecraft is shown in Figure 1-2 for the ATS-A (medium altitude) system. There are variations in the system to accommodate the individual requirements of the three flights. Table 1-2 lists these differences "as flown."

The two primary boom packages (A of Figure 1-1) erect booms tipped with weights in an X-configuration. DC motors in the boom package allow the length of each boom to be varied to effect changes in spacecraft moment of inertia magnitudes and the angle between booms to be varied - over a 20-degree range - to effect a variation in spacecraft moment of inertia ratios (scissoring function). Gravitational and centrifugal forces, acting on the tip weights and gravity gradient rods, provide small restoring forces to orient the spacecraft in the three principal axes.

The Damper Boom (B of Figure 1-1), consists of two self-erecting, 45-foot rods which are attached to a damper shaft. The shaft, in turn, is coupled to the rotor of the Combination Passive Damper. The Damper Boom is shown in its stowed position at the bottom of illustration C, Figure 1-1. The weight of the tip masses at the end of the Damper Boom, the boom length, and the restoring spring constant of the CPD are selected to "detune" the damper boom from the spacecraft oscillatory frequency, thus insuring relative motion of the spacecraft and the Damper Boom.

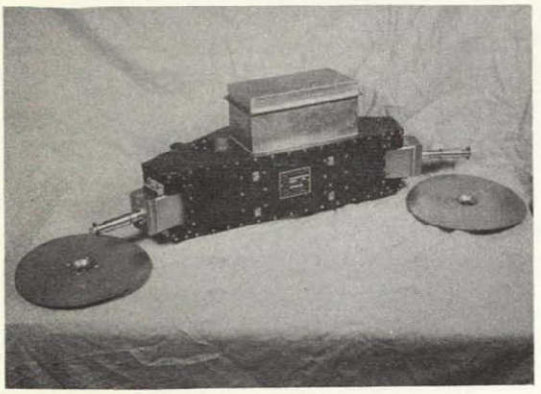

A. PRIMARY BOOM PACKAGE

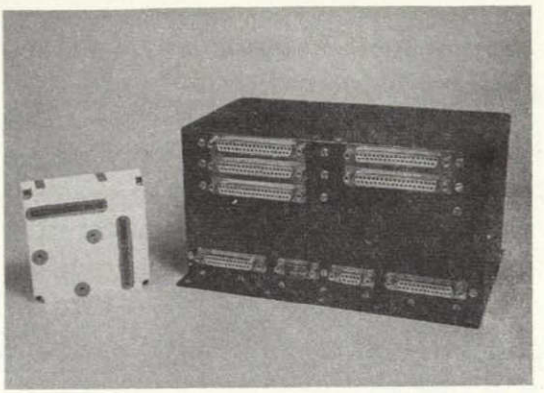

D. SOLAR ASPECT SENSOR

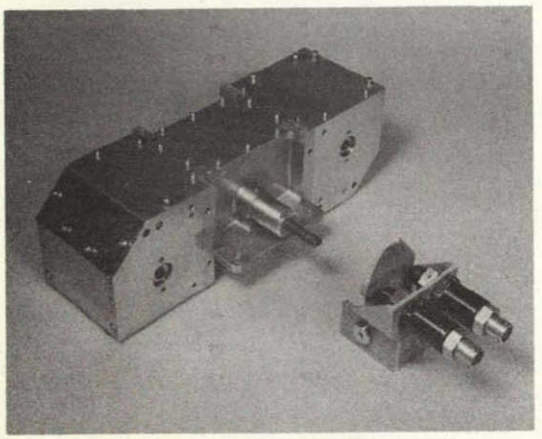

B. DAMPER BOOM

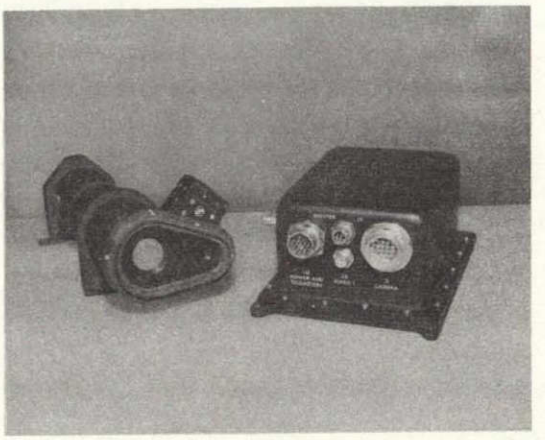

E. TV CAMERA SYSTEM

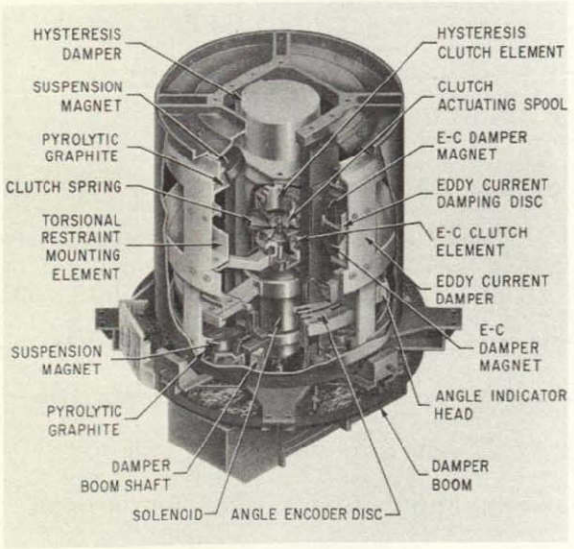

C. COMBINATION PASSIVE DAMPER

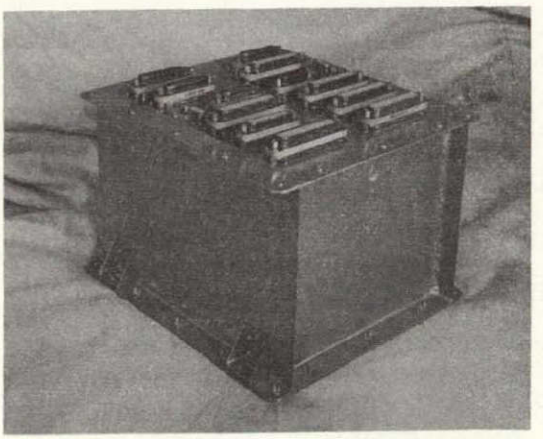

F. POWER CONTROL UNIT

Figure 1-1. ATS Gravity Gradient Hardware

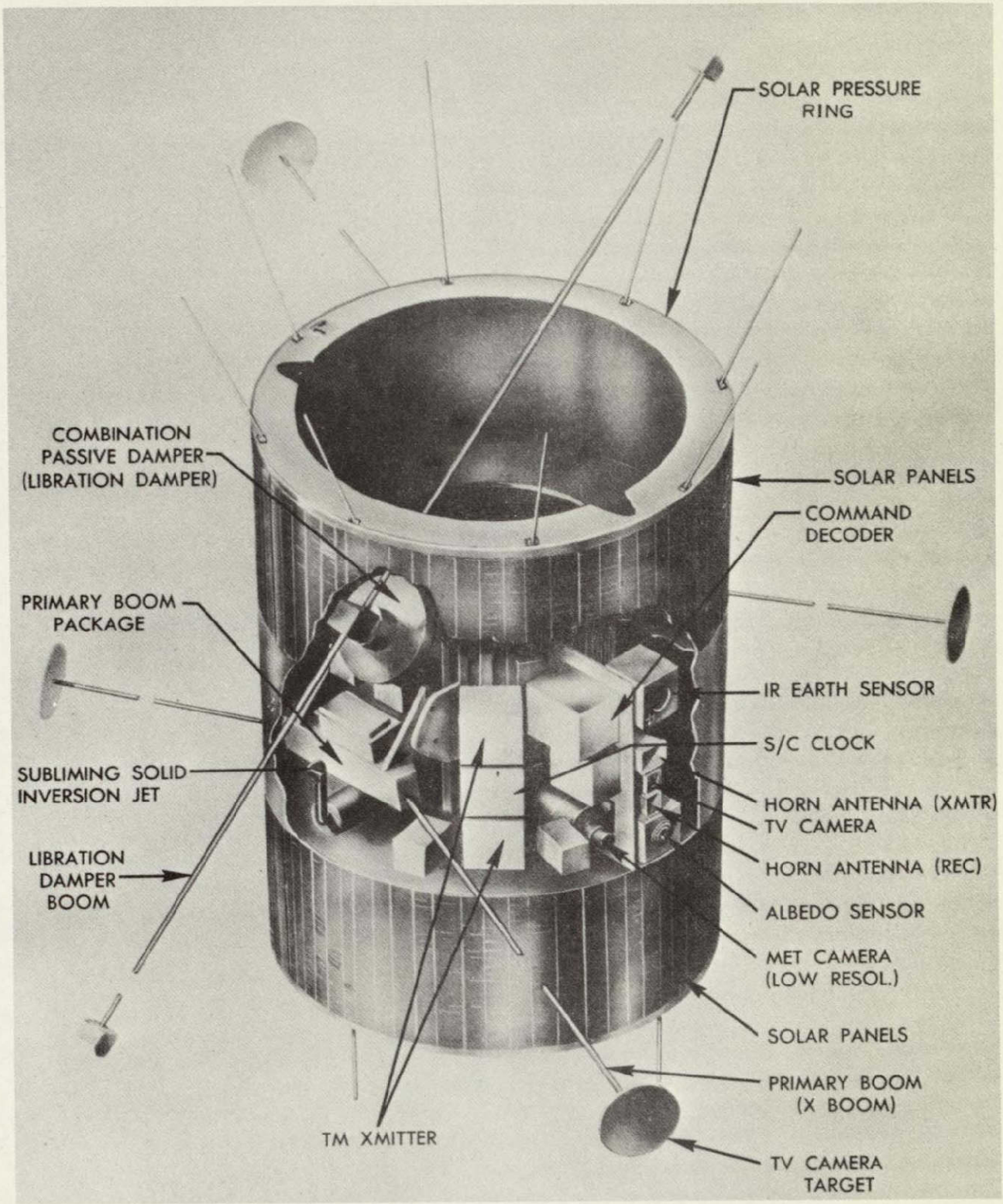

Figure 1-2. Packaging Arrangement for the ATS-A System

Table 1-2. Gravity Gradient Subsystem Parameters - "As Flown"

	ATS-A Medium Altitude		ATS-D Synchronous Altitude		ATS-E Synchronous Altitude	
Primary Boom Pkg. (2 Booms per Pkg)	2		2		2	
Boom Length (ft)	123		121		121	
Tip Weight/End (lbs)	2.8		8		8	
Erection Rate (ft/sec)	1.2		1.2		0.5	
Scissor Rate (deg/sec)	0.12		0.10		0.10	
Damper Boom Pkg. (2 Booms per Pkg)	1		1		1	
Boom Length (ft)	43.4		45		45	
Tip Weight/End (lbs)	2.09		4.06		4.06	
Erection Rate (ft/sec)	4		4		4	
Combination Passive Damper	1		1		1	
Damping Constant (ECD) (Dyne-Cm)/(Deg/Sec)	15,000		9250		11,470	
	Damper Angle	Torque	Damper Angle	Torque	Damper Angle	Torque
Damping Constant (PHD)	0^o - 45^o	185 Dyne-Cm	0^o - 10^o 10^o - 45^o	7 Dyne-Cm 2.9 Dyne-Cm/ Deg Slope	0^o - 10^o 10^o - 45^o	14 Dyne-Cm 2.6 Dyne-Cm/ Deg Slope
Spring Constant (Dyne-Cm)/Deg	24.1		3.73		4.11	
Solar Aspect Sensor (Electronics pkg + 5 detectors)	1		1		1	
TV Camera	2		1		1	
Power Control Unit	1		1		1	

The Damper Boom shaft is attached to one of two independently functioning dampers in the Combination Passive Damper (C of Figure 1-1) to dissipate the libration energy of the spacecraft by taking advantage of the relative motion between the damper boom and the spacecraft body. One of the dampers in the CPD is an eddy current device, and the other is a hysteresis damper. Either damper can be coupled to the Damper Boom shaft on command from the ground to permit evaluation of the rate of energy dissipation, amplitude of steady state oscillations, and other damper-related parameters.

The eddy current damper converts libration energy to heat by causing the induction of eddy currents in an aluminum disk that is coupled to the boom shaft. Rate of energy dissipation is proportional to the square of the angular velocity of the boom, while damper torque is directly proportional to the rate. The hysteresis damper utilizes the energy loss associated with the magnetization curve of chrome steel to convert libratory energy to heat. Its rate of energy dissipation is virtually independent of angular velocity.

The primary purpose of the TV camera is to obtain data on in-orbit thermal bending of the primary booms. The camera is a black and white TV system with standard scan (525 horizontal lines and a 30-frame vertical scan). The camera is mounted near the vertex of each pair of primary booms and focused onto a 9-inch eccosphere target at the end of each boom. The highly reflective surface on the target provides contrast against black space and makes boom identification easier when the boom is deployed to its full length. On the medium altitude system (ATS-A) there are two such cameras: one facing space and the second earth pointing, but only one camera is provided for the ATS-D and -E. A secondary function of the TV camera (on ATS-A and ATS-E) is as an earth viewing sensor.

Spacecraft attitude data (relative to the sun) is provided by the Solar Aspect Sensor. Two of the five SAS detectors are mounted on the ends of the spacecraft and three are mounted at 120-degree intervals around the spacecraft bellyband. One of these detectors is always the most illuminated by the sun according to vehicle attitude. This sun angle data is processed in the SAS electronics unit and telemetered to the ground to provide full spherical coverage. Complete three-axis attitude information is derived by combining the output of

the Solar Aspect Sensor with data from a GFE Earth IR sensor or measurements of antenna polarization angles by ground tracking stations (POLANG). Initially, the attitude sensing system included an RF Attitude Sensor which would have measured the angle of arrival at the satellite of an electromagnetic wave transmitted from the ground. However, this sensor was deleted by NASA early in the design effort.

A Power Control Unit (F of Figure 1-1) is included as an electrical interface between the gravity gradient system and the spacecraft. The PCU incorporated the power, command and telemetry interfaces as well as diagnostic measurement circuits.

Beginning with inception of the ATS contract and lasting through the critical design phase of the gravity gradient stabilization system, GE published a monthly interface report. Each document contained items pertinent to system interfaces with the spacecraft contractor. Such topics as weight and center of gravity allocations, power requirements, recommended alignment procedures, telemetry and command assignments, detailed interconnection diagrams, etc., were updated on a monthly basis. Table 1-2 contains a list of published interface reports by document number and publication date.

Development of the gravity gradient stabilization system was defined in the ATS Work Statement, approved by NASA, and issued by GE on April 20, 1965 as Document No. 65SD4293. This work statement required fabrication and test of three flight systems and two sets of ground test equipment and flight analysis and data reduction support following the launch of each flight system. The components delivered under contract are summarized in Table 1-3. Table 1-4 lists the associated aerospace ground equipment designed for use during development testing and later field testing. Table 1-5 summarizes the "make or buy" decisions which were finalized the latter part of 1964. Table 1-6 lists the requirements and subsystem specifications issued by GE, accepted by NASA and modified by the course of events during the engineering development phase of the program; dates shown are original release dates. The ensuing Acceptance and Qualification Test Instructions (Standing Instructions or "SI's") were prepared to describe the detailed test activity deemed necessary to insure compliance with the subsystem specifications and the acceptance and qualification test requirements of NASA Specification S2-0102, "Environmental Qualification and Acceptance Testing,"

Table 1-2. Interface Reports

Interface Report No.	Document No.	Publication Date
1	Letter report	---
2	Letter report	---
3	Letter report	---
4	64SD4365	October 1964
5	64SD4391	November 1964
6	65SD4202	December 1964
7	65SD4218	January 1965
8	65SD4242	February 1965
9	65SD4303	March 1965
10	65SD4307	April 1965
11	65SD4351	May 1965
12	65SD4370	June 1965
13	Letter report	July 1965
14	65SD4408	August 1965
15	65SD4462	September 1965
16	65SD4480	October 1965
17	65SD4520	November 1965
18	65SD4224	December 1965
19	66SD4245	January 1966
21	66SD4323	March 1966
22	66SD4368	April 1966
24	66SD4432	June 1966
26	66SD4486	August 1966
29	66SD4551	November 1966

Table 1-3. Definition of Gravity Gradient Stabilization Systems

Component	System and Quantity/System								
							Flight Systems		
	Thermal (ATS-A)	Dynamic(ATS-A)	E/U 1(ATS-A)	E/U 2(ATS-D/E)	P1 (ATS-A)	P2 (ATS-A)	ATS-A	ATS-D	ATS-E
1. Primary boom assembly (2 per system)	2	2	2	*	1	2	2	2	2
2. Damper boom assembly (1 per system)	1	1	1	*	1	1	1	1	1
3. CPD	1	1**	1	1	1	1	1	1	1
4. PCU	1	1	1	0	1	1	1	1	1
5. SAS (Electronics and 5 Sensors)	1	1	1	0	1	1	1	1	1
6. TV Camera	2	2	2	0	1	2	2	1	1

* Set of ATS-D/E tip masses to be provided to modify E/U 1.
** Same as E/U except for dummy diamagnetic suspension system and angle indicator.

NOTE:

1. ATS-A and 6000 NM Orbit Configuration are used interchangeably.
2. ATS-D and first 24 hr Orbit Configuration are used interchangeably.
3. ATS-E and second 24 hr Orbit Configuration are used interchangeably.

Table 1-4. Definition of Aerospace Ground Equipment (AGE)

Item	Set 1*	Set 2**
Sun Sensor Stimulator Source	1	1
Video Monitor	1 (GFE)	1 (GFE)
TV Target Lights and Complementary Equipment	1	1
GGSS Test Console	1	1
Test Console Cables (Set)	1	1
Damper Simulator	1	1
Squib Firing Box	1	1

*Contractor Use
**Field Use

Table 1-5. Make or Buy List

	Make (GE)	Buy (from)
Combination Passive Damper	GE/MSD	TRW, Inc. supplied the Passive Hysteresis Damper*
TV Camera System	-	Lear-Siegler
RF Attitude Sensor	-	GE Radio Guidance Operation
Power Control Unit	GE/MSD	-
Solar Aspect Sensor	-	Adcole Corporation
Primary Boom, Rods & Mechanism	-	deHavilland Aircraft of Canada
Damper Boom/Rods & Mechanism	-	deHavilland Aircraft of Canada

*PHD for ATS-A was supplied by TRW. GE built the Variable Torque Hysteresis Damper for the ATS-D/E systems.

Table 1-6. ATS Gravity Gradient Subsystem Specifications

Title	GE Specification No.	Release Date
ATS Gravity Gradient System Requirements Specification	SVS-7312	10/8/65
Gravity Gradient Boom System for Project ATS	SVS-7316	3/5/65
Gravity Gradient Digitated Damper Boom Assembly for Project ATS-E	SVS-7563	2/13/69
Combination Passive Damper	SVS-7314	4/29/65
Solar Aspect Sensor-Applications Technology Satellite	SVS-7306	1/4/65
TV Camera Subsystem-ATS	SVS-7310	4/15/65
RF Attitude Sensor Subsystem Design Specification	SVS-7305	7/20/64
Power Control Unit-Applications Technology Satellite	SVS-7307	9/27/65

and NPC 200-2, "Quality Control Provisions for Space Systems." These Standing Instructions formed the procedural basis for qualification and flight acceptance testing of each component of each gravity gradient stabilization system. Table 1-7 lists the published SI's by NASA approval date.

1.3 DELIVERABLE HARDWARE END ITEMS

1.3.1 THERMAL MODEL

The gravity gradient stabilization system thermal model was prepared for NASA acceptance in August of 1965 and shipped to the spacecraft contractor on September 9, 1965. The units were designed for use in system thermal test. Each model was fabricated to dissipate the

Table 1-7. ATS Gravity Gradient Subsystem Standing Instructions

Title	SI No.	Release Date
Qualification and Acceptance Test Instructions for the Primary Boom Assembly	237,036	9/2/66
Acceptance Test Instructions for the Combination Passive Damper	237,016	4/20/66
Acceptance and Qualification Test Instructions for the ATS Solar Aspect Sensor	237,012	4/20/66
Acceptance and Qualification Test Instructions for the ATS Television Camera Subsystem	237,013	4/20/66
Acceptance and Qualification Test Instructions for the ATS Power Control Unit	237,015	4/20/66

Note: The Standing Instructions for the Damper Boom Tests were published in deHavilland document DHC-SP-ST.110M, approved 4/20/66.

predicted nominal power of the flight units within 10 percent. Dissipation was achieved through power resistors mounted with each unit. The primary boom package contained separate resistors to simulate the power dissipation characteristics of the boom extension and scissoring motors. A "Thermal Model Interface Information" report (GE Document No. 65SD4421) was prepared for use in system thermal test and contained special handling instructions, thermal duty cycles, installed thermocouple locations, and a drawing of each unit.

1.3.2 DYNAMIC MODEL

The gravity gradient stabilization system dynamic model duplicated the mass properties of each of the flight units and was designed for use in system dynamic tests conducted by the spacecraft contractor. These components were accepted by NASA and shipped to Hughes Aircraft on September 13, 1965. A "Dynamic Model Interface Information" report (GE

Document No. 65SD4430) was prepared for use in system dynamic testing and contained special data requirements, interface drawings and a request for the installation of accelerometers in certain key locations.

1.3.3 ENGINEERING UNITS

Construction of engineering units was started early in 1965 along with a series of engineering design evaluation studies used to confirm or modify the chosen engineering approach. These efforts were supported by specialists in systems analysis and simulation, materials, reliability, manufacturing, parts and quality control procedures. The engineering units were to faithfully duplicate the electrical and mechanical characteristics of the 6000-mile ATS configuration and second units were to be built only in those instances where synchronous altitude mission requirements introduced unique changes in unit operational parameters. This plan led to the fabrication of a second CPD engineering unit and the fabrication of a second set of tip masses for conversion of primary and damper boom engineering units from ATS-A to ATS-D/E configurations. Only one engineering unit was developed in each of the other subsystem areas. The engineering units were used to establish proven design feasibility before commitment of efforts to prototype and flight unit fabrication. Development and testing of engineering units was essentially complete by early 1966.

1.3.4 PROTOTYPE UNITS

Assembly and initial testing of prototype units paralleled the final phases of engineering unit testing. Two prototype gravity gradient systems were built to flight drawings. Both were fabricated to the requirements of the medium altitude spacecraft (ATS-A). One set was used at GE for the component qualification test program and the second set was delivered to NASA for use in system qualification testing by the spacecraft contractor. Tests performed on each subsystem are summarized at the end of each of Sections 2 through 7.

1.3.5 FLIGHT SYSTEMS

Assembly and flight acceptance testing for three sets of gravity gradient stabilization system flight hardware was followed by NASA acceptance and delivery to the spacecraft contractor during the following time periods:

ATS-A	October - December 1966
ATS-D	August - September 1967
ATS-E	September - October 1968

The delivery of the ATS-D and ATS-E systems was proceded by an interim period of GE bonded storage. The bonded storage period was introduced in an effort to improve the efficiency of personnel and facility utilization through inauguration of a production-type approach to the assembly and test of the three flight units. The production-type approach allowed for continuity of shop and test personnel through critical periods of fabrication and initial test. The consequent early readiness of the ATS-D and ATS-E systems required the interim periods in bonded storage. During the period of storage, standardized inspection and preventive maintenance procedures were implemented and formal condition reports were issued to insure continuance of flight readiness status. Some modifications to the equipment were also made during these periods. For example, the automatic operation of the TV sun shutter in the "TV off" condition was eliminated on the ATS-E system due to the possibility of an excessive number of shutter operations during the interim spin mode.

1.4 FIELD AND FLIGHT SUPPORT

Following acceptance and delivery of the gravity gradient prototype and flight systems, GE continued to support NASA/Goddard and Hughes Aircraft, the spacecraft contractor, through provision of a fulltime field test representative and consultation during system testing at Hughes Aircraft and prelaunch activities at NASA/GSFC and Cape Kennedy. This support extended over more than a three-year period and frequently included on-site analysis (by the cognizant GE design engineers) of problems that arose during the field test operations.

The GE field test representative received and inspected all GE hardware and equipment delivered to the spacecraft contractor's plant and assured that delivery was accomplished without damage. Before spacecraft installation, the gravity gradient hardware was subjected to "short-form" testing using the Hughes Experimental Package Console (EPC). Following spacecraft installation, the field test representative (with "as required" on-site consultation and support by cognizant GE design engineers) participated intimately in system qualification

and flight acceptance testing of the total spacecraft system. The gravity gradient experimenter's role in system test was primarily concerned with the performance of "short form" and "long form" tests at prescribed intervals in the overall system test plan. These long and short form test procedures were established in detail, well in advance of their actual performance. GE's recommendations for testing of the prototype spacecraft system were included in the GE Gravity Gradient Systems Prototype Field Test Plan, Document No. 65SD4499-B, 18 April 1966. This document contained a detailed test procedure with data sheets for checking the gravity gradient components during spacecraft system qualification testing at Hughes. GE recommendations for system flight acceptance testing were included in the GE Gravity Gradient System Flight Field Test Plan, Document No. 66SD4553, December 8, 1966. This document contained block diagrams of all electrical interconnections between GE and Hughes components and a detailed test procedure, with data sheets, for checking the gravity gradient components during spacecraft flight acceptance testing. Information from these documents was extracted, reformatted and published in the form of a Hughes Acceptance Test Plan for each flight spacecraft. GE requirements and recommendations for gravity gradient stabilization system component installation and alignment were presented in Document No. 66SD4222, "Installation and Alignment Instructions for the Gravity Gradient Stabilization System," August 1, 1966. This document also contained information on parameter tolerances and a description of the special test jigs and fixtures provided for accurate alignment.

In addition to follow-on support in the field, a team of flight analysts was in place at GE (following each launch) to analyze and interpret performance of the orbiting gravity gradient system and provide consultation to the GSFC Project Office and ATSOCC on an "as required" basis. This was in addition to the regular requirement for attitude determination, gravity gradient orbit test consultation and readiness for evaluation of anticipated but never-performed gravity gradient stabilization experiments. These activities are covered in more detail in Volume I of this report.

SECTION 2

BOOM SUBSYSTEM

BOOM SUBSYSTEM FACT SHEET
(Both Primary and Damper Booms)

DESIGNER:

General Electric Company Space Division

SUBCONTRACTOR:

deHavilland Aircraft of Canada Limited

CONTROLLING DOCUMENTS AND DRAWINGS:

Specification	SVS-7316
Work Statement	GE 9970-GGEP-1
Primary Boom Assembly	GE Drawing 47J209567
Damper Boom Assembly	GE Drawing 47E207008

FUNCTION:

Primary Boom

- Provides large inertia for gravity gradient satellite
- Booms are configured to furnish proper inertia ratio for stabilization
- Scissoring capability provides means for altering inertia ratio in orbit
- Retraction capability provides for changes in inertia levels and a method for inverting the spacecraft

Damper Boom

- Provides gravity reference for dissipation of vehicle libratory energy
- Contributes to moment of inertia for vehicle stabilization

UNIT DESIGNATION:

Primary Booms

1	Engineering Unit
2	Engineering Unit
3	Engineering Unit
100	Component Qualification Unit
11	Prototype Unit
12	Prototype Unit
101	ATS-A Flight Unit
102	ATS-A Flight Unit
104	ATS-D Flight Unit
105	ATS-D Flight Unit
10	ATS-E Flight Unit*
103	ATS-E Flight Unit*
*	Used as backup to the Westinghouse booms

Damper Booms

2	Engineering Unit
11	Component Qualification Unit
10	Prototype Unit
100	ATS-A Flight Unit
102	ATS-D Flight Unit
101	ATS-E Flight Unit

SECTION 2

BOOM SUBSYSTEM

2.1 INTRODUCTION

The boom subsystem of the ATS Spacecraft consists of three separate packages containing gravity gradient booms. The two primary packages each contain two rod erection devices coupled to a mechanism for extending and scissoring the two primary booms. The third package contains two rod storage units (tip masses) attached to a structural center body and includes a separate housing containing the explosive portion of the tip mass release system.

The basic requirements for the boom subsystem are as follows:

1. Provide a set of four erectable primary booms which can be stowed within the confines of the ATS Spacecraft during launch and be deployed at separation to form an "X" configuration about the spacecraft. Weights are installed at the boom tips to achieve a prescribed set of inertias about the three principal axes of the spacecraft.

2. Provide a means of retracting the primary rods on command to desired lengths.

3. Provide a means of changing the angles included between the primary booms in a manner that maintains a symmetrical configuration about the satellite yaw axis. This action, which is limited to a total of 20 degrees on each boom, is referred to as scissoring.

4. Provide a set of two damper borne secondary booms which will each extend along the same straight line in opposite directions. These booms are to carry tip masses on their ends which will provide the proper inertia for the operation of the damper. After initial deployment, no mechanical connection or wiring is to extend from the damper boom platform to the spacecraft body. The damper booms are not required to retract.

5. Accomplish the above within the tolerance/disturbance constraints.

The basic extendible boom selected for this mission is the Storable Tubular Extendible Member (STEM) developed by the deHavilland Aircraft of Canada, Limited. This technique involves the formation of a tubular section from a flat metal strip which is formed and heat-treated in the tubular form then flattened under stress and wound onto a storage drum.

Subsequent erection in orbit is accomplished by paying out the stowed strip through a set of guides which allow the boom to form into its natural tubular shape. The edges of the metal strip overlap each other to render stiffness to the operating section. Storage/erection units for the STEM tubing are of both motorized and self-erecting type. The motorized type employs a motor to drive the storage drum and thereby provide a means of retracting the extended booms. The self-erecting type units use the strain energy in the stowed metal strip to rotate the storage drum and erect the boom. The STEM concept is shown in Figure 2-1.

Motorized units were selected for the primary booms due to the requirement to retract. Self-erecting units were selected for the secondary (damper) booms. Initial considerations for the scissoring mechanism included several which provided mechanical coordination of the motion for all four primary booms.

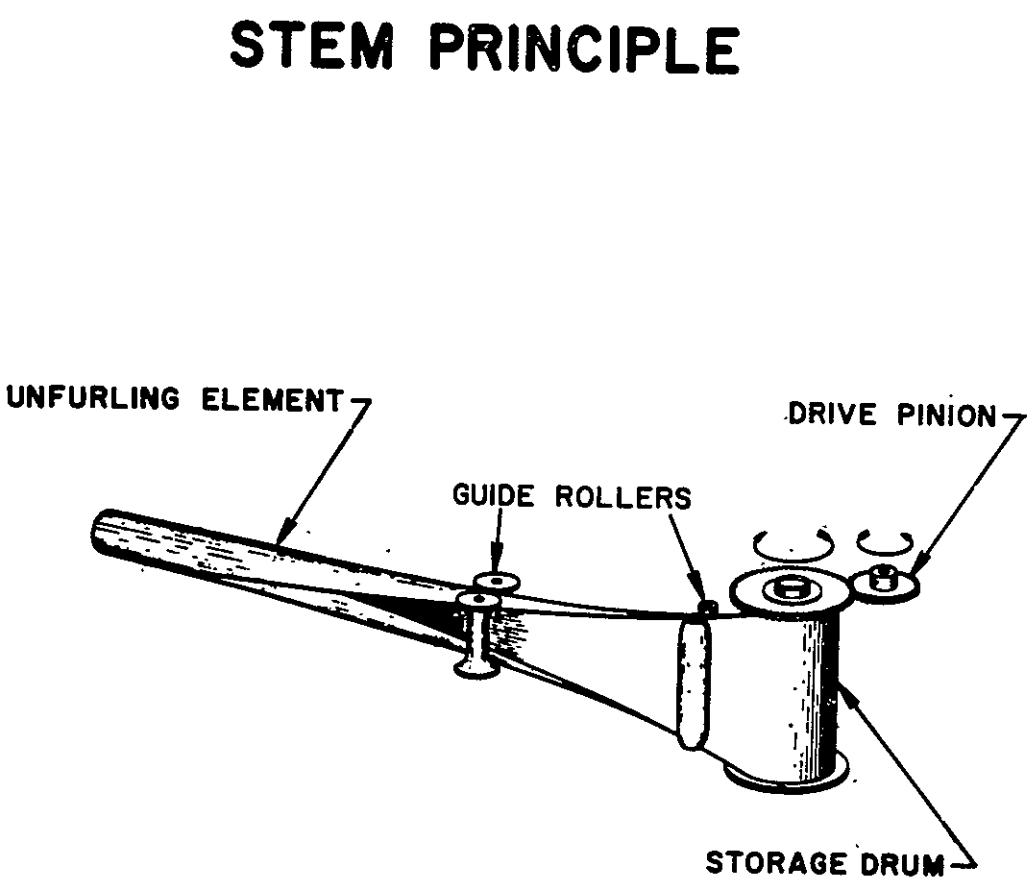

Figure 2-1. STEM Principle

Design studies included versions using bull gears, pulley systems, bellcrank linkages, and jackscrews. However, the constraints imposed by spacecraft size and other equipment in the boom mounting area proved the mechanical connection of all booms to be impractical. An evaluation of the coordination required between booms for both extension and scissoring showed that a system which depended on electrical synchronization was not impractical. Accordingly, the following system was devised:

1. The four primary boom erection units are divided into two pairs.

2. The two erection units making-up each pair are mounted as close as possible to one another and are coupled by a bell-crank linkage to transmit scissoring motion and a gear train to coordinate extension drum drive.

3. Each pair of erection units is provided with one motor for extension and one motor for scissoring. The motors are encased in a hermetrically sealed container to preserve their useful life in space, torque being delivered through flexible membranes.

4. The two erection units of each pair, their drive train, motors, and scissoring linkage are all mounted with a single framework. The erection units are pivoted to this framework.

5. Motion between the two pairs of units is coordinated electrically.

One half of a primary boom system is shown in Figure 2-2 with the booms in the stowed position.

Damper boom design was less complex than the primary boom since there was no requirement for retracting the booms after they were deployed. Two boom elements move away from the center body in opposite directions as a result of the stored energy in the tapes. Release is effected by two (redundant) linear actuators that are each initiated by a pyrotechnic device. Figure 2-3 shows the damper boom in the stowed position with the linear actuator at the right.

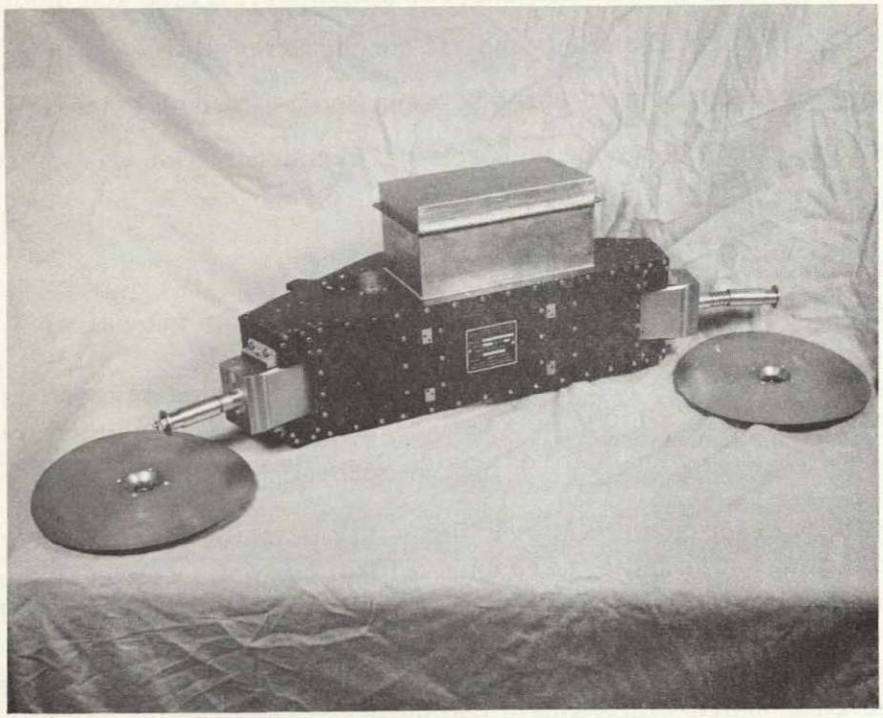

Figure 2-2. Primary Boom Assembly (1/2 system)

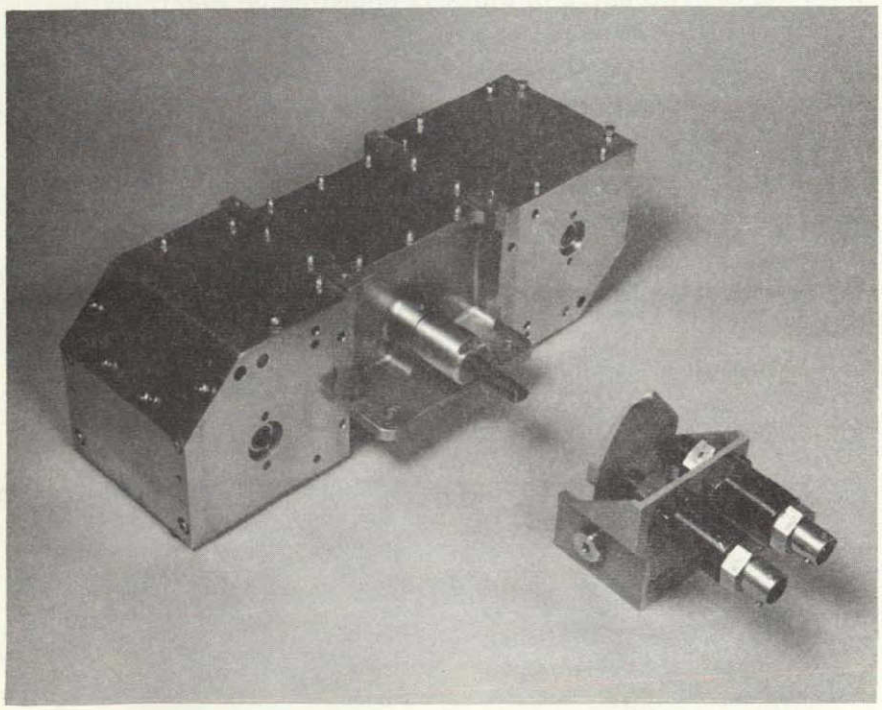

Figure 2-3. Damper Boom with Linear Actuator at Right

2.2 ENGINEERING DEVELOPMENT

2.2.1 MAJOR SUBCONTRACT

Since the basic component of this subsystem (erectable STEM type booms) was previously manufactured solely by the Special Products Division of the deHavilland Aircraft of Canada Limited, it was decided to let a subcontract for the deployment, manufacture and qualification of the boom system components. This was done with the approval of NASA-Goddard Space Flight Center.

2.2.2 INTERFACE CONSIDERATIONS

2.2.2.1 Spacecraft Interface

2.2.2.1.1 Damper Boom

The damper boom unit is designed to mount directly to the Combination Passive Damper (CPD) and as such does not have a direct interface with the spacecraft structure. However, the damper boom unit does require certain clearances with respect to spacecraft equipment in the course of its oscillation about the CPD axes. These clearances are dependent upon the location of the CPD within the spacecraft. In general the damper boom/spacecraft interfaces are as follows:

1. A hole in the solar array substrate in the general vicinity of the CPD in order to pass one damper boom tip assembly as the boom is deployed. This hole is configured to allow for the angular motion of the damper boom about the CPD axis.

2. The swing of the damper boom which extends toward the aft end of the spacecraft necessitates local slots at the edge of the aft solar cell skirt.

   The exact size and location of these cutouts is defined by the CPD position within the spacecraft.

2.2.2.1.2 Primary Booms

The major interface between the boom subsystem and the spacecraft is the installation of the primary boom packages. There are two primary boom half systems per spacecraft, each package containing two erection units and their associated drive train and scissoring linkage.

Each primary boom package has five interfaces with the spacecraft. They are:

1. Location within the volume of the spacecraft (interference with other equipment)
2. Mounting attachments
3. Clearance for boom scissor travel (slots in solar array, etc.)
4. Cushions for tip target on solar array
5. Alignment with spacecraft center of mass, center of pressure and satellite axes (also requiring proper balance of spacecraft CM & CP).

The location within the spacecraft volume (item 1 above), clearance for scissor travel (item 3 above), and alignment with the spacecraft (item 5 above) were the subject of numerous negotiations between General Electric and Hughes Aircraft Company. The following agreements were reached:

1. The boom packages will be symmetrically located about the overall spacecraft CG.
2. The booms will extend in planes parallel to one another.
3. The boom packages will be equidistant from and on opposite sides of a plane passing through the overall spacecraft CG (at Station 22.5) and making an angle of 20.5 degrees with satellite yaw/roll plane. The angular relationship of the boom package to this plane will be such that the center of gravity for each boom assembly will lie in this plane. This angular relationship will be symmetrical.
4. The center of pressure of the spacecraft body (not including booms) will be balanced to be coincident with center of gravity of the spacecraft body.

5. Slots will be provided in the solar array and other spacecraft equipment will be located to accommodate the scissor travel. In response to a HAC request, the primary boom package design was reviewed with regard to mounting on only three bolt hole locations. It was determined that, with a heavier gauge material in the component skin, the package could sustain the loads imposed by such a mounting. It was also determined that 1/4-inch diameter bolts would be required. This information was relayed to NASA/GSFC at a meeting held at GE on May 6, 1965. A detailed interface requirements drawing was prepared as a result of this meeting and delivered to NASA/GSFC on May 14, 1965.

   GE and deHaviland worked out the mechanical details of the thermal boot recommended by HAC. The thermal boot is inserted on the primary boom package at the boom clearance slots provided in the spacecraft. Details of the thermal boot were incorporated into the primary boom interface drawing which was one of the drawings corrected at the NASA/HAC/GE interface meeting on May 19, 1965.

2.2.2.2 Sensor Interface

2.2.2.2.1 Primary Boom

Since the gravity gradient primary booms extend distances greater than 100 feet from the spacecraft, they enter the field of view of various sensors located on board. Because the presence of the booms in the field of view of certain of the sensors might have deleterious effects on sensor performance, an investigation was undertaken to determine the extent of the boom transgression of sensor fields of view. In addition it is required that the TV camera be able to "see" the tips of the booms over the full travel of possible boom tip excursion. Accordingly, the following layouts were prepared:

1. A layout of TV field of view camera/boom intercepts
2. A layout of RF Attitude Sensor field of view/boom intercepts
3. A polar coordinate plot of possible positions of the primary booms within the field of view of the IR earth sensor.

A 3-inch displacement between camera lens and boom location will have only a slight effect. It was determined from Layout 1 that, for the camera field of view lined with the satellite axes, there is a slight risk that the tips of the boom will be outside the field of view during the worst case condition of maximum scissor angle and maximum thermal bending. However, a rotation (about the lens centerline) of approximately 12 degrees will enable the camera to "see" the boom tips at all times due to diagonal effect. This amount of rotation was planned for TV camera installation.

Layout 2 was based on an RF sensor location near the forward end of the vehicle. Layout 3 was generated at the specific request and per the instructions of NASA/GSFC. This plot and explanatory notes were delivered to NASA/GSFC as required.

2.2.2.3 Power and Telemetry Subsystems Interface

The boom subsystem interfaces directly with the Power Control Unit (also supplied by GE).

2.2.3 150-FOOT ROD CONSIDERATIONS

2.2.3.1 Primary Boom

One of the initial requirements for the primary booms was that the rods for MAGGE* and SAGGE* be 100 feet long. The different inertial levels for the medium and synchronous vehicles were to be achieved by different weighted tip masses; the heavier tip mass would be used on the SAGGE. The use of 150-foot rods was investigated to establish the weight savings that could be effected by the longer rods for the same inertial levels as the shorter rods.

The investigation also included a consideration of results when the tip mass weight was held to the original requirement (2.5 and 10 pounds respectively) while increasing the rod lengths to 150 feet.

* MAGGE - Medium Altitude Gravity Gradient Experiment (6000 nm orbit)
SAGGE - Synchronous Altitude Gravity Gradient Experiment (23,000 nm orbit)

2.2.4 MOTOR SELECTION

2.2.4.1 Primary Boom

The boom system employes four DC motors per satellite, two for primary boom deployment and two for primary boom scissoring.

The types of dc motors considered for this application were:

1. Permanent magnet type
2. Split series wound type
3. Shunt wound type

The shunt wound motor was selected for this application because the shunt wound motor offers a much finer speed control over the range of possible variations in applied voltage and ambient temperature. Examination of typical curves in the expected loading areas readily shows that the shunt wound motor speed will vary much less with variations in loading, temperature, and voltages. It is necessary to limit the variations in motor speed in order to preclude deleterious effects on boom structural integrity and capture performances.

The use of shunt wound motors requires a slightly more complex power switching system than the split series motor, but this is offset by the attendant advantages in speed control.

The use of the permanent magnet type is precluded by the residual magnetic dipole remaining after power is removed.

2.2.5 POTENTIOMETER BOOM LENGTH INDICATOR

2.2.5.1 Primary Boom

The original design concept employed a magnetic reed switch to monitor primary boom erection. This system, although simple in sensor concept, easy to calibrate, and not susceptible to boom erection jeopardization, had the disadvantage of requiring a counter

circuit in the telemetry set to measure boom length. In the event of power interruption, the count would be lost. In order to have up-to-date boom length information readily available at the ground station at all times, it would be necessary to design a memory circuit into the telemetry set. The complexity that this requirement introduced into the telemetry set was not considered offset by the advantages associated with the reed switch. Accordingly, a rotary potentiometer was included in the extension drive transmission box to monitor boom length in orbit.

2.2.6 BOOM ELECTRICAL ISOLATION

2.2.6.1 Primary Boom

GE was requested to provide dc electrical isolation of the primary booms from the spacecraft and to reduce the capacitance between the boom and the spacecraft to a minimum.

The resistance between each primary boom and the spacecraft structure is to be a minimum of 10^8 ohms when measured at laboratory ambient conditions. The design goal for capacitance between the boom assemblies and the spacecraft is to be 50 picofarads with a maximum allowable capacitance of 200 picofarads.

2.2.7 TIP TARGET CONFIGURATION

A tip target configuration change from an articulated 6-inch diameter disc to a 9-inch diameter disc fixed at a 50 degree angle to each primary boom was incorporated. This configuration simplified the tip target design in that the targets could be stowed tangent to the spacecraft solar array during launch without the use of an articulated joint. Evaluation for TV camera visability resulted in a change in disc material from aluminum to lexan treated with eccospheres.

2.2.8 RELEASE MONITOR

2.2.8.1 Damper Boom

In order to provide a telemetry event monitor of damper boom release, a design improvement was undertaken to add two microswitches to the upper damper surface. These microswitches

are triggered by motion of the tip assemblies of the damper booms as they move away from the CPD. These switches were mounted so that they would not interfere with the motion of the damper booms after deployment. This design requires no wiring between the damper booms and the CPD.

2.2.9 DESIGN DETAILS

2.2.9.1 Erectable Booms

The basic erectable boom is a flat beryllium copper element two inches wide, 0.002 inch thick, and of a length equal to the desired boom length. The element is rolled about its longitudinal axis into an overlapped, right, circular cylinder. The element is heat treated in this form such that its natural stress tree condition is the overlap tube. Storage of the boom is effected by elastically flattening the tape and coiling it about a storage spool. Subsequent erection is accomplished by rotation of the storage spool in the direction which drives the stowed tape through the guidance until it reforms into the tubular shape. A sample section of the rod element is shown in Figure 2-4.

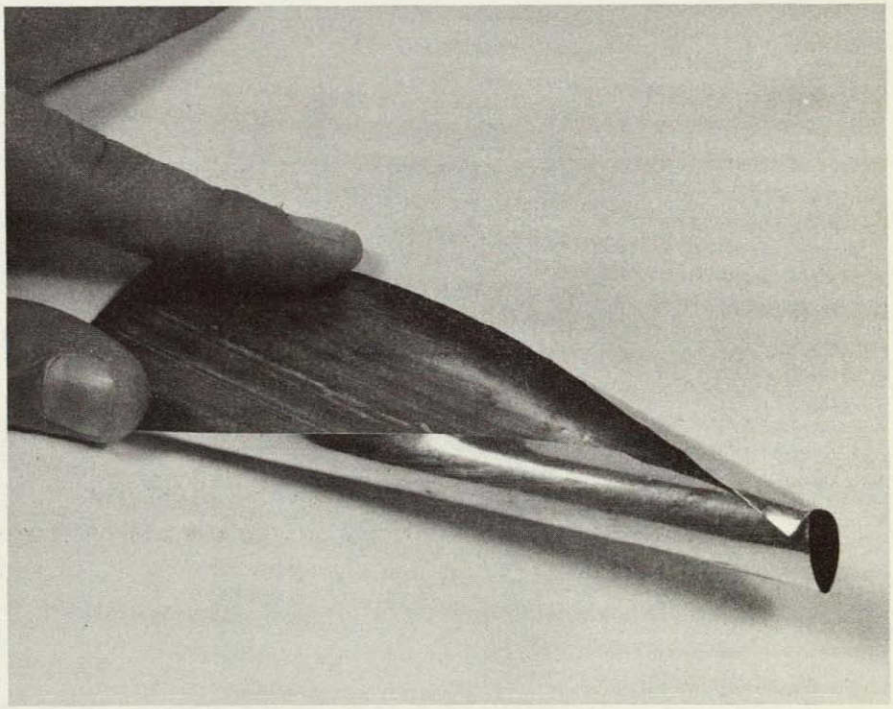

Figure 2-4. Gravity Gradient Rod Sample

2.2.9.2 Primary Boom

2.2.9.2.1 Erection Units

The erection units for the primary booms house the storage spool and guidance and are driven externally by means of a gear train. They take the form of a roughly rectangular prism 8.25 inches long, 4.5 inches high, and 3.0 inches wide. A schematic is shown in Figure 2-5.

The erection units also secure the inboard ends of the tip weight assemblies. (Additional lateral support during launch is rendered the tip weight by the overall assembly housing at a point near the CG of the tip weight.)

The attachment of the tip weight to the erection unit is so fashioned as to release the tip weight upon initial motion of the boom tape at erection.

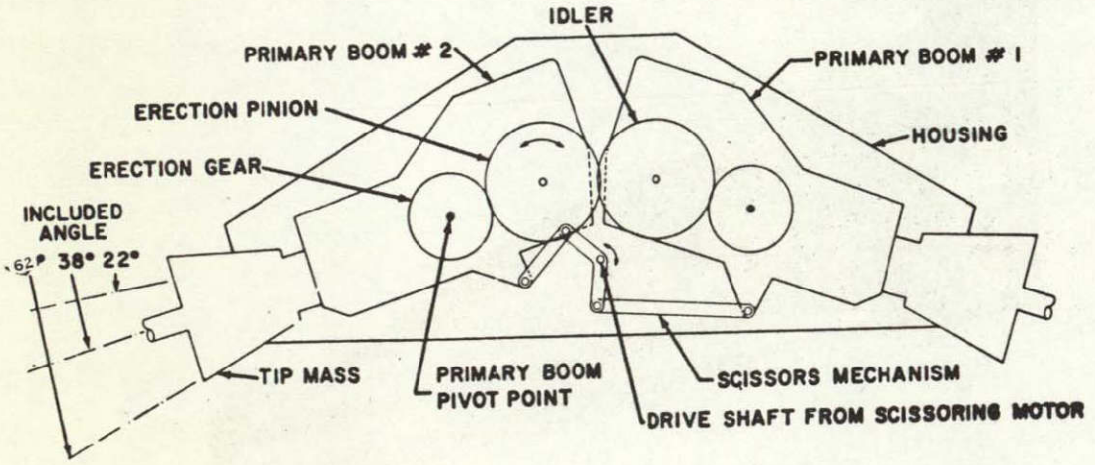

Figure 2-5. Primary Boom Assembly Schematic (1/2 system)

In the stowed condition, the boom tape is wound on the storage spool and fed through the guidance up to the point where it passes just outside of the erection unit and fastens to the tip weight assembly. Torque applied to the spool will drive the stowed tape through the guidance and free the tip weight from its attachment to the erection unit. Continued application of torque will erect the boom to its full length in the tubular configuration, at which time the full extension microswitch will engage a hole in the storage spool and cut-off motor power, as well as provide a telemetry event monitor.

Reversal of the direction of applied torque will retract the booms. A rotary potentiometer mounted external to the erection unit will provide telemetry input of boom length, thereby providing the capability of stopping the erection or retraction process on command at points other than full extension or full retraction.

The storage spool bearings are mounted in arc-shaped slots. This allows the spool centerline to move in the direction necessary to keep the point of tangency to the stowed tape always in line with the entry to the guidance at the tape pay-off point. This motion is necessary since the diameter of the stowed tape will decrease as the boom is extended. The motion is controlled by a roller that rides on the stowed tape just below the tape pay-off point. The drum is spring loaded against this roller by the tension in the spring belt system which serves the additional function of keeping the strain flattened tape wound tightly on the storage spool.

Since the storage spool centerline moves relative to the housing, external troque can not be delivered directly to the spool. Therefore, a set of drive gears is provided. This consists of two gears (one at each internal side of the erection unit) that are pinned to a common shaft which is driven externally. Each of these gears meshes with gear teeth cut in the side cheeks of the storage spool. The slot in which the spool bearing rides is an arc-shaped slot centered at the drive gear shaft. Therefore, the storage spool is constrained to move in an arc type motion about the drive gear, always maintaining tooth engagement at the pitch diameter of the drive gear. The double gear (one at each cheek) is provided in order to stabilize the spool and maintain the spool centerline always parallel to the drive gear shaft.

The housing of the erection unit is constructed of chem-milled aluminum side and end plates and of a light aluminum top and bottom covers. The end of each tip mass assembly will be equipped with a lexan disk to serve as a TV camera target. Each tip target is fully articulated in order to allow it to lie flush against the spacecraft "skin" during launch, and erect itself normal to the boom centerline upon boom erection. Each ATS boom subsystem requires four such erection units and tip mass assemblies.

2.2.9.2.2 Scissoring

It is a basic requirement of the system that the primary boom be "scissored" that is the angles, in the plane of the basic "X", between the primary booms must be changed over a prescribed range while in orbit; the scissoring geometry is shown in Figure 2-6. In order to mechanize this feature, it is necessary to pivot the primary boom erection units. The motion must be coordinated such that all four primary booms move simultaneously in order to maintain a symmetrical configuration about the satellite yaw axes. This is accomplished by pairing the four primary erection units into two sets. The centrally located bellcrank in the scissoring linkage for each set is driven by a shaft which extends from the drive unit. Rotation of this bellcrank is transmitted through the push-pull links to the bellcranks on the erection units. Each erection unit is pivoted with respect to the overall package at a point concentric with the drive gears. Therefore, rotation of a single shaft (the central bellcrank drive shafts) manifests itself in equal and opposite rotation on the part of two primary erection units.

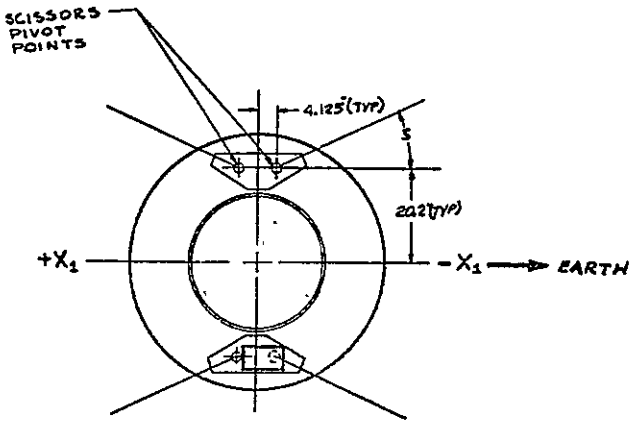

Figure 2-6. Primary Boom Package Locations Showing Scissoring Pivots

The two separate sets of paired erection units are synchronized electrically so that all four booms move in the fashion required for proper scissoring. At launch each boom unit will be caged at the nominal caging angle which is 32 degrees included angle between the booms at the top and bottom of the satellite. After initial boom deployment, the booms are free to move on command after their scissor axes. (The method of caging the tip masses also cages the erection units about their scissor axes. Therefore, release of the tip masses by boom erection also releases the scissor caging and the nominal scissor angle of 38 degrees is achieved.) The range of included angles over which the scissor linkage can move the booms is 22 degrees minimum and 62 degrees maximum. These included anges are shown on the left side of Figure 2-5. All pivots in the scissor linkage are of the flex-pivot type in order to minimize the number of bearings to be protected from the space environment.

2.2.9.2.3 Deployment

The primary boom erection units require externally applied torque at the drive gear shaft, as mentioned above. This is provided by a train of four gears for each pair of primary erection units. One of the center gears of the train is driven by the transmission unit. It, in turn, drives one erection unit directly and drives the second erection unit by means of an idle gear. Both erection units are thus driven by a single motor and their spool rotations are mechanically synchronized by the gear train.

The center of the erection unit drive gear is concentric with the axes about which the erection unit are pivoted in order to allow the gear train to remain engaged during scissoring motion.

2.2.9.2.4 Transmission Unit

Each primary boom unit pair is equipped with one drive unit which provides the torque required by the scissors bellcrank and the deployment gear train. Each drive unit contains two brush GJY type motors, one for boom extension drive (via gear train) and one for scissors drive (via bellcrank linkage). The scissors drive motor is equipped with an integral gear reducer to reduce speed to that required for scissoring rate. The original concept of the transmission unit provided for a clutch arrangement to switch motor functions in the event either motor failed. This standby mode operation was deleted during the prototype phase of the program.

The transmission unit enclosure confines the motors and drive trains in a vacuum tight envelope and uses a bellows type coupling to deliver the torque through the pressure shell. Two drive shafts protrude from the enclosure; one for the deployment gear train and one for the scissors bellcrank. The transmission unit also houses the potentiometers to readout scissor position and boom length. The linkage is illustrated in Figure 2-7.

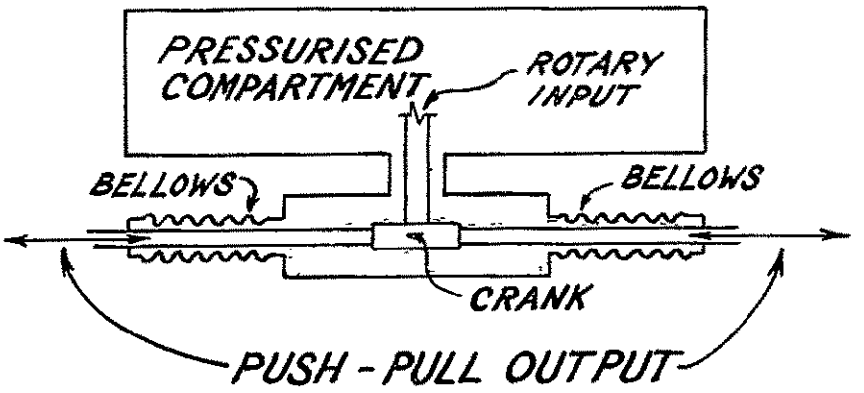

Figure 2-7. Scissoring Linkage Seal, Primary Boom System

2.2.9.2.5 Gears and Bearings

The design involves certain gears and bearings which will be at least partially exposed to the space vacuum and will be expected to operate after a long period of soak in orbit.

2.2.9.2.6 Structural Housing

Each pair of primary boom units, together with the associated drive train and scissor linkage, are housed by a local structure which coordinates the locations of all pivots and bearing supports, and provides structural support and caging of all components as a single unit. This unit will be mounted to the spacecraft structure, in the appropriate attitude, by means of bracketing. Alignment adjustments of this housing will be made relative to the satellite body axes. This housing is fabricated from chem-milled aluminum plate and aluminum sheet. Two such assemblies, make up one spacecraft set of primary gravity-gradient boom equipment.

2.2.9.3 Damper Boom

Each ATS boom subsystem requires one damper boom unit to be mounted on the damper borne platform and to act as a gravity anchor for the damper. The damper boom unit will extend two 45-foot long booms in diametrically opposite directions from the damper axes of rotation and in a plane normal to the same.

The erection technique for this unit is the self erecting scheme. The ends of the booms are fastened to that portion of the unit which remains at the damper axes (center body). The two storage spools, however, are each mounted in a section of the unit which is propelled away from the damper axes (tip masses) as the strain energy in the stowed tape causes the tape to unwind off of the spool.

The portions of the unit which house the storage spools are sized to weigh 1.6 pounds each, which is the amount required to provide the proper inertia for MAGGE (Medium Altitude Gravity Gradient Experiment). These units will be ballasted to provide inertia for SAGGE (Synchronous Altitude Gravity Gradient Experiment).

Release of the damper booms is accomplished by the action of squib-activated thrusters. When a single ball-lock is actuated, lift-off springs initiate the motion of the tip assemblies.

Then, the elastically wound tape begins to erect itself and continues to propel the tip assembly to the full length of the booms. Erection speed control is effected by a centrifugal brake. The tip assembly is restrained at the end of the fully erected boom.

2.2.10 TEST PROGRAM

2.2.10.1 Damper Boom

The Engineering Test program as originally envisioned would entail testing on only one Damper Boom Assembly. The intent of this program was to verify the design, determine problems in design and demonstrate the capability of the design surviving the qualification test program.

Prior to delivery of the T1 engineering unit, vendor test problems arose with the Conax bolt cutter employed in the tip mass release system with coordination due to the centrifugal brakes employed during the tip mass deployment. After delivery of T1 engineering unit test problems arose at General Electric on this unit with the Avdel Ball Lock and Holex Linear Actuator which replaced the Conax bolt cutter in the release system. At about the same time vendor test problems arose during the testing of the prototype units which resulted in further configuration changes to the centrifugal brake system.

Following is a listing of the tests performed on the T1 engineering unit:

1. Functional Tests
2. Solar Vacuum/Squib Firings
3. Vibration
4. Humidity
5. Acceleration
6. Ambient Squib Firings
7. Magnetic Dipole

The T1 engineering Damper Boom was deployed mechanically in initial tests conducted at deHavilland, but both booms did not deploy at the same rate. The problem was attributed to a change in friction on the nickel plated copper brake shoe. Continuing difficulty with the squib-actuated bolt cutters resulted in a postponement in the planned coordination testing with an actual bolt cutter.

An agreement was reached which enabled deHavilland to deliver the T1 engineering Damper Boom with a mechanical release rather than the pyrotechnic device. Plans included a retro-fit to incorporate the new tip mass release system after it was developed. T1 engineering Damper Boom was received by General Electric on 23 September 1965. The unit was functionally tested at General Electric at ambient conditions.

While the T1 engineering Damper Boom was undergoing ambient functional testing at General Electric, deployment coordination tests were being conducted at de Havilland on a SPAR model engineering unit.

After completion of the coordination tests and the redesign of the new pyrotechnic release system, the T1 engineering unit was returned to de Havilland for retrofit.

The retrofitted T1 engineering Damper Boom was received at General Electric on December 1965. The basic retrofit consisted of a new center-body to accommodate the new tip mass release mechanism, new brake lever arms, new spools with new boom elements, and all the associated modifications.

The series of engineering tests begun on the retrofitted T1 engineering Damper Boom in December 1965, were performed in accordance with the Engineering Test Plan for the Damper Boom which was documented in PIR 4171-085.

A solar vacuum test was conducted with the T1 Damper Boom unit mounted to CPD engineering unit 1 (summarized in PIR 41M2-104). This test closely simulated the insulation conditions of the ATS vehicle. The Damper Boom squibs were fired successfully at a chamber temperature of -15°F. After the squibs fired, Damper Boom travel was restricted to a 1/8 inch travel by tip weight catchers installed during the test.

A diamagnetic suspension test of the center body of the T1 engineering Damper Boom was completed on the Low Order Force Fixture (shown in Figure 3-40, Section 3) in the continuing series of engineering tests. In the demagnetized condition, there was a 2-dyne magnetic attractive force. In the magnetized condition, a 3-1/2 dyne repulsion force was measured.

The functional tests conducted on T1 engineering Damper Boom gave an insight into the difficulties to be encountered in utilizing the specialized deployment test trollies and the mechanical rewind equipment. Subsequent functional tests and problems on the prototype

and flight hardware resulted in the evolution of the present test trolley configuration with its oscillation dampers and motorized rewind equipment.

Although the T1 engineering Damper Boom vibration test indicated no significant problems, the subsequent qualification vibration test uncovered an element cracking failure. The failure, as the qualification test report No. 4315-QC-031 outlines, resulted from the lack of drum torque application after rewind. During mechanical rewind of T1 this drum torque application was a standard operational procedure. However, when the motorized rewind was introduced on the prototype units, due to inherent difficulties with the mechanical rewind, this drum torque application was not believed to be necessary.

In addition to the rewind procedural change introduced on the prototype units, the brake system underwent a configuration change to pivoted brakes which were not tested on the engineering unit.

2.2.10.1.1 Tip Mass Release System

The Conax bolt cutter originally developed for the Damper Boom release operation employed dual redundant squibs firing into the same explosion chamber. The primary function of the bolt cutter was to sever the solid cylindrical tie bar which maintained the tip masses in intimate contact with the center body, the schematic is shown in Figure 2-8. Its secondary function was to shear the primer leads when the bolt cutting was accomplished.

On July 9, 1965 a malfunction occurred at de Havilland during a deployment test of the T1 engineering Damper Boom. When the Conax bolt cutter was fired, the tip mass tie bar was not severed but the primer leads were sheared and no deployment resulted. Prior to returning the failed bolt cutter to Conax, the firing circuit utilized by de Havilland in the test was suspected to be the cause of the malfunction. However, the Conax failure analysis report suggested that the most likely cause of the malfunction was lack of proper confinement of the potting compound due to voids in the primer cavity.

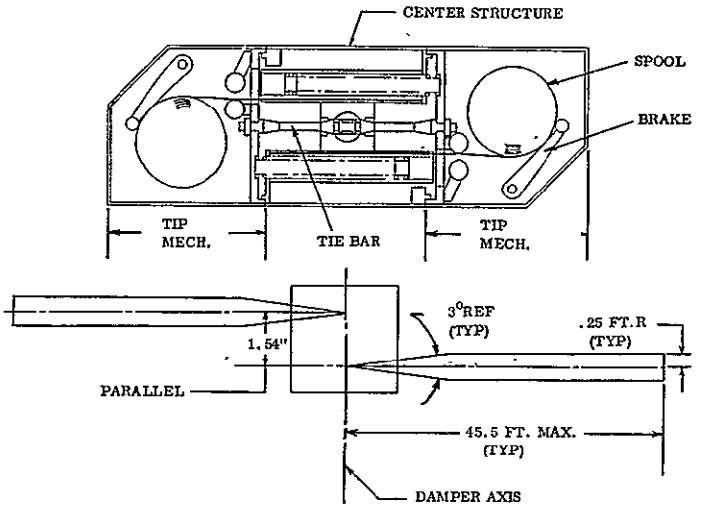

Figure 2-8. Damper Boom Schematic

Investigation of the redundant squib circuits which actuated the bolt cutter revealed that the connector ram sheared the primer leads within 100 microseconds after the first primer fired, thus cutting off power to the second primer. Since primers have in excess of one millisecond variation in firing time, redundancy could be guaranteed. The Conax failure analysis report stated that reliability cannot be guaranteed without testing a fairly large number of cutter operations under varying environmental conditions.

A test program to determine design adequacy, was negotiated between Conax, de Havilland and General Electric. However, this test program was not implemented. After further review, it was decided to drop the bolt cutter design approach because of the pyro device development problems. Several alternate boom release designs were investigated for possible replacement of the Conax cutter; two were examined in detail.

The first alternate design employed a Hi-Shear explosive nut in conjunction with a clevis type tip mass tie bar. On 13 September 1965, this concept was tested at de Havilland in a makeshift set up on a tensile tester. A severed explosive nut base resulting from this test was subsequently attributed to improper base support during testing.

According to Hi-Shear, frequent failures of this type in industry have prompted them to strengthen the base of this design for future units, although they state that this failure will not occur if the mounting is proper. On 15 September 1965, two additional tests on this first alternate design were conducted at de Havilland in the same test setup but with proper base support. The nut base remained intact, but in both tests the bolt did not move to separate the clevis tie rod. These failures were attributed to the lack of margin between the basic variations to be expected from the power cartridges and the force required to separate the clevis mechanism. Therefore, this approach was also dropped.

The second alternate design utilized an Avdel ball-lock device for holding and releasing the tip masses. This ball lock release mechanism was actuated by a Holex explosive thruster, the scheme is shown in Figure 2-9.

Other tie rod and release device combinations were given consideration in selecting alternate designs for actual testing. All combinations contained merit but in discarding each one the main consideration was that of reliability of operation.

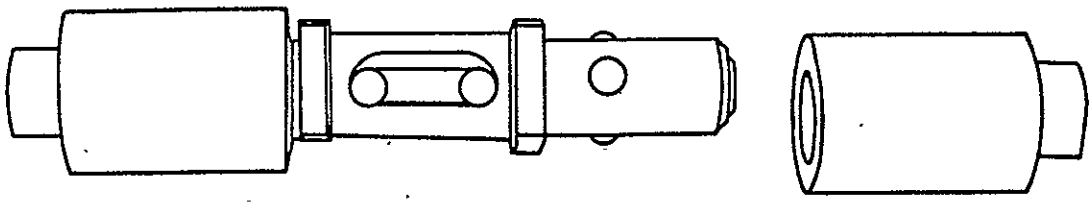

Figure 2-9. Damper Boom Ball Lock Release Scheme

The Avdel ball lock mechanism, de Havilland plunger and lever arm, and Holex linear actuator (squib/thruster) combination selected to replace the original Conax bolt cutters for the Damper Boom tip mass release, underwent functional testing during testing at General Electric on T1 engineering Damper Boom. The ball lock mechanism and plunger are integral parts of the Damper Boom Assembly and the linear actuator and lever arm are mounted in a separate actuator assembly on the base plate of the CPD. The two receptacles at the ends of the ball lock mechanism provide the coupling between the tip mass housing and the centerbody when the Damper Boom is in the stowed position. At deployment, the plunger travels through the slot in the center of the ball lock assembly and contacts the two spindles which permit the balls to depress inside the housing and release the receptacles. The plunger movement is initiated by either or both the electroexplosive squib-linear actuator devices. The tip masses then separate from the center body. In the actual system, the end of each element is secured to the center body. A spring at the end of the center body provides the initial separation force and guide pins ensure coaxial separation. Although the above combination was proven adequate for releasing the tip masses, individual parts experienced secondary failures during accomplishment of the releases.

Two Avdel ball lock mechanisms were used during the T1 tests. Each mechanism was subjected to one single and one double squib/thruster firing. The mechanism subjected to a single firing first showed no visible abnormal spindle damage after the first firing but sustained one broken spindle during the second (double) firing. This mechanism also underwent two mechanical releases at de Havilland prior to shipment of the T1 Damper Boom Assembly. The mechanism subjected to a double firing showed no visible abnormal spindle damage after the first firing but sustained two broken spindles during the second single firing.

Six Holex linear actuators (squib/thruster) were used during the T1 tests. Each actuator was fired only once. There were two single firings and two double or simultaneous firings. The second double firing only resulted in breakage of one piston at the end of its travel.

None of the other firings resulted in any noticeable abnormal piston damage. Simultaneous firing of both linear actuators is a system requirement but cannot be absolutely guaranteed from a pyrotechnic standpoint. Redesign of the thruster piston was undertaken to prevent piston failure when fired into no load as may occur with simultaneous firing of two linear actuators.

Only one de Havilland plunger was used during the T1 tests. During the first single firing, the threaded end protruding through the ball lock mechanism and its nylon guide, were damaged when the plunger contacted the overlapping support arms of the General Electric tip mass catcher at the end of the plunger travel. These unnecessary overlapping support arms were cut off before the second firing to eliminate this plunger damage at the end of its travel. During the second firing (double) the damaged plunger end failed and the other two firings were conducted with no guide on this portion of the plunger. Based on these two successful tip mass releases, without the guide and the guiding prior to and within the ball lock mechanism, this back guide was eliminated. Adequacy of this guide elimination was determined during future planned vibration testing.

Only one de Havilland lever arm was used during the tests. No noticeable abnormal damage resulted from the first firing (single). During the second firing (double), the lever arm overtraveled and became wedged beneath the end of the plunger protruding from the Damper Boom Assembly.

Uncaging of the damper within the CPD released the lever arm and allowed it to return to its normal fired position. The top edge of the lever arm was damaged and the roll pins in the lever arm and its mechanical stop were bent. The other two firings were conducted with a spacer placed beneath the actuator assembly to compensate for lever arm overtravel. Redesign of the lever arm and its mechanical stop were undertaken at de Havilland. The lever arm was made longer and stronger and its mechanical stop became an integral part of the actuator housing.

At Holex no load firing tests were conducted on the redesigned linear actuator at temperatures of $-225^{\circ}F$ and $-80^{\circ}F$ at a vacuum of 10^{-5} torr in order to determine their ability to retain the pistons. Three firings were conducted at each temperature. During one of the hot test firings, the piston was not retained. The vendor (Holex) suggested the use of a 17-4 PH stainless steel piston. One such firing was successfully carried out with a stainless steel piston at high temperature.

The piston used in the test had been previously fired once. General Electric stress analysis indicated a large margin for the stainless steel piston. The no-load firing tests were repeated at high and low temperature vacuum with stainless steel pistons. All six firings were successful.

Due to the above stated problems encountered with the release system, a reliability demonstration program was instituted and conducted at General Electric.

2.2.10.2 Primary Boom

The Engineering Test Program as originally envisioned would entail testing on two Primary Boom Assemblies. The intent of this program was to verify the design, determine problems in design and demonstrate the capability of the design surviving the qualification test program.

Prior to delivery of Engineering units vendor test problems arose with the test equipment utilized in track deployment tests, clutch operation and enclosure pressurization. After delivery, electrical test equipment, deployment, clutching and vibration problems were encountered. Of all the problems encountered the vibration induced failures were by far the most difficult to overcome. The severity of the vibration problems necessitated occasional utilization of the prototype units which were being processed concurrently with the T1-B engineering unit for more representative vibration test beds.

The following is a listing of the tests performed on each of the engineering units:

T1-A (S/N 2)	T1-B (S/N 3)
Electrical	Electrical
Leak	Leak
Functional	Functional
Magnetic Dipole	PCU Compatibility
Electrical Isolation	Magnetic Dipole
Vibration	Electrical Isolation
Functional	Humidity
Vibration	Acceleration
	Thermal Vacuum
	Vibration
	Functional
	Vibration

2.2.10.2.1 T1-A Engineering Unit

T1-A was tested at de Havilland to the requirements of specification SVS-7316 and Work Statement 9770-GGEP, bought off, and shipped to General Electric on 17 September 1965. The unit was bought off with the boom lengths, scissor angle, clutch solenoid operational voltage and pressurization not conforming to the requirements.

Buy off of the pressurization "out-of-spec" conditions was on stipulation that General Electric would locate the source of leak and de Havilland would retrofit to correct leakage problems at a later date.

2.2.10.2.1.1 Pre-Environment Testing at General Electric. A complete circuit isolation, continuity and dc resistance check, conducted at General Electric prior to performance testing, disclosed a short between -5 vdc and the chassis. Trouble shooting traced the problem to damaged wire insulation at the extension potentiometer hold-down strap. Switch relocation undertaken for subsequent units eliminated repetition of this problem.

A helium "sniffer" pinpointed the pressurization leak at the center (not near any weld) of the stainless steel scissor bellows on the No. 2 erection unit side of the assembly. This

leak was attributed to handling damage since the assembly had been successfully sealed prior to teardown to correct other problems at de Havilland. Redesign for subsequent units incorporated beryllium cooper bellows instead of the stainless steel bellows.

Deployment tests were conducted with the unit mounted at the intersection of a long (150 foot) section of track and a short (10 foot) section, Figure 2-10. The tip weight of one boom (excluding target) was mounted to a trolley which travels along the 150 foot section. The other boom was connected to a special boom take-up mechanism. In this way, one boom could be fully deployed while the other boom was reeled-up by the take-up mechanism (this reducing the required total test area).

Initial deployment tests were hampered when slight missynchronization of take-up and extension motor speeds resulted in loading of the boom taps, rather than loading on the wheel borne take-up mechanism. This problem with the test equipment was overcome when the nylon wheels provided by the manufacturer were replaced with the ball bearing mounted, stainless steel wheels.

In addition to deployment and scissoring performance, other pre-environmental tests performed on the T1-A Primary Boom Assembly included a preliminary magnetic dipole test and boom electrical isolation. The dipole test indicated a well-defined dipole of approximately 152 pole-cm with tip masses removed. The skewed orientation of the dipole axis with respect to component principal axes appeared to result from the location of permeable materials in the motors, motor gearhead, clutching solenoid, and sealed drive unit. The specification limit of 80 pole-cm was not met, however, calculations indicate that a fully magnetized 0.25 x 0.25 x 0.75 inch bar magnet, suitably positioned, should reduce the net dipole to within specification limits.

The tip mass dipoles are 13 pole-cm each. The test data showed some lack of correlation about different axes. The final test fixturing for performing this test provided more accurate test data. The test was repeated on engineering unit T1-B using updating fixturing and procedure.

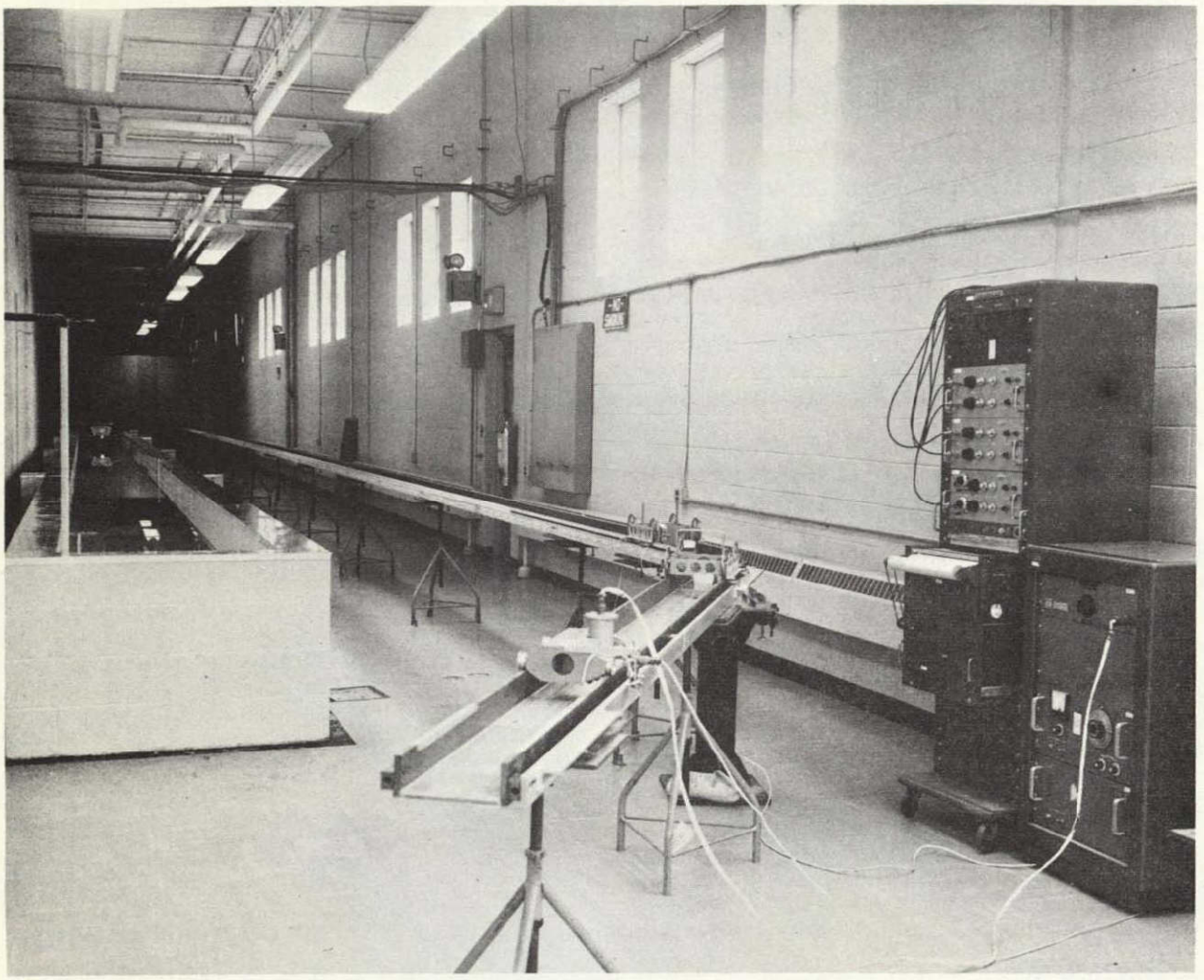

Figure 2-10. Boom Straightness Measuring Tank (left), Boom Deployment Track (right)

2.2.10.2.1.2 Vibration Testing. Vibration tests were conducted at General Electric on the T1-A Primary Boom Assembly using the C-125 shaker facility.

The component axes definition used during the tests was marked on the fixture. Due to an error in marking the fixture, this axis definition does not exactly correspond to the vehicle axes definition. Table 2-1 correlates vehicle axes to component axes definition used in this report.

Table 2-1. Primary Boom/Vehicle Axes Relationship

Component Axis	Vehicle Axis
Z-Z	Z-Z
X-X	Y-Y
Y-Y	X-X

Initial resonance search at 1.5g in the Z-Z axis resulted in the tip mass of Boom 1 becoming uncaged. Subsequent trouble-shooting pinpointed the cause at the external (to erection unit) drive gear set screws. Replacement set screws of a slot end configuration had been previously installed and were found not properly seated. This screw allowed the gear to drop out of engagement and the spool to rotate, thereby moving the boom and uncaging the tip weight. The installation of the proper allen-head set screws retained these gears in position during further resonance testing. This initial search indicated resonance for the entire unit at 175 cps and other resonances of the erection unit and tip mass at 70 cps and 500 cps.

The initial sinusoidal vibration was started in the Z-Z axis and was initiated at one-half of the qualification vibration levels (approximately three-fourths of the acceptance vibration levels). At the 5.8g level, both of the tip masses became uncaged at 39 cps. After removal of all access covers, the exact cause of uncaging was not readily discernible. However, the carbofil gears did show indications of possible rotation and vibration hammering on faces. Also, the erection unit polycarbonate housings showed signs of crazing at the mounting holes. In an effort to pinpoint the exact nature of the uncaging, resonance searches were again

conducted, but with all the access covers removed for observation with a strobotac. During the 2.5g resonance search, movement of boom tape on the spool was detected. Subsequent marking of relative positions on tapes, spools, and gears confirmed suspicions that boom stacking, and not gear rotation, was the cause of uncaging. During vibration the boom tape tends to tighten up on the spool and resultant tip plug movement is sufficient to allow the tip weight to become uncaged.

After defining the uncaging problems, resonance searches were completed in the Z-Z, X-X and Y-Y axis at 1g and 2.5g levels by artificially restraining the tip plugs from moving during vibration. Redesign efforts were initiated to make uncaging of the tip weights in future units independent of boom tape movement on the spool. Upon completion of resonance searches, normal mode performance tests were conducted and the unit was still functionally operative. Since resonance searches in all three axes revealed no problems other than those stated, sinusoidal vibration testing was undertaken with spacers placed in the tip target standoffs to restrain the tip plugs from moving during vibration.

Vibration of T1-A was conducted in the Y-Y, Z-Z and X-X axes with the following sequence in each axis:

1. 1g resonance search
2. One-half qualification level sinusoidal run (shaped spectrum)
3. 1g resonance search
4. Full qualification level sinusoidal run (shaped spectrum)
5. 1g resonance search
6. Full qualification level random run
7. 1g resonance search

Performance testing after vibration in the Y-Y axis was limited to tip weight uncaging which was satisfactory. Performance testing after vibration in the Z-Z axis was limited to tip weight uncaging and partial deployment (about 3 feet). Both operations were satisfactory, however, an inspection revealed cracks at two separate locations on each boom (at attachment to tip plug and at drum support rollers).

Performance testing after vibration in the X-X axis (after retrimming booms) was limited to uncaging, partial deployments (about 3 feet and 56 feet), and normal and standby scissoring. All operations were satisfactory, however, inspection of both booms during the 3 foot deployment revealed that Boom 2 was cracked again at the drum support rollers while Boom 1 sustained only wrinkles. Both booms showed evidence of cracking at the attachment to the tip plug.

The other partial deployment with Boom 2 on the test track trolley and Boom 1 in the take-up mechanism resulted in a dramatic boom 2 element failure. At a deployed length of 56 feet, the trolley stopped its forward motion. When power was removed from the unit, inspection revealed that the element had split from both edges diagonally toward the center at the entrance to the guide within the erection unit and had reverse wound approximately one half turn on the storage drum. Inspection after removal of erection unit 2 from the assembly revealed that the storage drum support bearings had hung up in the kidney shaped guide slot.

Inspection of the deployed portion of both booms revealed a regular pattern of creases starting at the erection unit and gradually decreasing in severity until they disappeared at approximately 20 feet away from each erection unit. The pattern could be seen developing in the guidance. These patterns suggested the possibility of a condition of unnatural deployment developing on both booms which gradually worsened as more boom was deployed. Disassembly of the unit subsequent to the above failure revealed the following:

1. The storage drums of both booms were found to be hung-up in the kidney slots in a position consistent with zero extended boom length.

2. The thin spacer under the bearing flange was found to be badly deformed in the area where it is contacted by the bearing flange.

3. A bearing stress failure of the side plate material was found in the area just under the bearing flange (in booms stowed position). Fretting corrosion was also visible in the area contacted by the spacer.

4. This bearing stress failure was found to have moved metal in a feather edge fashion into the kidney slot, thereby reducing its width. This reduction in bearing slot width was found to restrict motion of the bearing along the kidney slot, resulting in the hang-up.

Both sideplates of the disassembled erection unit (Boom 2) were found to be similarly affected. The Boom 1 drum bearings were found to be hung-up in a like manner but this unit was not completely disassembled at the time.

Since speculation existed that the reverse wind type failure experienced by Boom 2 might not be entirely due to the drum hang-up, an attempt was made to repeat the failure on Boom 1 in a manner conducive to close observation. Accordingly, the unit was set up at the test track and the drum drive gear was manually driven, after the erection unit was disconnected from the drive motor.

The results of this manual repetition of the failure are:

1. The reverse wind failure was duplicated with no unit discrepancies except drum/guidance misalignment due to kidney slot hang-up.

2. No edge damage (crack) was evident before or after test.

3. The ductile tear as in Boom 2 was not duplicated but this could be attributed to the vast difference in deployment speeds.

4. The wrinkle pattern (as in Boom 2) was found on the deployed position of the boom but not on the undeployed portion, indicating that misalignment between drum and guidance caused the wrinkling.

It was therefore concluded that the kidney slot hang-up (and resultant misalignment) was the problem to be attacked in precluding the reverse-wind failure. The redesign for this condition provided a much larger bearing area under the flange.

Concurrence on the resolution of the four vibration induced problem areas resulted in the submittal of detailed drawings by de Havilland for rework of T1-A parts.

2.2.10.2.1.3 Retrofit. A retrofit kit was received by General Electric from de Havilland, and installed in the T1-A unit during January 1966. Functional performance tests were conducted to ensure the adequacy of the retrofit.

The bearing hang-up in the kidney slot and element cracking at the attachment to the tip plug were eliminated by the retrofit. However, tip weight uncaging and element cracking at the drum support rollers remained problems. The testing that was done to confirm these results is discussed in the following paragraphs.

After the satisfactory completion of the following post retrofit functional performance tests, T1-A was rescheduled for vibration testing.

T1-A performance tests were conducted early in January 1966. Normal mode deployment on erection unit No. 2 (with modifications and fixes) performed at low voltage to determine lowest operating voltages for extension and retraction (12.7 vdc required for extension and 15.7 vdc required for retraction). Normal mode scissoring, emergency mode operation and mode alternation were satisfactory. Misalignment of the storage drum and guidance in erection unit No. 1 limited deployments to manual. This was considered satisfactory to verify recurrences of previous vibration failures (this erection unit was unmodified). The tip masses were latched into the unit and the erection unit covers were bonded on prior to vibration testing.

A 3-axis vibration was completed early in February 1966 to qualification levels in both sinusoidal and random, with one manual deployment on the test track after the first (ZZ) axis. The manual deployment tentatively verified that the element had not cracked at either tip plug attachment point or the drum support rollers and also that full deployment could be accomplished without bearing hangup in the kidney slot. Unfortunately the tip mass unlatching still occurred, but only during random testing, signifying that although the latching cable

was an improvement it still was not quite adequate. Observations during vibration showed that partial drive gear rotation (about 2-3 degrees) occurred during sinusoidal, and an equal or greater amount occurred during random. The maximum amount of gear rotation observed was about 15-21 degrees which occurred during random in the axis parallel to the boom axis.

Discussions at General Electric on the element cracking at the drum support rollers experienced on T1-A resulted in a number of approaches for attempts at resolution of the cracking. The first attempt at revibration with modifications incorporated into the erection units convinced personnel involved that considerable teardowns and modifications were required before this particular assembly would be fit to continue revibration for investigation of cracking problem.

Continued vibration of T1-A still resulted in tip mass unlatching despite manual removal of all back lash in the transmission unit. Marking of gears and subsequent inspection showed that drive train rotation occurred all the way back to the spiroid gear adjacent to the extension motor output. Complete snubbing of the kidney slot was accomplished, but element cracking still occurred at the drum support rollers.

High speed motion pictures were taken of the boom element motion during vibration of a hard mounted primary boom erection unit from the T1-A as an aid for studying the mechanism of failure associated with the element cracking in the area between the storage drum and the guidance. The films were studied and together with on-the-spot observation of the component under test resulted in a set of fixes to be incorporated on the erection unit. These fixes were incorporated and vibration tested on the hard mounted erection unit.

The results of this hard mount testing led to the incorporation of the most promising fixes in the complete T1-A component and further vibration testing.

The transmission unit was removed from the T1-A Primary Boom package and mounted in a special fixture to permit vibration of the transmission unit alone. The vibration testing was accomplished while a torque was externally applied to represent erection unit loading. Special

viewing ports were machined into the side of the transmission unit to allow direct observation of the spiroid gear set and the remainder of the extension drive train. Excessive spiroid pinion (motor shaft) rotation was noted at 260 and 400 cps, both with and without external torque applied. This rotation indicated that the motor brake was not effective in these ranges. In these same frequency ranges, the motor and its mount were observed to be responding excessively in a cantilever mode. When the brake end of the motor was manually restrained the rotation stopped at 260 cps and reversed itself at 400 cps.

Vibration tests were re-run on the transmission unit under the same conditions as the first test, but this time the armature leads of the erection motor were shorted. Motor rotation occurred again as in the first test while the unit was undergoing vibration. The transmission unit was repositioned and vibrated along the motor axis to qualification level (9.2 g rms). Motor shaft rotation was also observed during this test. These vibration tests showed that the erection motor brake was ineffective at 260 and 400 cps causing shaft rotation and tip mass unlatching.

The transmission housing for units subsequent to T1-A are of a design that is somewhat stiffer than T1-A in that the housing is machined out of two basic parts rather than the assembly of several parts that exist in T1-A. It was at first hoped that this stiff box would alleviate the vibration problem observed with the T1-A transmission. Accordingly, a series of vibration tests were undertaken with the stiff transmission box.

The stiff transmission box with motors and the applicable portions of the gear train, was obtained from de Havilland and the unit was vibrated along the axis parallel to the extension motor axis, which is the worst axis from the standpoint of the brake based on results of the T1-A unstiff box. Both random and sinusoidal vibration were applied. Although shaft rotation occurred, the rate of rotation was reduced significantly over the unstiff design. Motor shaft rotation throughout a complete random cycle only resulted in about four turns of the motor shaft. This, however, would result in about ten degrees of rotation of the erection unit drive gear, thus releasing the latching cable. Response to any particular sinusoidal

frequency was eliminated in the stiff box design. The application of power to the motor field while the armature was shorted did not significantly reduce rotation during random vibration.

These tests indicated the possibility of successful tip mass caging with the removal of a brake plate positioning spring. A meeting with the motor supplier (Globe Industries) and de Havilland on the topic revealed certain differences between the motors used in the engineering equipment and the prototype (Suprel) motors which could alter brake performance. Accordingly, Globe shipped two Suprel motors to General Electric for vibration testing. However, vibration testing of the Suprel motors on the stiff transmission box also resulted in motor shaft rotation.

Additional tests were performed on the stiff box configuration in an effort to eliminate the problem of motor shaft rotation. Tests were conducted with the spiroid gear eliminated, and using a coarse surface on the surface of the brake, both tests had negligible effect in reducing shaft rotation.

The T1-A component was vibrated with the clutch in the standby mode, thereby allowing the large gear reduction ratio of the scissor motor to act as a brake on the extension drive train. This technique resulted in successful retention of the tip masses during vibration. This technique appeared to be the solution to the tip mass uncaging problem due to motor rotation.

2.2.10.2.2 T1-B Primary Boom Unit

The T1-B Primary Boom Engineering unit (1/2 system) was delivered to General Electric from de Havilland on March 19, 1966. The transmission unit had been sealed to permit thermal vacuum testing. The unit did not incorporate any vibration fixes, but extension motor stiffener, needle bearing, clutch and solenoid helper spring were included.

2.2.10.2.2.1 Pre-environment Testing at General Electric. T1-B was electrically and functionally tested in accordance with the established procedures for engineering evaluation. The Primary Boom test console was used in place of the Power Control Unit to provide power. The functional tests included switching to emergency mode, scissoring, clutching and a leak test. Although the leak test showed a leak rate of about 3×10^{-6} cfm, results of all the functional tests were satisfactory.

A compatibility check was then performed with the T1-B and the PCU. All functions of the boom package were successfully exercised by the PCU with the exception of full extension to the unit switch. This procedure resulted in a jamming of the brake lever arm in the drum spool and prevented subsequent boom retraction. The problem was traced to the fact that the PCU internally jumpers-out the boom system switches which cutt off the field and brake. This condition was artificially simulated using an auxiliary power supply, and the same jam-up occurred. The brake lever arm was identified as the item that was jammed, and manual release of this arm resulted in proper retraction. The problem was identified as the motor brake not being allowed to act when the full extension microswitches are activated and the inertia of the drive train acting on the drum spool brake lever arm.

2.2.10.2.2.2 Environmental Testing. The primary purpose of T1-B was as a thermal vacuum test bed, and later as a vibration test bed, after the completion of the temperature test series. As delivered to General Electric, the transmission unit of T1-B was sealed with a pressure of 7 psia internal to the transmission. This unit was the first one delivered that was pressurized and sealed, T1-A was not sealed when delivered.

T1-B was tested in the 8 by 10 foot thermal vacuum chamber at temperatures of 0° and 140°F. One series of tests included uncaging at the two temperature extremes in both the normal and standby modes. Another series of tests was run to simulate the boom functions in orbit after uncaging. As a condition for these latter tests, the tip masses were removed and the unit was exposed to high and low temperature soak, then the booms were extended, retracted and scissored in both modes. These tests were all successfully performed, no degradation of the hermetic sealed unit was observed.

Tip mass uncaging resulted from stacking the element on the drum during vibration. Essentially the element became more tightly wound on the drum and this tightening resulted in enough movement of the tip plug so that the caging springs were disengaged from the locking grooves within the tip weights, thus releasing the tip masses. The basic problem was that tip weight uncaging is directly dependent upon boom element movement. One modification thereafter incorporated included a flexible latching cable with ensured that tip weight uncaging would be independent of element movement due to stacking.

The flexible cable was inserted into the unit through the end of the tip weight and guided to a special worm gear attached to the internal polycarbofil drum drive gear. Engagement was accomplished by screwing the cable into engagement with the special gear and locking in place. Disengagement occurs only with rotation of the drum drive gear.

Other methods for solving the tip mass uncaging during vibration which included launch in standby mode and a negative spring concept, were evaluated. These methods attempted to solve the uncaging difficulty while preserving the clutching function wich provides a backup in the event of a drive motor failure. However, the approach that finally solved the problem involved retention of the gear train during launch vibration but it excluded emergency mode operations.

One of the techniques employed to prevent extension drive train rotation was to clutch from the extension drive train to the scissor motor (standby mode). The 3000 to 1 gear ratio of the scissor motor gear head would thus act as a motor brake and retain the extension drive train during launch environment. This configuration was implemented on T1-B, and this caging scheme was pursued through extensive engineering evaluation beginning in April 1966. T1-B was subjected to vibration testing in a standby mode in an attempt to prove that the tip masses would remain caged with the scissor motor holding the extension motor drive train. The tip masses did uncage, however, due to clutch slippage. T1-B was also vibrated in normal mode and the same slippage was observed. T1-B was returned to de Havilland for their investigation of clutch slippage. The unit had been subjected to some damage which caused rounding of the clutch teeth, in addition, one of the gears in

the extension drive train was stripped. T1-B was then abandoned as a test bed for evaluation of this caging scheme, and Prototype P2-b was used in succeeding tests. P2-b was vibrated in the standby mode at General Electric, but it failed to remain caged. Further testing was stopped because NASA required P2-b at HAC for vibration testing on the dynamic vehicle. The component was rigged to artificially constrain the tip masses against unlatching during vibration, and it was sent to HAC on 7 June 1966.

A method of caging the primary booms which utilizes a detent in a manner similar to a ratchet to hold the extension gear train during vibration was suggested by de Havilland. The deployment sequence would require the booms to be retracted for about one half inch to release the detent before the booms could be deployed. De Havilland chose to use the T1-B engineering unit as a test bed for evaluation of their design.

In the negative spring approach to the uncaging problem, the spring that normally pushes the tip plugs toward the uncaged position was reversed so its force would be exercised toward the caged position. The negative spring thus assisted in retaining the tip masses while in the caged position, the force was transmitted through the boom element to the tip plugs. However, the force exerted by each spring would have to be overcome by the extension motor upon deployment in orbit. The first series of tests of the negative spring caging approach resulted in failure because of slippage of the latching cable with respect to the drum drive gear. The depth of engagement was too small to be tolerant of movement between the mating worm gear and the erection unit gear.

These gears were redesigned to provide approximately twice the depth of engagement. Tests were performed using a 7/10 of a pound per inch spring at zero pre-load which resulted in successful endurance of qualification vibration levels and successful deployment upon command. Because of the extremely small margin between uncaging force deliverable after vibration and caging force required during vibration, the lighter spring was replaced by a 1-1/2 pound spring at zero pre-load. This modification also incorporated a teleflex cable to increase the compressive force delivered from the drum drive gear to the tip plug over that provided by the boom tape. The teleflex cable replaced the former

latching cable which proved to be incapable of transmitting sufficient compressive force to the tip plug. Although tests proved this method to be feasible, both NASA and General Electric felt that the available uncaging force was to be used as a reliable method for uncaging. Therefore, NASA directed the implementation of a positive caging method that would utilize pyrotechnic devices to uncage the tip masses.

The pyrotechnic gear holder caging method prevents the extension drive train immediately external to the erection unit from rotating during launch vibration environment. In addition, since the clutch is pinned in the normal mode, commands which had formerly been designated for interchanging extension and scissor motors and returning them to normal mode are now available for firing the squibs on the gear holder to initiate primary boom deployment. The pyrotechnics involved were identical to the linear actuator design used for initiation of damper boom deployment. As used in the primary boom uncaging sequence, the linear actuator thrusts against a lever assembly which rotates the locking arm out of mesh with the teeth on a gear in the extension drive train. Since the clutching function was abandoned, no additional squib driver circuits were required. In the course of analyzing this caging method, two other methods were considered either of which could have preserved all existing functions. However, because of the difficulties experienced in mechanizing the clutch, NASA directed the use of the former clutch commands to fire the uncaging squibs and further investigation of the clutch difficulties became non sequetor. The squib circuitry had some range safety ramifications for the reasons that:

1. The squib fire commands were transmitted through a connector that also carries other power and signal leads.

2. The clutch solenoid driver circuits in the PCU were not standard squib driver circuits, and attendant protective drives were not available.

NASA obtained a waiver to operate the uncaging squibs in this manner, since the payload power switch through which all boom system power is directed will be in the open position when the vehicle is in the launch mode, and the system is thus protected from spurious signals.

The gear holder design had been successfully tested at General Electric. Engineering and prototype units were modified to incorporate the caging method with the results as presented in Table 2-2.

Table 2-2. Gear Holder Evaluation

Primary Boom Unit	Vibration Test	Post Vibration Results
T1-B	Qualification Level	Unit modified with bread-board model of gear holder design. Success-fully deployed.*
P2-A	Qualification Level	Successfully deployed
P2-B	Acceptance Level	Successfully deployed

* Successful deployment is considered to be boom extension to a distance of 1 foot.

The circuits in the PCU which were formerly designated "Rod Assembly Normal Mode" and "Rod Assembly Standby Mode Clutch Solenoid Drivers" are now designated Primary Boom Squib Drivers and used to apply firing power to the squibs in the caging assembly. These circuits became available because of the decision to pin the clutches and not use the solenoid drivers.

Retrofits were completed at General Electric on T1-B and the causes for element cracking were eliminated as previously described for T1-A.

The success of these modifications was further demonstrated as evidenced from the results of the many vibration tests that were performed in connection with the investigation of the tip mass uncaging problem.

Clutching was originally included in the primary boom design to enable either the extension motor or the scissor motor to drive the opposite function in case one of the motors should fail while in orbit. In normal mode, each motor would perform its designated function. In

emergency mode, however, the extension motor or scissor motor could perform the other task through the action of a clutch that interchanged the gear trains. Four commands were assigned by NASA to permit clutching on ground command. However, several problems became evident in an attempt to implement the hardware. At one point, a problem existed because the clutch could not be disengaged in the normal mode at the extremes of scissor angle. The clutch was redesigned, the most significant difference being a reduction in the height of the clutch teeth which in turn reduced the stroke requirements of the clutch solenoid. These changes were incorporated into both prototype units. When the modification was evaluated, the most repetitive problem was that the clutch continued to jump out of mesh at the extremes of scissor angle (where loads are the highest). Several modifications of this design were attempted, but the clutch never performed to the satisfaction of NASA or General Electric.

It was concluded that instead of increasing reliability, the normal mode operation was being compromised because of the difficulties encountered with the clutch mechanisms. It was agreed jointly by NASA and General Electric to eliminate the backup mode. The clutches were de-activated and parts such as the solenoid and the solenoid force transmission linkage were removed.

The booms are now operated only in the normal mode wherein the extension motor drives the extension drive train and the scissor motor drives the scissor drive train.

Prototype units P2-a and P2-b were modified for normal mode operation before they were shipped to HAC. The clutch in both units was mechanically constrained to stay in mesh in the normal mode. This modification was accomplished at General Electric on T1-B during the vibration tests involving a breadboard pyrotechnic gear holding mechanism.

Subsequent retrofit of T1-B to the ATS-D/E configuration tip masses was accomplished at General Electric after completion of the ATS-A qualification program and launching of the ATS-A Flight Spacecraft. Initial vibration testing of T1-B in this configuration resulted in both tip masses coming uncaged. Retrofit of the prototype qualification unit to ATS-D/E was in process at the time of the T1-B uncaging failure so use of T1-B as a further vibration test bed was discontinued.

Basically the ATS-D/E vibration problems encountered and solved during the qualification program were tip mass uncaging and latching spring cracking. Resolution of the cracking failure was attained by reconfiguring and stiffening the spring plate assembly and latching springs. The uncaging failure resulted from excessive movement of the latching spring locking insert within the tip weight during vibration and was corrected by addition of shimming to minimize insert movement during vibration.

2.2.11 DAMPER BOOM DIGITATION PROGRAM

The boom subsystem of the ATS-E spacecraft consists of three separate packages containing gravity-gradient booms. The two primary packages each contain two rod erection devices coupled to a mechanism for extending and scissoring the two primary booms. The third package contains two secondary rod erection units (tip masses) attached to a structural center body and includes a separate housing containing the explosive portion of the tip mass release system.

The boom digitation program reported herein pertains only to refurbishment of the third package specifically for use on ATS-E boom subsystem (SVS-7563 in Appendix 2A contains modification requirements). The third package is known as a Damper Boom Assembly. Refurbishment of the ATS-E damper booms with edge-interlocking digitations was submitted to the NASA-Goddard Space Flight Center in proposal No. F-20423, dated January 17, 1969.

The objective of the boom digitation is an improvement in the torsional stiffness of the deployed damper booms and a consequent reduction in the concern over postulations of damper boom thermal flutter.

The basic extendible boom selected for this mission was the storable tubular extendible member (STEM) developed by SPAR Division of de Havilland Aircraft of Canada, Ltd. (now SPAR Aerospace Products, Ltd.). This technique involves the formation of a tubular section from a flat metal strip which is formed and heat-treated in the tubular form, then flattened under stress and wound onto a storage drum. Subsequent erection in orbit is accomplished by paying out the stowed strip through a set of guides which allow

the boom to form into its natural tubular shape. The edge-interlocking version of the basic STEM allows the edges of the metal strip to interdigitate while overlapping each other thereby increasing the stiffness of the operating section. The self-erecting damper booms utilize the strain energy in the stowed metal strip to rotate the storage drum and erect the boom.

2.2.11.1 Design Details

2.2.11.1.1 Erectable Booms

The basic erectable booms utilized for the ATS-E damper boom digitation are flat beryllium copper elements two inches wide and 0.002 inch thick. Previously the elements were heat treated into an overlapped, right circular cylinder about their longitudinal axis such that their natural stress free condition was an overlapped tube, .500 inch in diameter. Originally the intended usage for these particular elements was in the Primary Boom Assemblies.

Interlocking teeth were cut, by electrical discharge (ELOX) machining, on the edges of the boom element over 43 of the 45 feet extended length. These interlocking teeth were centrally located on the boom in equally spaced groups. Each digitation group covered a span of 2 inches which is shorter than the shortest element wrap circumference at the storage drum core. The digitation groups were separated from each other by a span of smooth unbroken edge of 13.5 inches which is longer than the longest element wrap circumference at the storage drum outside circumference. Digitation details are shown on GE drawing 47E217400.

Accordingly, when the digitated booms are stowed on the storage drums, the tips of the interlocking teeth are sandwiched between layers of smooth-edged element which carry the loads imposed by the drum cheeks. These loads result from element inertia during dynamic environments and from side cheek preload. Upon deployment the interlocking teeth, which are pre-formed for proper engagement, engage each other and are held in engagement by the forming stresses in the element.

2.2.11.1.2 Erection Units

The basic erection units (tip masses) utilized for the ATS-E digitated damper booms are as configured when shipped to Hughes Aircraft Company in October 1968. The sole change incorporated into each erection unit was a new roller assembly. This was in addition to the existing roller assembly.

The edge-interlock concept feasibility was demonstrated in August 1968 through development of a demonstration erection unit from a Prototype Damper Boom Assembly. Testing of an entire unit, however, necessitated further unanticipated development activity. The above roller assembly resulted from this further development activity, as well as significant digitated element and associated tooling configuration improvements.

2.2.11.2 Test Program, Digitated Damper Boom

2.2.11.2.1 Background

The entire six-week Damper Boom Digitation Test Program, as originally envisioned, would entail fabrication of five 45-foot edge-interlocked elements and one short-length, flight-quality, edge-interlocked specimen. Incorporation of the digitated booms would involve retrofit plus Engineering/Qualification testing on one Prototype Damper Boom Assembly, and retrofit plus Acceptance testing on one Flight Damper Boom Assembly. The intent of the Prototype program was to determine the effects of tooth forming on straightness and deployment rates, and demonstrate the capability of the digitated boom surviving storage and the Qualification vibration environment.

In the interests of expediting the program, electroexplosive releases were eliminated from the deployment tests in favor of manual ball lock release, and installation pinning of the plunger was eliminated for vibration tests. Justification for these two actions was that the basic Damper Boom package was fully qualified (Qualification Test Report 4315-QC-031) and the reliability of the release system was adequately demonstrated (GE Report 41M3-001). As stated above, qualification of the digitated booms was the prime consideration and these eliminations in no way compromised the validity of the test program for this purpose.

2.2.11.2.2 Test History

The test history of the entire digitated damper boom program is presented in Appendix 2A. Review of this history shows that the previously mentioned unanticipated development activity involved considerably more than the originally envisioned number of edge-interlocked elements.

Following is a list of the tests performed on the Prototype and Flight units during the Qualification and Acceptance Test cycles, respectively:

Prototype S/N 11		Flight S/N 101	
Pre Digitation	- Hardness - Bending - Torsion - Straightness - Deployment	Pre Digitation	- Deployment
Post Digitation	- Bending - Torsion - Straightness - Deployment - Vibration (Sine and Random) - Deployment - Storage - Deployment	Post Digitation	- Deployment - Vibration (Random) - Deployment - Adhesion - Reflectivity

The results of the Prototype Test Program are discussed in Section 2.2.12.3.

2.2.11.2.3 Test Results

2.2.11.2.3.1 Hardness. To alleviate concern about the possibility of the flight boom element being softer than expected, a series of hardness tests were conducted by Space Science Laboratory Materials personnel, after consultations with their counterparts at NASA. These tests involved boom samples from both plated and unplated full-length elements utilized during the digitation program. Results reported in Table 2A-1 of Appendix 2A are indicated in Diamond Pyramid Hardness Numbers (DPN). Conversion to Rockwell C has not been made

due to possible variations in conversions resulting in conflicting Rc numbers. In general, the results confirm that the hardness of the flight elements is as anticipated.

2.2.11.2.3.2 Bending/Torsion. A series of bending and torsion tests were conducted to determine the degree of improvement in the torsional stiffness of the deployed damper booms. These tests involved pre- and post-digitated boom samples. An increase in torsional stiffness by two orders of magnitude to preclude thermal flutter, as discussed in PIR 1450-ATS-004, was the desired test result.

2.2.11.2.3.3 Straightness. Pre-and post-digitation engineering type straightness tests were conducted to determine the effects of tooth forming on the straightness profile. The pre and post profiles are shown in Figure 2A-1 of Appendix 2A. The digitation process resulted in an overlap different from that used in the pre-digitation straightness test and the profiles are therefore not directly related. However, the resulting profile differences are not too different from those experienced throughout the ATS program on both primary and damper overlapped booms.

2.2.11.2.3.4 Deployment. In conjunction with the previously mentioned hardware configuration changes, the following test equipment modifications were required to achieve satisfactory deployment test results with a Damper Boom Assembly containing digitated boom elements:

1. Rewind. Motorized rewind eliminated in favor of manual rewind. Excessive rewind speed caused degradation of edge-interlocking teeth.

2. Tip Mass Oscillation Dampers. Oscillation damper eliminated on tip mass No. 1. Tip mass unable to attain necessary angle fast enough after release and resulted in failure to attain full deployment. During deployment, tip mass No. 2 rotates in a direction which does not compress the damping fluid while tip mass No. 1 rotates in the direction of fluid compression. Thus, tip mass No. 2 is able to attain the desired angle more rapidly than tip mass No. 1.

3. Tip Mass Counterbalance Weights. Repositioned weights on counterbalance arms. Improper tip mass balance caused excessive boom degradation during deployment.

4. Boom Support. Boom No. 1 support provided at track top level during deployment and boom No. 2 support provided on track bottom during deployment. Excessive sag of the booms onto bottom of test track prevented proper interdigitation of edge-locking teeth.

Considering deployment of one tip mass as one deployment test, there was a total of 35 deployments on digitated boom elements during the entire program, of which only 13 can be considered as successful full deployments. Six full deployments were attempted with the flight configuration roller boom combination and all were successful.

Pre- and post-vibration deployments on both the Prototype and Flight units showed no deployment anomalies or degradation in the deployment rates with the flight configuration roller/digitated boom combination. The Prototype deployment rates were 2.4 ft/sec as compared to 1.9 ft/sec and 2.0 ft/sec on the Boom Serial Flight Unit with overlapped booms prior to shipment to HAC in October 1968. (Reference Report No. 1315-050 Amendment A dated 10/25/68.) The 10 percent increase from the Prototype to Flight rates with digitated booms is undoubtedly due to cleaning of flight bearings and brakes. The 25 percent increase of rates indicated in the flight unit when digitated booms are installed rather than overlapped booms results from the increase in inherent strain energy in the smaller (.500 dia) digitated boom over the larger (.560 dia) overlapped boom. With the present digitation configuration the boom diameter when deployed is approximately midway (.530 to .540) between the above basic diameters.

2.2.11.2.3.5 Vibration. Neither Qualification nor Acceptance vibration to the levels indicated in Specification SVS-7563 resulted in degradation of the edge-interlocking booms.

2.2.11.2.3.6 Storage. After completion of the post vibration deployment, the Prototype unit was placed in storage. The prototype post storage deployment test was planned for approximately six weeks prior to launch (mid August 1969) when the flight spacecraft was scheduled to be at NASA-Goddard Space Flight Center.

2.2.12 SUMMARY AND CONCLUSIONS OF DEVELOPMENT PROGRAM

The boom system engineering units were subjected to a very complete and comprehensive test program. The test program was in some instances carried out in parallel with both the qualification and flight testing programs. This situation occurred because marginal performance conditions which passed on the engineering units (and were not evident as

being marginal) failed on either the qualification or the flight units and overcoming the vibration-induced failures required an inordinately long period of extensive testing.

In general the engineering test program was considered very successful even though many difficulties and failures were encountered, it is evident that it did uncover a majority of design, manufacturing, test and workmanship problems that could in most cases be corrected on prime hardware.

2.2.12.1 Damper Boom

As a result of the centerbody diamagnetic suspension test, it was concluded that the magnetic forces due to magnetic materials in the Damper Boom centerbody should have no significant effect on the CPD after the tip masses were deployed.

The adequacy of the Avdel ball lock and Holex linear actuator combination for accomplishing the release of the tip masses has been proven by the functional tests on the T1 Damper Boom Assembly and the release system reliability demonstration program.

2.2.12.2 Primary Boom

The T1-A Primary Boom Assembly performed satisfactorily at General Electric at ambient conditions with regard to tip mass release, boom extension and retraction rates, scissor rates, repeatability of boom extension and retraction positions, telemetry functions, and standby mode operation. Deficiencies found in the unit with respect to its ability to endure the qualification vibration environment necessitated an extensive redesign effort. The results of this redesign effort were incorporated and tested on T1-B and refinements were incorporated into the prototype and flight units until the present qualified configurations emerged.

It was not fully realized during the engineering test program, but as prototype testing highlighted dramatically, mechanical redundancy, as was attempted with the standby mode of operation, it would be almost impossible to attain without greatly sacrificing reliability of normal functioning.

It was evident from the engineering testing that the original specification requirements could not be fully met. Subsequent prototype and flight unit testing resulted in requirement alterations which the finalized design could readily attain. However, the severity of the qualification environments was not relaxed as a prerequisite for satisfactory completion of the qualification program.

2.2.12.3 Digitated Boom Retrofit

The Prototype and Flight Damper Boom Assemblies retrofitted with digitated booms were subjected to test programs adequate enough to qualify the edge-interlocking concept and verify the flight worthiness of the prime ATS-E Damper Boom Assembly.

In general the Engineering Developmental Testing performed on the Prototype unit was considered successful even though many difficulties and failures were encountered. It is evident that it did uncover a majority of design and test problems that could have been overcome earlier if the original feasibility demonstration had been more representative.

Taking all aspects of the Engineering, Prototype and Flight testing of the digitated damper booms into consideration, it was the opinion of the cognizant QC engineer that no qualms should occur about the flight worthiness of the ATS-E prime unit with the finalized roller/boom configurations installed.

The one concern on this particular unit expressed by the GE Audit Team, in October 1968, in Report 68SD-4346, has been eliminated. This concern was on overtorquing of the storage drum. No such anomaly occurred during preparation of the unit for shipment with the digitated booms installed. Therefore, the Audit Team conclusion that "there is no indication that Boom Assembly Serial No. 101 represents more risk than previous flights" is still valid even with the digitated booms.

2.3 QUALIFICATION TESTS, PRIMARY BOOM

Two prototype Boom System packages (designated as component and system qual) were subjected to similar environments at more severe levels than the anticipated operating environments in order to establish confidence that the design was valid under extreme operating conditions. Following tests, the component qual unit was not further dispositioned, but the system qual unit was included in the spacecraft qualification tests conducted by the vehicle contractor following the GE tests. A summary of these environments and references to the appropriate test reports are listed below. These documents are on file at GE and will be made available on request of the Contract Administrator for NASA programs.

2.3.1 COMPONENT QUALIFICATION, PRIMARY BOOM

Serial No.:	100			
Part No.:	47J209567			
Test Report:	4315-QC-027	(8/02/67)		
Failure Analysis Reports:	311-E-51	(7/13/67)	225-E-16	(8/18/66)
	316-E-52	(7/26/67)	264-E-30	(10/9/66)
	319-E-53	(8/17/67)	295-E-45	(3/24/67)
	224-E-15	(8/18/66)		

Test Sequence

1. Visual and Mechanical Inspection
2. Circuit Isolation and DC Resistance
3. Isolation Resistance
4. Dielectric Strength
5. Electrical Isolation
6. Scissoring
7. Extension and Retraction
8. Leak Test
9. Humidity
10. Circuit Isolation and DC Resistance
11. Vibration
12. Circuit Isolation and DC Resistance
13. Acceleration
14. Circuit Isolation and DC Resistance
15. Thermal Vacuum
16. Magnetic Dipole
17. Leak Test
18. Circuit Isolation and DC Resistance
19. Insulation Resistance
20. Dielectric Strength
21. Electrical Isolation
22. Scissoring
23. Extension and Retraction
24. Straightness and Alignment

2.3.2 SYSTEM QUALIFICATION, PRIMARY BOOM

Serial No.:	12	
Part No.:	47J209567	
Test Report:	4315-QC-016	(10/14/66)
Failure Analysis Report:	292-E-43	(03/20/66)

Test Sequence

1. Circuit Isolation and DC Resistance
2. Insulation Resistance
3. Dielectric Strength
4. Scissoring
5. Extension and Retraction
6. Vibration
7. Extension and Retraction
8. Scissoring
9. Circuit Isolation and DC Resistance
10. Leak Test
11. Vibration
12. Leak Test
13. Circuit Isolation and DC Resistance
14. Extension and Retraction
15. Scissoring
16. Magnetic Dipole
17. Insulation Resistance
18. Dielectric Strength

Serial No.:	11	
Part No.:	47J209567	
Test Report:	4315-QC-01	(10/5/66)
Failure Analysis Reports:	212-E-11	(8/2/66)
	183-E-2	(5/10/66)
	223-E-14	(8/18/66)
	300-E-5	(5/4/67)

Test Sequence

1. Visual and Mechanical Inspection
2. Circuit Isolation and DC Resistance
3. Insulation Resistance
4. Dielectric Strength
5. Electrical Isolation
6. Scissoring
7. Extension and Retraction
8. Leak Test
9. Vibration
10. Circuit Isolation and DC Resistance
11. Thermal Vacuum
12. Magnetic Dipole
13. Leak Test
14. Circuit Isolation and DC Resistance
15. Insulation Resistance
16. Dielectric Strength
17. Electrical Isolation
18. Scissoring
19. Extension and Retraction
20. Straightness and Alignment

2.4 FLIGHT ACCEPTANCE, PRIMARY BOOM

Each of the Boom System flight units were exposed to vibration and thermal-vacuum environments at levels anticipated during flight to verify that the design had not degraded during manufacture. A summary of these environments and references to the applicable test reports are listed below. These documents are on file at GE and will be made available on request of the Contract Administrator for NASA programs.

2.4.1 ATS-A

Serial No.:	101	
Part No.:	47J209566	
Test Report:	4315-QC-022	(2/13/67)
Failure Analysis Report:	247-E-23	(10/7/66)
	255-E-26	(10/10/66)
	266-E-31	(11/15/66)

Test Sequence

1. Visual and Mechanical Inspection
2. Circuit Isolation and DC Resistance
3. Insulation Resistance
4. Scissoring
5. Extension and Retraction
6. Leak Test
7. Vibration
8. Circuit Isolation and DC Resistance
9. Thermal Vacuum
10. Magnetic Dipole
11. Thermal Vacuum
12. Circuit Isolation and DC Resistance
13. Insulation Resistance
14. Electrical Isolation
15. Magnetic Dipole
16. Leak Test
17. Circuit Isolation and DC Resistance
18. Performance
19. Vibration
20. Circuit Isolation and DC Resistance
21. Performance
22. Thermal Vacuum
23. Extension and Retraction
24. Straightness and Alignment
25. Leak Test

Serial No.: 102
Part No.: 47J209567
Test Report: 4315-QC-023 (2/21/67)

Test Sequence

1. Visual and Mechanical Inspection
2. Continuity and DC Resistance
3. Insulation Resistance
4. Electrical Isolation
5. Scissoring
6. Extention and Retraction
7. Leak Test
8. Vibration
9. Thermal Vacuum
10. Magnetic Dipole
11. Alignment and Straightness

2.4.2 ATS-D

Serial No.: 104 and 105
Part No.: 47J209567
Test Report: 039 (9/28/67)
Failure Analysis Reports: 320-E-54 (8/17/67)
321-E-55 (9/14/67)
322-E-56 (9/27/67)

Test Sequence

	Test	Serial No. Tested
1.	Visual and Mechanical Inspection	105
2.	Circuit Isolation and DC Resistance	105
3.	Insulation Resistance	105
4.	Uncaging	105
5.	Scissoring	105
6.	Visual and Mechanical Inspection	104
7.	Circuit Isolation and DC Resistance	104
8.	Insulation Resistance	104
9.	Uncaging	104
10.	Scissoring	104
11.	Extension and Retraction	104
12.	Extension and Retraction	105
13.	Caging	104
14.	Vibration	104
15.	Caging	105
16.	Circuit Isolation and DC Resistance	104
17.	Thermal Vacuum	104
18.	Uncaging	104
19.	Vibration	104
20.	Circuit Isolation and DC Resistance	104
21.	Thermal Vacuum	104
22.	Vibration	105
23.	Circuit Isolation and DC Resistance	105
24.	Circuit Isolation and DC Resistance	104

	Test	Serial No. Tested		Test	Serial No. Tested
25.	Insulation Resistance	104	35.	Straightness and Alignment	105
26.	Scissoring	104	36.	Extension and Retraction	105
27.	Electrical Isolation	104	37.	Straightness and Alignment	104
28.	Thermal Vacuum	105	38.	Straightness and Alignment	105
29.	Circuit Isolation and DC Resistance	105	39.	Leak Test	104
			40.	Leak Test	105
30.	Isolation Resistance	105	41.	Straightness and Alignment	105
31.	Electrical Isolation	105	42.	Caging	104
32.	Straightness and Alignment	104	43.	Weight and Center of Gravity	104
33.	Scissoring	105	44.	Caging	105
34.	Extension and Retraction	104	45.	Weight and Center of Gravity	105

2.4.3 ATS-E

Serial No.:	10	
Test Reports:	1315-QC-005	(10/25/68)
	PIR 1315-QCE-147	(11/5/68)
Failure Analysis Reports:	249-E-25	(10/7/66)
	256-E-27	(10/17/66)
	268-E-32	(10/17/66)
	269-E-33	(12/12/66)
	277-E-37	(12/13/66)
	382-E-59	(1/3/69)

Test Sequence

1. Performance
2. Extension and Retraction
3. Leak Test
4. Uncaging
5. Vibration
6. Thermal Vacuum
7. Uncaging
8. Post Environmental Functional
9. Extension and Retraction (unit was reworked after failure to retract)
10. Preliminary Acceptance after rework
11. Vibration (interference between polycarbofil gear and housing at minimum scissor angle; housing was replaced)
12. Uncaging (following series of design changes)
13. Extension and Retraction (Unit stalled during retraction due to excessive drive train loading. Unit was refabricated and changed to ATS D/E configuration.
14. Environmental Functional

Serial No.:	103	
Test Reports:	1315-QC-005	(11/5/68)
	PIR 1315-QC-145	
Failure Analysis Reports:	389-E-60	(10/24/68)
	299-E-49	(4/4/67)
	331-E-57	(12/12/67)

Test Sequence

1. Visual and Mechanical Inspection
2. Leak Test
3. Extension and Retraction
4. Uncaging
5. Scissoring
6. Visual and Mechanical Inspection
7. Leak Test
8. Extension and Retraction
9. Vibration
10. Thermal Vacuum
11. Leak Test
12. Inspection (Retrofit to ATS-D/E configuration and four months storage
13. Thermal Vacuum
14. Vibration
15. Functional
16. Eight Months Storage
17. Completed Flight Acceptance including: Extension and Retraction, Alignment and Caging

2.5 QUALIFICATION TESTS, DAMPER BOOM

Two prototype Damper Booms (designated as component and system qual) were subjected to similar environments at more severe levels than the anticipated operating environments in order to establish confidence that the design was valid under extreme operating conditions. Following tests, the component qual unit was not further dispositioned, but the system qual unit was included in the spacecraft qualification tests conducted by the vehicle contractors following the GE tests. A summary of these environments and references to the appropriate test reports are listed below. These documents are on file at GE and will be made available on request of the Contract Administrator for NASA programs.

2.5.1 COMPONENT QUALIFICATION, DAMPER BOOM

Serial No.:	11	
Part No.:	47E207008	
Test Report:	4315-QC-031	(4/28/67)
Failure Analysis Reports:	228-E-17	(9/13/67)
	279-E-38	(1/13/67)

Test Sequence

1. Visual and Mechanical Inspection
2. Electrical Check
3. Performance Test (deployment on 50-foot test track; pyrotechnic actuated)
4. Alignment and Straightness Check
5. Electrical Check
6. Magnetic Dipole Measurement
7. Thermal Vacuum
8. Electrical Test
9. Humidity
10. Electrical Test
11. Vibration (mated to CPD)
12. Electrical Test
13. Acceleration (mated to CPD)
14. Visual Inspection
15. Electrical Test
16. Performance Test (same as Item 3)
17. Alignment and Straightness Check

2.5.2 SYSTEM QUALIFICATION, DAMPER BOOM

Serial No.:	10	
Part No.:	47E207008	
Test Reports:	4315-QC-229	(1/20/67)
	4315-QC-005	(8/18/66)
	4315-QC-005-1	(2/26/67)

Test Sequence

1. Visual Inspection
2. Electrical Check
3. Alignment
4. Performance (deployment on 50-foot test track; pressure actuated. Deployment Rage = 1.76 ft/sec)
5. Electrical
6. Performance (similar to Item 4)
7. Visual Inspection
8. Performance (similar to Item 4)
9. Alignment
10. Electrical Check
11. Thermal Vacuum
12. Post Thermal-Vacuum Inspection
13. Vibration
14. Post Vibration Inspection
15. Performance (similar to Item 4)
16. Alignment

2.6 FLIGHT ACCEPTANCE, DAMPER BOOM

Each of the Damper Boom flight units were exposed to vibration and thermal-vacuum environments at levels anticipated during flight to verify that the design had not degraded during manufacture. A summary of these environments and references to the applicable test reports are listed below. These documents are on file at GE and will be made available on request of the Contract Administrator for NASA programs.

2.6.1 ATS-A

Serial No.:	100
Part No.:	47E207008
Test Report:	1315-040
Test Procedure:	DHC-SP-AT-69M, Rev. 4, issued by De Havilland Aircraft Co.
Failure Analysis Report:	229-E-18 (8/20/66)

Test Sequence

This unit was subjected to a performance test per de Havilland procedure DHC-SP-AT-69M. Both boom elements extended at an average velocity of 2 ft/sec. The respective boom lengths were 44.88 feet and 44.96 feet.

2.6.2 ATS-D

Serial No.:	102
Part No.:	47E207008
Test Report:	040 (1/3/68)
Test Procedure:	DHC-SP-AT-69M (deHavilland)

Test Sequence

Test	Serial No. Tested	Test	Serial No. Tested
1. Visual Inspection	101	4. Electrical	101
2. Electrical Check	101	5. Thermal Vacuum	101
3. Performance (Both booms were deployed on a test track at a maximum rate of 2.4 ft/sec. Electro-explosive released.)	101	6. Post Thermal-Vacuum Check	101
		7. Vibration	101
		8. Post Vibration Inspection, Electrical Check and Performance	101

9.	Visual Inspection	102	18.	Performance (See Item 3)	102
10.	Electrical Check	102	19.	Visual Inspection	101
11.	Performance (See Item 3)	102	20.	Performance (See Item 3)	101
12.	Electrical Check	102	21.	Electrical Check	101
13.	Thermal Vacuum	102	22.	Thermal Vacuum	101
14.	Post Thermal-Vacuum Inspection	102	23.	Post Thermal-Vacuum Check	101
			24.	Vibration	
15.	Vibration	102	25.	Post Vibration Inspection,	101
16.	Post Vibration Inspection, Electrical Check and Performance (See Item 3)	102		Electrical Check and Performance (See Item 3)	
			26.	Alignment Check	101
17.	Alignment Check	102	27.	Performance (See Item 3)	101

2.6.3 ATS-E

Serial No.:	101
Part No.:	47D212101 (Modified 47E207008)
Test Report:	040 (4/16/69)
Failure Analysis Report:	296-E-46 (3/23/67)

Test Sequence

See paragraph 2.10.3/

Damper Boom 101 was retrofitted with digitated elements (Dwg. No. 47E217400), then subjected to a performance test and a vibration test. Vibration levels were to flight acceptance standards with the damper boom mounted to the CPD.

APPENDIX TO

SECTION 2

APPENDIX 2A

DIGITATED DAMPER BOOM HISTORY

1/21/69	Digitation program initiated.
1/23/69	Hand release - both sides fully deployed/overlapped damper boom elements to checkout test equipment and familiarization.
1/24/69	Plated 45-foot overlapped primary boom work elements installed - both sides fully deployed/hand release. These elements to be digitated and reinstalled for qual testing.
2/3/69	Unplated digitated 19-foot, PB element installed in side No. 2 and plated digitated 19-foot, PB element installed in side No. 1. Spreader modified for use with digitated booms.
2/3/69	Hand release - both sides fully deployed but digitating not satisfactory.
2/3/69	Digitation tabs rebent slightly prior to rewind. Hand release side No. 1 fully deployed/counter balance and oscillation damper removed and tip mass fixed at constant angle. Digitating properly.
2/3/69	Hand release side No. 1 - fully deployed/tip mass fixed at constant angle. Digitating properly.
2/6/69	Digitated plated 45-foot, PB elements installed in both sides. Motorized rewind eliminated due to degrading effect of excessive rewind speed on digitation tabs experienced during test sequence on 2/3/69.
2/7/69	Reassembled unit/ball lock and drum torqued.
2/8/69	Manual ball lock release - both sides hesitated after release. Side No. 2 attained full deployment with only this hesitation but side No. 1 stopped and continued to full deployment by itself when side No. 2 attained full deployment. Both sides 75 percent digitated. Crossovers experienced on both sides and crack appeared on side No. 2.
2/8/69	Unit reassembled/ball lock and drum torques. Manual ball lock release/ side No. 2 counterbalance weight removed and side No. 1 weight repositioned - both sides fully deployed at same rate although side No. 2 hesitated several times and side No. 1 stopped momentarily. Side No. 1 85 percent digitated and side No. 2 50 percent digitated. Crossovers experienced on both sides.

2/8/69 Hand release of side No. 1/drum torqued and new engineering configuration rollers and rewind gear installed. Required hand assist to attain full deploy--all but one group digitated properly. Suspect new roller adjustment.

2/8/69 Hand held and released side No. 2/proper roller adjustment on new roller assembly and rewind gear installed. All groups digitated properly and now crossovers experienced.

2/8/69 Six feet of side No. 1 plated boom removed from bending/torsional tests. Replacement 50-foot plated element prepared from another PB work element.

2/11/69 Pre-digitation engineering type straightness test conducted on plated replacement boom element.

2/12/69 Tip mass No. 2 mounted on side No. 1/engineering configuration, new rollers installed. Hand release/drum torque--high speed movies taken within first 4 feet of deployment.

2/12/69 Boom No. 2 and engineering configuration rollers removed and installed in tip mass No. 1. Tip mass No. 1 hand held and released for high speed movies of boom leaving drum.

2/13/69 Replacement unplated 50-foot digitated boom and engineering configuration rollers installed in tip mass No. 2 for repeat of 2/12/69 tests due to high speed movies being poor. This unplated boom is of new configuration--has removed and bent group edges and improved bending tools/techniques.

2/13/69 Removed boom and rollers from tip mass No. 1--unit reassembled/ball lock and drum torqued--no boom in side No. 2. Manual ball lock release/side No. 1 having no oscillation damper. Fully deployed satisfactorily but did not digitate properly in two groups - no crossovers.

2/13/69 Removed boom and rollers from tip mass No. 2 and installed same new configuration unplated boom in tip mass No. 2. Unit reassembled/ball lock and drum torqued - no boom in tip mass No. 2. Manual ball lock release/side No. 2 having no oscillation damper. Side No. 2 deployed fully but deployment and digitation very unsatisfactory due to extreme buckling.

2/14/69 Retrimmed boom and installed with engineering configuration rollers in side No. 1. Unit reassembled/ball lock and drum torqued - no boom in side No. 2. Manual ball lock release/no oscillation damper and new fixed position for counterbalance weight. Full deployment with proper digitation very satisfactory.

2/14/69 Removed boom and rollers from tip mass No. 1 and installed in tip mass No. 2. Unit reassembled/ball lock and drum torqued - no boom in side No. 1. Manual ball lock release/oscillation damper and new fixed position for counterbalance weight. Full deployment satisfactory but two of last three groups not digitated properly.

2.15/69 Three full deployments of side No. 2 satisfactorily completed with hand release - engineering configuration rollers and same latest configuration unplated boom installed.

2/15/69 Post digitation engineering type straightness test conducted on same plated element tested on 2/11/69. This boom has pre-digitation crease along the entire length of the underlapped edge.

2/18/69 Installed two new plated elements - one is from straightness test. Unit reassembled/ball lock and drums torqued. Side No. 2 contains creased boom and engineering configuration rollers. Side No. 1 contains prot. configuration rollers.

2/18/69 Manual ball lock release/same test equipment configuration that was successful on 2/13 and 2/14. Side No. 2 fully deployed very successfully with proper digitation. Side No. 1 however deployed slowly and required assistance to attain full deployment - digitated properly. Failure caused by improper adjustment of prototype configuration rollers.

2/19/69 Unit reassembled/ball lock and drums torqued. Side No. 2 contains creased boom and engineering configuration rollers. Side No. 1 contains flight (reworked prot) configuration rollers.

2/20/69 Pre-vibration deployment completed satisfactorily/manual ball lock release - both rates identical at 2.2 ft/sec and all digitations were proper with no crossovers.

2/21/69 Qual level sine and random vibration tests completed/unit mounted on prototype CPD.

2/21/69 Post-vibration deployment - side No. 2 deployed satisfactorily and all groups digitated properly. Rate was 2.2 ft/sec and flight roller was installed in this side. Side No. 1 experienced hesitation and stopping prior to attaining full deployment with assistance.

2/21/69 Side No. 1 rewound and manually released - same hesitation occurred. Cause detected as interference between protruding counterbalance weight locating tape and trolley end plate.

2/21/69	Side No. 1 rewound and manually released after eliminating interference - full deployment satisfactory and all groups digitated properly. Rate was 2.0 ft/sec.
2/21/69	Unit reassembled/ball lock and drums torqued - covers installed and unit subsequently placed in storage for post launch storage test at six weeks prior to launch.
2/24/69	Damper boom removed from ATS-E flight CPD.
2/25/69	Manual release of ball lock/pinned plunger and overlapped booms (as received from HAC). Side No. 1 fully deployed successfully but Side No. 2 hung up on center body. Side No. 2 fully deployed when hand pushed away from center body. Cause was excessive force applied to shear pin which resulted in shifting of mtg bracketry and jamming of tip mass.
2/25/69	Installed two 50-foot digitated booms and cleaned bearing/brakes reassembed unit/ball lock and drums torqued.
2 26 69	Manual ball lock release - very smooth and successful. Full deployment of both sides at almost exactly same rate of 2.4 ft/sec. All groups digitated properly with no crossovers.
2/27/69	Three-axis acceptance level random vibration completed/damper boom mounted on prot. CPD.
2/27/69	Manual ball lock release - very smooth and successful full deployment of both sides at almost exactly same rate of 2.4 ft/sec. All groups digitated properly with no crossovers.
2/27/69	Booms trimmed to 45 feet - unit reassembled/ball lock and drums torqued.
2/28/69	New plunger/shear pin installed and unit remounted on ATS-E flight CPD.
2/28/69	ATS-E CPD/digitated damper boom assembly shipped to HAC.

Table 2A-1. Hardness Data (Diamond Pyramid Hardness)

Specimen Number	DPN	DPN (av)
1	292 287 292 292	291
2	260 254 264 264	260
3	264 276 264 260	266
4	270 262 264 264	265
5	276 268 264 268	269

NOTES:

Each of the five specimens were individually metallographically mounted in bakelite. Each mount contained a 3/4 inch diameter steel tube which surrounded the specimen for rigidity. Transverse sections were prepared, ground and polished.

Microhardness testing was done on a Kentron Microhardness tester using a pyramid diamond endenter. A 100 gm load was used and DPN* (diamond pyramid number) was determined four times for each specimen. The resulting DPN data included in Table 2A-2 was originally contained in PIR 2410-362.

* DPN obtained from conversion charts relating to size of indent as supplied by Kentron (Riehle Testing Machines, Division of Ametsk, Inc.).

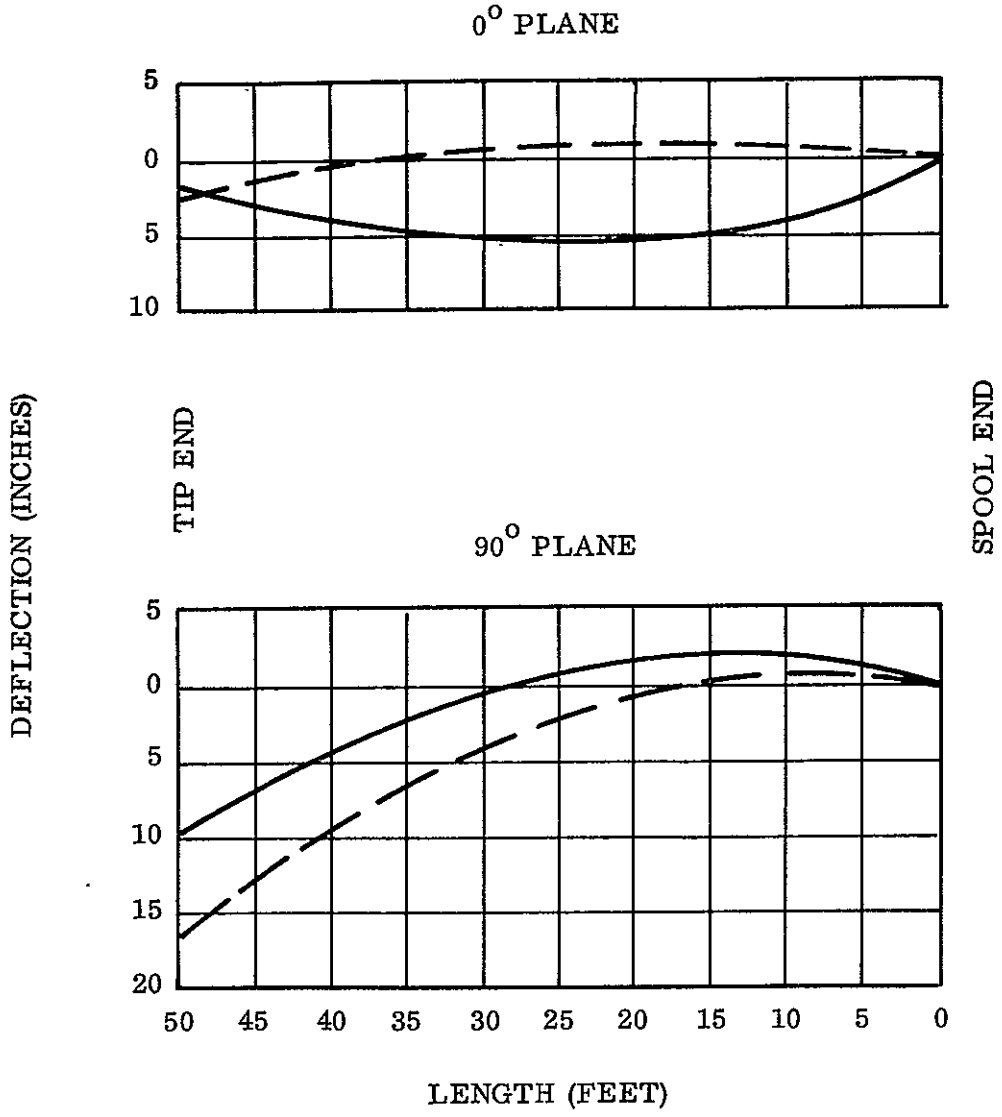

Figure 2A-1. Damper Boom Straightness Profile

BIBLIOGRAPHY

1. ETR 1315-040 Amend. B - ATS-E Flight Damper Boom Engineering Test Report by M. Hammer, dated March 1969.

2. PIR 1450-ATS-004 - Thermal Flutter Investigation Report by R. Freelin, dated 12 March 1969.

3. F20423 - Proposal for ATS-E Edge Interlocked Damper Booms Using Existing Self-Erectible Flight Units, dated 17 January 1969.

4. G8SD-4346 - Audit Team Report on Flight Readiness of ATS-E Gravity Gradient Stabilization Subsystem Components by S. Drabek, J. B. Gudikunst and C. A. Taylor, dated 31 October 1968.

5. ETR 1315-040 Amend. A - ATS-E Flight Damper Boom Engineering Test Report by M. Hammer, dated 25 October 1968.

6. PIR 41M2-221 - Boom Subsystem Engineering Report by R. A. Lohnes, dated 28 July 1967.

7. ETR 4315-QC-031 - Damper Boom Qualification Test Report by M. D. Hammer, dated 28 April 1967.

8. PIR 41M3-001 - Damper Boom Release System Reliability Demonstration Test Report for ATS Program by R. Monteiro, dated 1 November 1966.

9. PIR 2410-362 - Microhardness Tests on BeCu by M. Birenbaum, dated 15 February 1969.

SECTION 3

COMBINATION PASSIVE DAMPER

COMBINATION PASSIVE DAMPER FACT SHEET

DESIGNER:

General Electric Company Space Division

SUBCONTRACTOR:

TRW ATS-A (Passive Hysteresis Damper)

CONTROLLING DOCUMENTS:

Specification	SVS-7314
Outline Drawings	47E207100, CPD Assembly
	47E207098, CPD Envelope
	47E207083, Passive Hysteresis Damper
	47E207008, Damper Boom Assembly

PERFORMANCE REQUIREMENTS:

- Select and supply one of two forms of damping (eddy current or hysteresis)
- Provide spring restraint for damper boom, essential for spacecraft damping
- Indicate angular position between damper boom and spacecraft

UNIT DESIGNATION:

1	Engineering Unit
2	Engineering Unit
5962027	Component Qualification Unit
5962028	Prototype Unit
5962029	ATS-A Flight
5962030	ATS-D Flight
5962031	ATS-E Flight

SECTION 3

COMBINATION PASSIVE DAMPER

3.1 PURPOSE OF THE CPD

The Combination Passive Damper (CPD) was designed for use on the ATS spacecraft as a major part of the satellite's attitude control system. The function is to dampen the vehicles oscillatory motion and thereby achieve stabilization. This is accomplished by using a passive damping system using permanent magnets only.

Stabilization using the CPD is accomplished by affixing damper booms to the rotor of the CPD. The damper booms want to orient themselves to the local vertical, due to the earth's gravitational field, but are held horizontal by the torsional restraints within the CPD. This provides a "stable" position. Relative motion, and therefore damping, between the spacecraft and damper boom is assured by choosing system parameters which essentially "detune" the frequency response characteristics of the respective bodies.

The CPD is so placed within the spacecraft that only a single axis damper is required. Damping in all axes is obtained by taking advantage of the inherent crosscoupling between axes on this particular spacecraft configuration.

Design of the CPD incorporates two different damping systems, the Passive Hysteresis Damper (PHD) and the Eddy Current Damper (ECD), to obtain comparative performance characteristics of the two different systems on the same spacecraft. This fact adds considerable complexity to the CPD. Also adding to the complexity is the instrumentation for monitoring the CPD experiment.

This section presents a detailed history of the CPD engineering development effort and supporting engineering tests. A list of all qualification and acceptance tests is included as well as references to the resulting test reports.

3.2 ENGINEERING DEVELOPMENT

3.2.1 CPD UNIT NOMENCLATURE

The following is the designation and definition for all CPD's on the ATS Program.

Serial No.	Unit	Configuration	Use
-	EU 1	MAGGE*	Engineering Evaluation**
-	EU 2	SAGGE*	SAGGE Confidence Unit
5962027	Prototype (2nd Unit Built)	MAGGE	Component Qualification Unit
5962028	Prototype (1st Unit Built)	MAGGE	Systems Qualification Unit at HAC
5962029	Flight 1	ATS-A (MAGGE)	1st GG Flight in Series
5962030	Flight 2	ATS-D (SAGGE)	2nd GG Flight in Series
5962031	Flight 3	ATE-E (SAGGE)	3rd GG Flight in Series

*MAGGE - Medium Altitude Gravity Gradient Experiment (ATS-A)
*SAGGE - Synchronous Altitude Gravity Gradient Experiment (ATS-D/E)
**Also used as a structural qualification unit due to problems on Prototype Unit 1.

3.2.2 CPD DESCRIPTION

All CPD units were built from the same drawings and in general the prime units are identical to the engineering units, with the exception of high-reliability parts used on only prime units, i.e., prototype and flight. Other differences include items such as finish changes and redesign of certain elements due to testing results that were not retrofitted into the engineering unit. Other than performance characteristics there is no difference between Flight A and Flights D & E. This was done to simplify the design.

Figures 3-1 and 3-2 are a schematic representation and a functional isometric respectively which give the major components and their functions. Figures 3-3 and 3-4 are of the detail assembly. The numbers in the circles refer to the text description that follows.

The CPD package was integrated into the Hughes Aircraft Company structure and is attached to it at the inboard face of the four projecting beams of the base plate (1). The damper boom package (2), by de Havilland, is attached at the outboard end of the boom shaft (3).

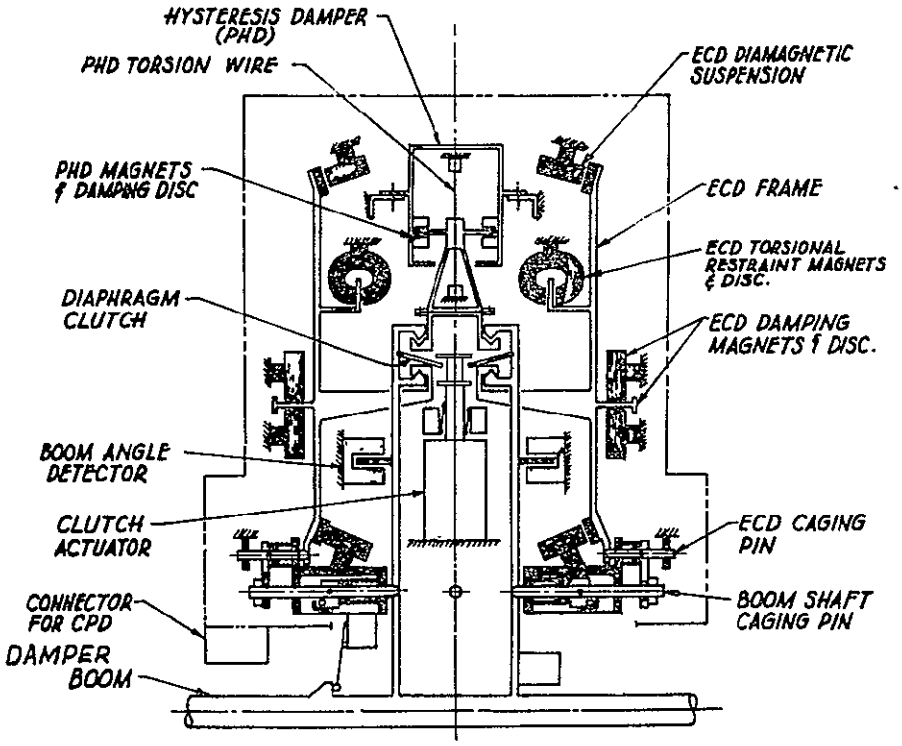

Figure 3-1. Combination Passive Damper Schematic

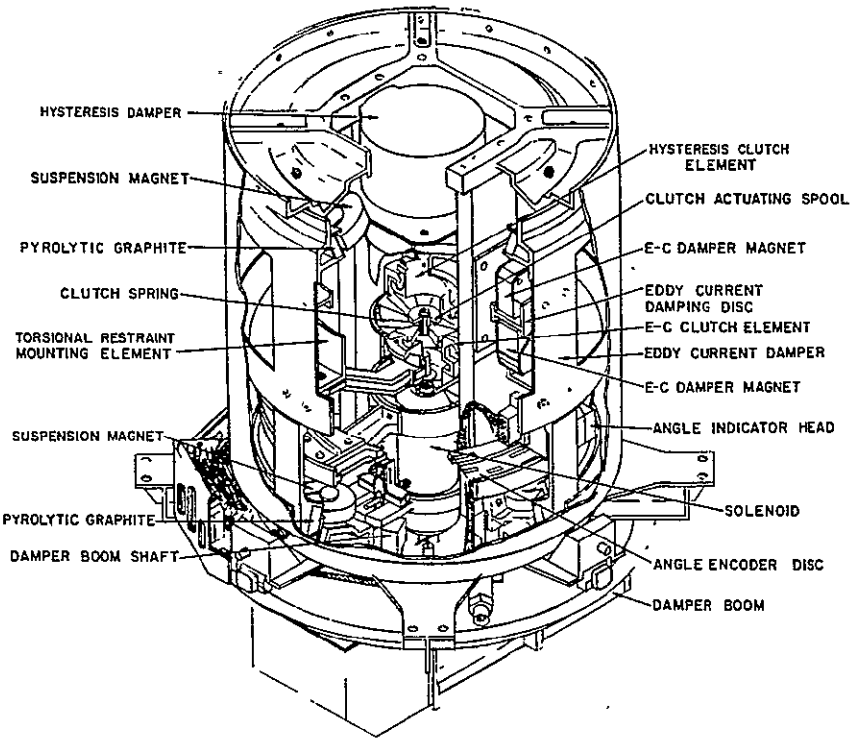

Figure 3-2. Combination Passive Damper for ATS

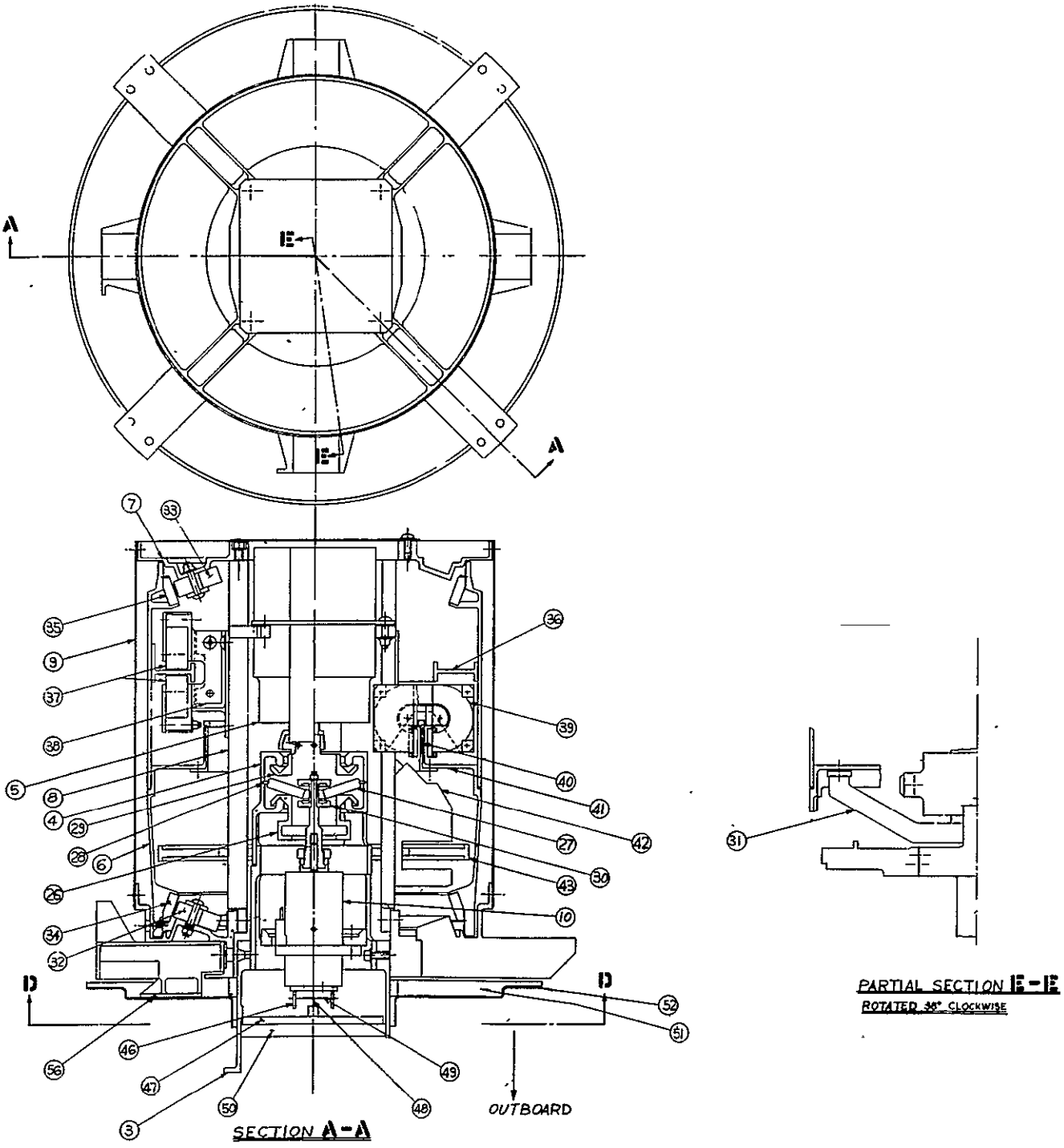

Figure 3-3. Combination Passive Damper Package (Elevation View)

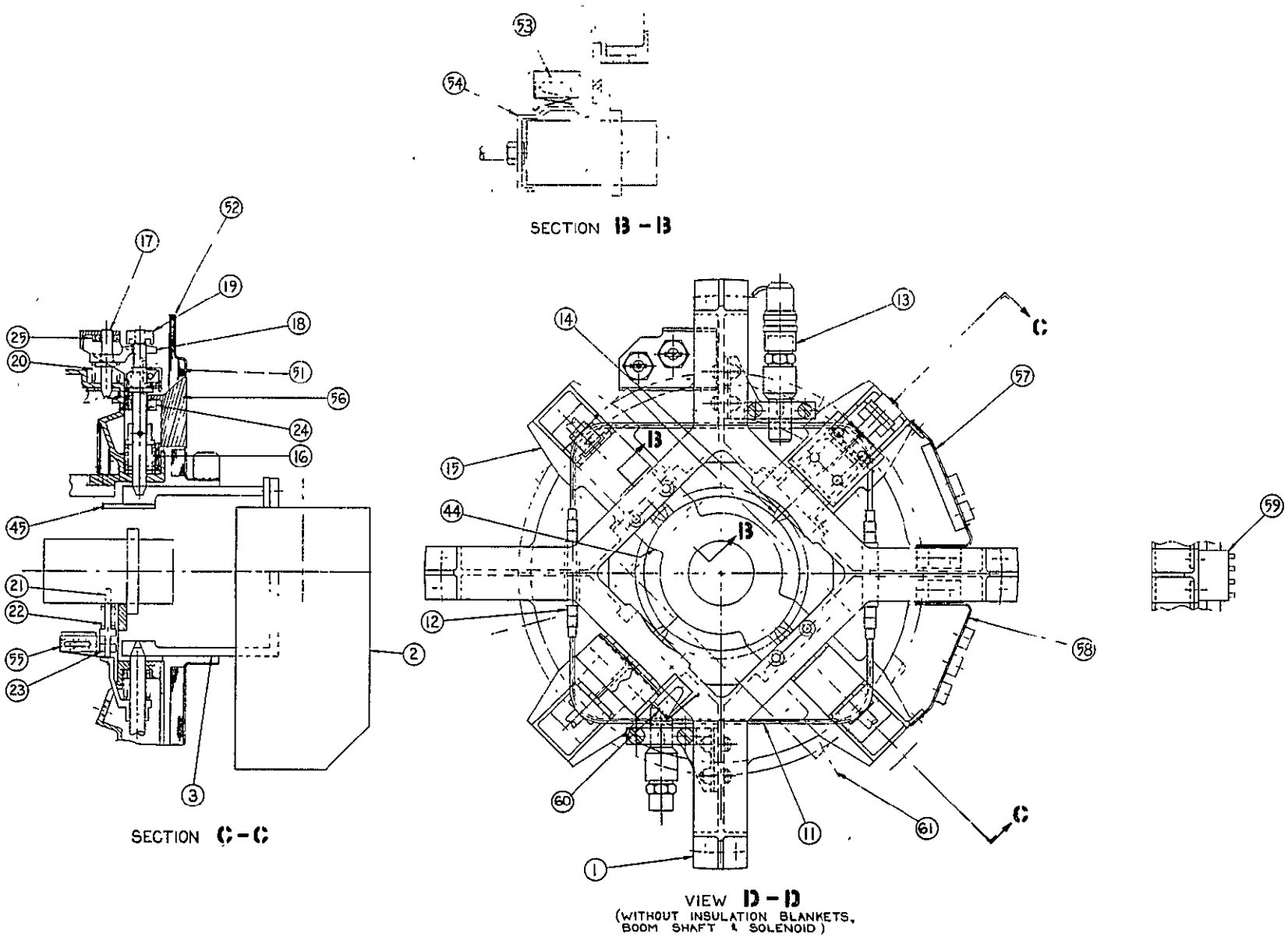

Figure 3-4. Combination Passive Damper Package (Plan View)

In operation, the damper booms rotate ±45° from a null position, and about the axis of the damper package.

There are four main parts to the CPD Package:

1. The boom shaft (3), which connects the booms to the clutch housing (4).
2. The hysteresis damper (5), procured from TRW, Inc., which is connected to the booms in one position of the clutch.
3. The eddy current damper rotor (6), which is connected to the boom in the other position of the clutch.
4. The structure, which consists principally of the base plate (1), the inboard plate (7) at the inboard end of the damper, the two posts (8) connecting the inboard and base plates internally, and the cover (9), connecting the inboard and base plates externally.

At launch the boom shaft (3), the eddy current rotor (6), and the core of the solenoid (10) (used to shift the clutch) are all caged to the structure. They are supported on pins which are held in the caged position by the 0.125 inch diameter cable (11). The cable is tensioned by the turnbuckles (12). To uncage, the cable is cut by a pyrotechnic fired guillotine (13) and/or its diametrically opposite redundant mate. The cable is roved through saddles on the main caging pins (14). The pins have tapered points where they enter tapered holes in the boom shaft (3). The cable, when tensioned, holds the pins snugly in the tapered holes. The pins pass through a hole in the baseplate (1) and another hole in the pin bracket (15), (with clearances of 0.004 inch to 0.008-inch diameter). A 49-pound spring (16) retracts the pin when the cable is cut.

The eddy current rotor is caged by a pin (17) which also has a tapered point that seats in a tapered hole in the rotor. This pin also passes through a hole in the baseplate and another hole in the bracket (with clearances of 0.004 to 0.008-inch diameter). The pin is engaged by a fork (18), loaded by a nut (19) on the end of the main caging pin. When the cable is cut and the main caging pin retracts, it allows the eddy current pin to be retracted by the 25-pound spring (20). The core of the solenoid is caged by pin (21) held in engagement by a foot on a sleeve of one of the main caging pins. When the main caging pin retracts it

allows a 10-pound spring (22) to disengage the solenoid pin. The pin is straight and fits in the solenoid and in the guide (23) (with 0.005-inch to 0.008-inch diametral clearance). Pin (61) is provided for manually caging the eddy-current rotor during handling and testing of the hysteresis damper. This feature is required because the diamagnetic suspension will not support the eddy-current damper in the earth's gravitational field. Buna-S rubber cushions (24) and (25) are provided to absorb the energy of the main and eddy-current caging pins, at release and thus to prevent distortion of the bracket (15), particularly under repeated operation during testing.

The loads generated by launch vibration in the boom package and in the boom shaft and clutch are transferred to the baseplate by the main caging pins. The launch loads from the eddy-current rotor are carried to the baseplate by the eddy-current caging pins. The loads in the posts and the parts attached to them are either carried directly into the baseplate or to the top plate. The loads in the top plate, plus the loads from the mass of the top plate itself and the parts attached to it, are carried by the cover, along with the loads due to the mass of the cover, into the baseplate. The baseplate is designed for adequate strength and rigidity to take these loads into the HAC structure.

In normal operation, the boom shaft structure is designed to have a nominal radial clearance of 0.1 inch between it and the baseplate. Within the CPD, the boom shaft structure connects to the clutch housing (4). This clutch housing has two circular vee clutch faces. These faces mate with matching vee-groove clutch plates. The eddy-current clutch plate (26) is shown in the engaged position in Figure 3-3. It is held in contact by the coned diaphragm (27). The reaction of the force that holds the clutch faces in engagement is taken by the pivot ring (28). When the clutch is shifted the diaphragm pivots about this ring, over center, and "flips through" in the opposite direction, to force the hysteresis clutch plate (29) into engagement with the other vee face of the clutch housing. The diaphragm is pushed over center by the actuator spool (30), which is moved by the solenoid (10). The positioning and stroke of the solenoid and diaphragm are such that the actuator does not touch the diaphragm during damping operation. Also, the dimensioning and locations of the clutch faces are such that the disengaged faces do not contact during damping operation. The two clutch plates are held in position by the suspension systems of either the hysteresis or eddy-current damper.

Thus, when the clutch is shifted, the clutch housing and everything attached to it (including the damper booms) must move axially a distance equal to the clearance between the disengaged clutch faces. This distance is about 0.14 inch. In the caged position the clutch is engaged in the eddy-current mode. The booms move outboard, about 0.14 inch, when shifted to the hysteresis mode.

The hysteresis clutch plate (29) is attached to the hysteresis damper (5) by screws. The damper is attached to posts (8) by bolts through oversized holes and with shims. This method will allow proper alignment of the clutch faces and the boom shaft when engaged.

The eddy-current damper rotor (6) is attached to the eddy-current clutch plate (26) by arm (31) . The arm is attached to the rotor by bolts in oversized holes and shims to allow proper alignment as in the case of the hysteresis damper. The rotor is supported by 10 magnets (32) attached to the baseplate and by 10 magnets (33) attached to the inboard plate. Each set of suspension magnets will be mounted, poles facing out, in a flat cone of total included angle of about 140° apex. The magnets support the rotor by the diamagnetic repulsion of the pyrolytic graphite rings (34) and (35) set in each end of the rotor. The angular arrangement of the magnets is such that the largest force is supplied in the radial direction, which is the direction of greatest loads. The axial component resulting from the angle of the cone produces sufficient axial force to support the imposed loads in that direction. There is a nominal clearance of 0.050 inch between the graphite and the magnet face. The ends of the rotor are shaped such that they fit, with clearance, corresponding surfaces on the baseplate and inboard plate to form stops. These stops prevent the magnets and the pyrolytic graphite rings from contacting in the event that transient forces experienced are greater than the design operating loads. No physical damage will occur when the stops are engaged.

The aluminum eddy-current damping ring (36) is riveted to the rotor. Two sets of magnets (37) are bolted to brackets (38) on the posts (8) through oversized holes to allow alignment with the damping ring. The eddy-current damping is created by the magnetic flux of the two sets of two magnets each that cause electrical currents to flow in the aluminum ring. The interaction of the flux resulting from the current flow in the aluminum and the flux of the magnets produces the damping force and consequently the torque. The faces of the magnets are spaced approximately 0.050 inch away from the aluminum surface.

Torsional restraint for the eddy-current damper is provided by an arrangement of magnets (39) and a thin crescent of magnetic material (40) mounted on a cylindrical extension of a flange (41) of the eddy-current rotor. The wider portion of the thin crescent has a greater attraction for the magnets producing the torque that returns the rotor to the null corresponding to this wider portion. There are two sets of torsional restraint magnet arrangements disposed symmetrically about the centerline of the damper. This arrangement tends to balance loads induced on the diamagnetic suspension. The magnets are bolted through oversized holes, to a face on bracket (38) to allow the 0.25-inch gap between the pole piece to be centered on the magnetic material (40) .

Two angle indicator heads (42) are located diametrically opposite each other and attached to the posts (8). The angle indicator disc (43) is attached to the boom shaft (3). Shaft position readout is accomplished by light being projected from a double filament lamp (2nd filament is redundant and is ground command controlled) through a fiber optic divider which separates the light into 5 bundles from whence it is relayed by lenses through the disc onto detectors. The disc is .010 beryllium copper with an expanded gray code pattern etched through it.

Faces (44) on the solenoid support bracket form one side of the rotational hard stop for the damper booms. Arms (45) which are part of the boom shaft will contact the faces at about ±45° from the damper null position.

The spider (47) supports an insulation pad (50) consisting of aluminized mylar. An insulation blanket (51) , 13 inches in diameter, is located on the outboard face of the baseplate (1). The blanket consists of 30 layers of aluminized mylar. It is attached, at its outboard face, to an aluminum sheet (52) , which is flanged to fasten it to the HAC insulation/blanket. The aluminum sheet is attached, through plastic spacers, to the baseplate. The outboard face of the aluminum sheet and other parts on the outboard end of the damper are coated with a thermal control paint. The remainder of the damper is thermally black, both outside and inside, to provide thermal control. Black on the inside of the damper will also be of benefit in reducing light reflection for operation of the angle indicator. The space between the aluminized sheets and the face of the baseplate is used to run electrical wiring.

Two switches (60) are mounted on a clip on the outboard face of the baseplate to indicate when the damper booms have extended. Two additional switches (53) are mounted to a clip on the solenoid support bracket (44) and activated by a ramp (54) on the solenoid core. They indicate, by the position of the solenoid plunger, whether the damper is in the hysteresis or eddy-current mode. Another switch (55) is mounted on a clip on the solenoid caging pin guide, to sense when a caging pin has been retracted, thus indicating that uncaging has been effected.

A foundation (56) is provided to accommodate the actuator assembly for the damper boom package. The actuators are redundant and either one releases the booms by releasing a ball lock assembly in the damper boom. The electrical connector for the wires from the actuator fit into bracket (57) . The wires from the uncaging guillotine (13) also go to a connector in bracket (57) . HAC connects directly to the second guillotine. All other wires will go to connectors in bracket (58) . An electronic module (59) is mounted on the inboard face of the baseplate beam between the two connector brackets. The purpose of this module is to provide common tie points for various circuits and to mount electronic components required for telemetry and temperature sensing circuits.

The following figures will help identify the components as discussed in the text. These photographs are of Engineering Unit 1.

Figure 3-5 shows the assembly with the cover and thermal shield removed as it is instrumented for vibration testing. The electrical wiring in the right of the picture was used for accelerometer and strain gage connections which were used in the vibration testing evaluation. The T-1 Damper Boom package is in place on the CPD. The switches that indicate damper boom extension, together with the actuator, are shown adjacent to the Damper Boom tip masses. The baseplate at the CPD is resting on the assembly stand.

Figure 3-6 shows the eddy-current rotor and upper magnet mounting plate from a different angle than that shown in Figure 3-5. The nominal clearance gap (0.040 inch) between the eddy-current rotor and upper magnet mounting plate can be seen at the bottom of Figure 3-6. The eddy-current damping magnets on each side of the damping disc are shown

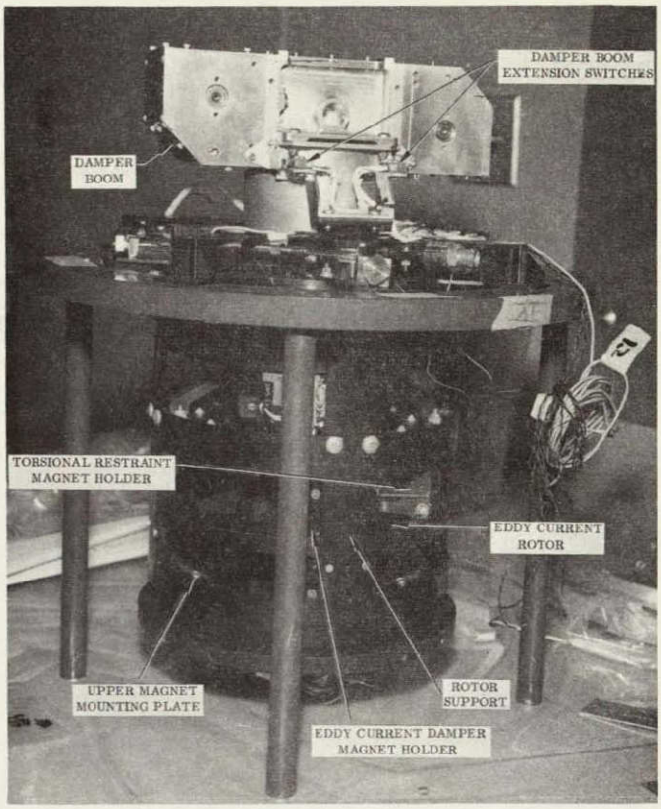

Figure 3-5. CPD Engineering Unit Assembled (Cover Removed) and T-1 Damper Boom Package in Place

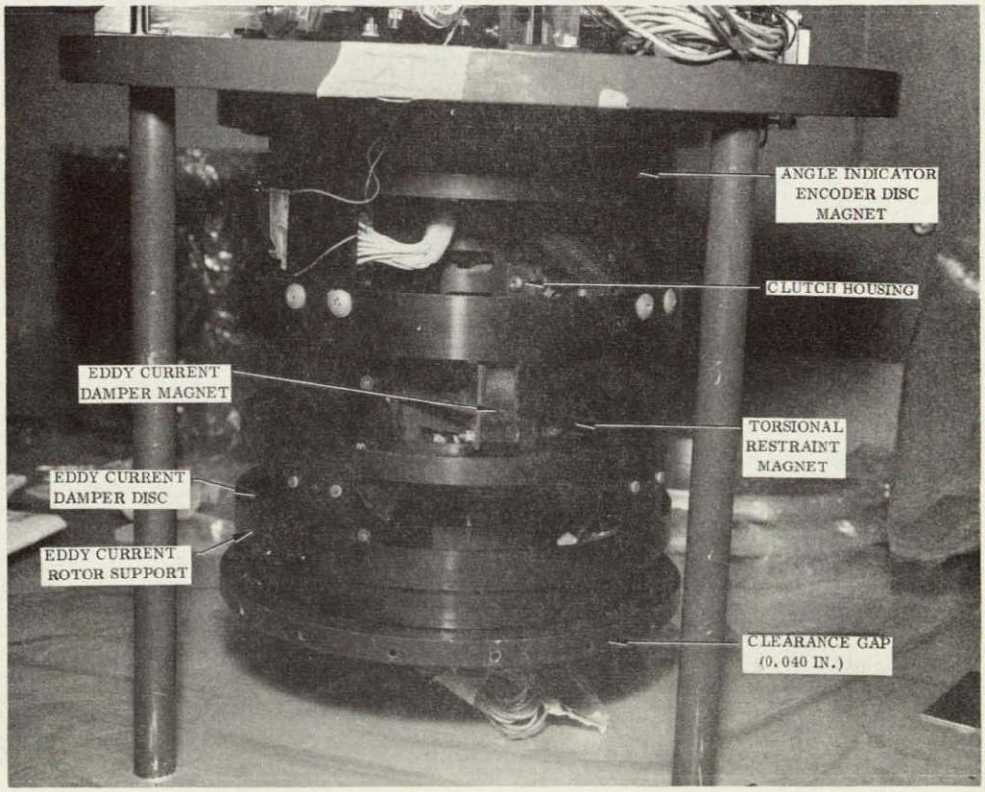

Figure 3-6. Details of CPD Engineering Unit 1

together with the end of the torsional restraint magnet. The clutch housing is also shown, and the edge of the angle indicator encoder disc support is seen above the clutch housing.

Figure 3-7 clearly shows the attachment of the Damper Boom package to the bottom shaft on the CPD and the boom release mechanism which is attached to the caging pin bracket on the baseplate. The boom shaft and eddy-current damper caging cable is shown in the tensioned (caged) position with the pyrotechnic device, boom shaft caging pins and eddy-current caging pins evident.

The first test performed following assembly of Engineering Unit 1 was an uncaging exercise. The guillotine cable cutters were electrically detonated. Figure 3-8 shows that all strands of the caging cable were completely cut by the uncaging guillotine.

The wiring (along with the conformal coating which holds the wiring), the connectors, and the boom extension switches are also shown. The thermal insulation in the center of the boom shaft can be seen at the top center.

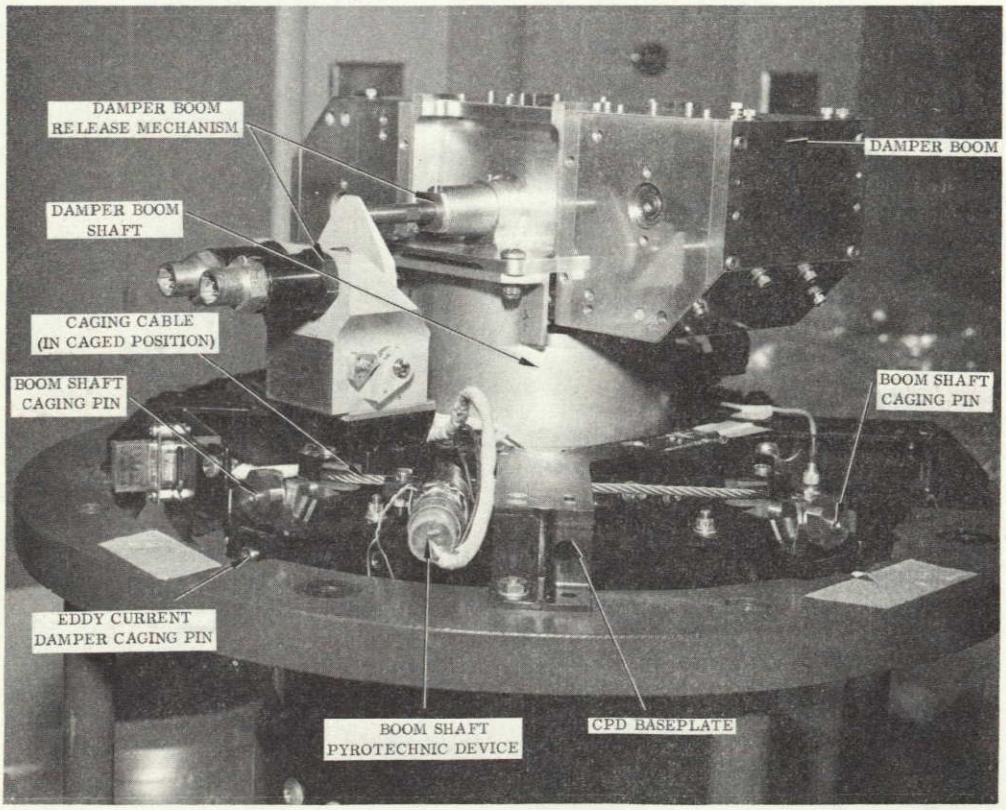

Figure 3-7. Baseplate and Caging Mechanism of CPD Engineering Unit 1 with Damper Boom Package in Place

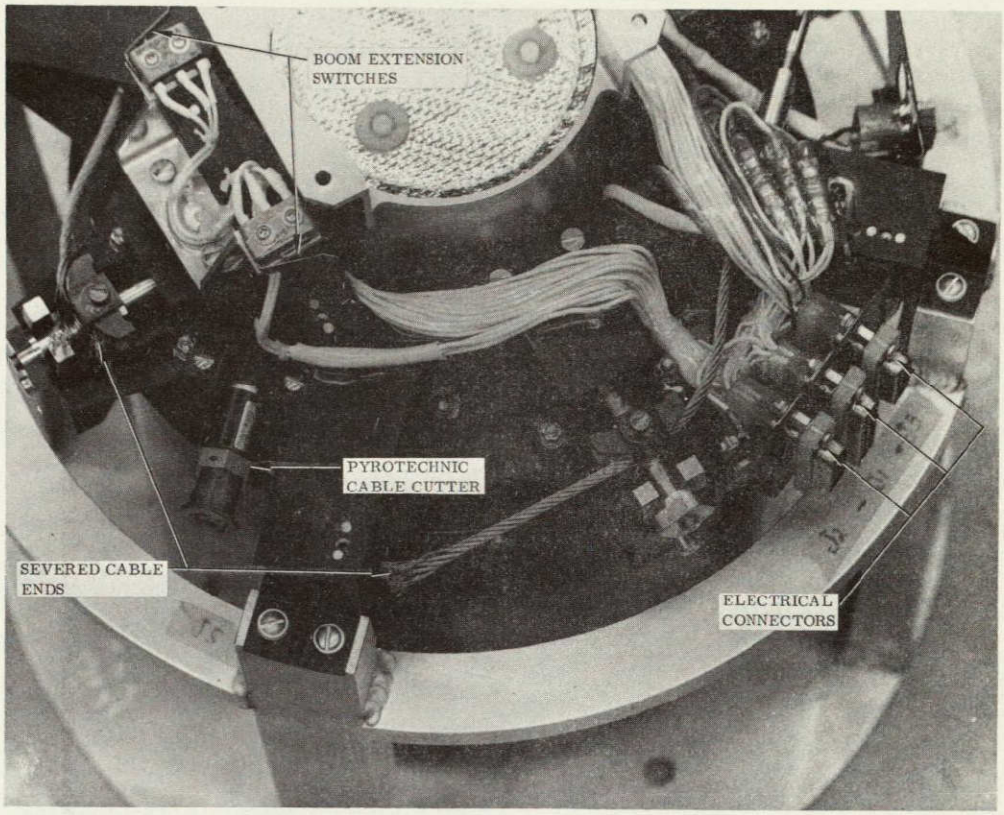

Figure 3-8. Caging Cable and Baseplate (with Pyrotechnic Device 2) After Uncaging Operation, CPD Engineering Unit 1

3.2.3 DETAILS OF MAJOR SUBSYSTEMS

3.2.3.1 Eddy Current Damping

The damping coefficient of an eddy-current damper may be expressed as follows:

$$b = K \gamma B^2 D^2$$

where

b = damping coefficient (torque/angular velocity)

K = proportionality constant

γ = electrical conductivity of damper disc material

B = flux density through disc

D = distance of magnet from axis of rotation

n = number of magnets

From this equation the fruitful areas for application of development engineering effort can be identified. Each factor will be discussed in turn to illustrate its effect on the damper design. As in all equations of this type, the proportionality constant assures dimensional compatibility, is independent of these factors, and is fixed. The diameter of the circle at which the magnets are placed is limited by the physical dimensions allowed for the package. In the physical design of the CPD, the eddy-current magnets are placed at the maximum radius possible which is outside of all other functional elements of the package. Only two pairs of magnets are used for this damper because of physical constraints on the mechanical design of the CPD.

The electrical conductivity of the disc is affected by the:

1. Material used in its construction
2. Thickness of the disc
3. Configuration of the return path for the eddy current generated in the disc.

As will be discussed later, the design can utilize an aluminum disc and still provide adequate damping torque. Increasing the thickness of the disc not only increases its conductivity but also reduces the flux density obtainable from a given magnet. Since thickness directly affects conductivity, and damping is proportional to the square of flux density, a tradeoff evaluation is necessary before the thickness can be chosen for the final design. It has been found that if the magnets are placed too close to the edge of the damper disc, the conductivity of the return path for the eddy current in the disc is too low. Therefore, care must be taken to assure adequate clearance from the magnet to the edge of the disc. The remaining factor, flux density, has been the object of considerable engineering effort. Measurements have been made using a CU-507 magnet, the same magnet that was used in the damper built for the Passive Orientation and Damping System (PODS) by General Electric in 1963. Tests were made to be certain that the method used to charge the magnets resulted in maximum stored energy being imparted to the magnet for every measurement point. The results of these flux tests are shown in Figure 3-9 and 3-10 where flux density is potted as a function of air gap and for various magnetic circuit configurations. Since flux density is a parameter which is difficult to measure accurately, the data plotted in Figure 3-9 was taken

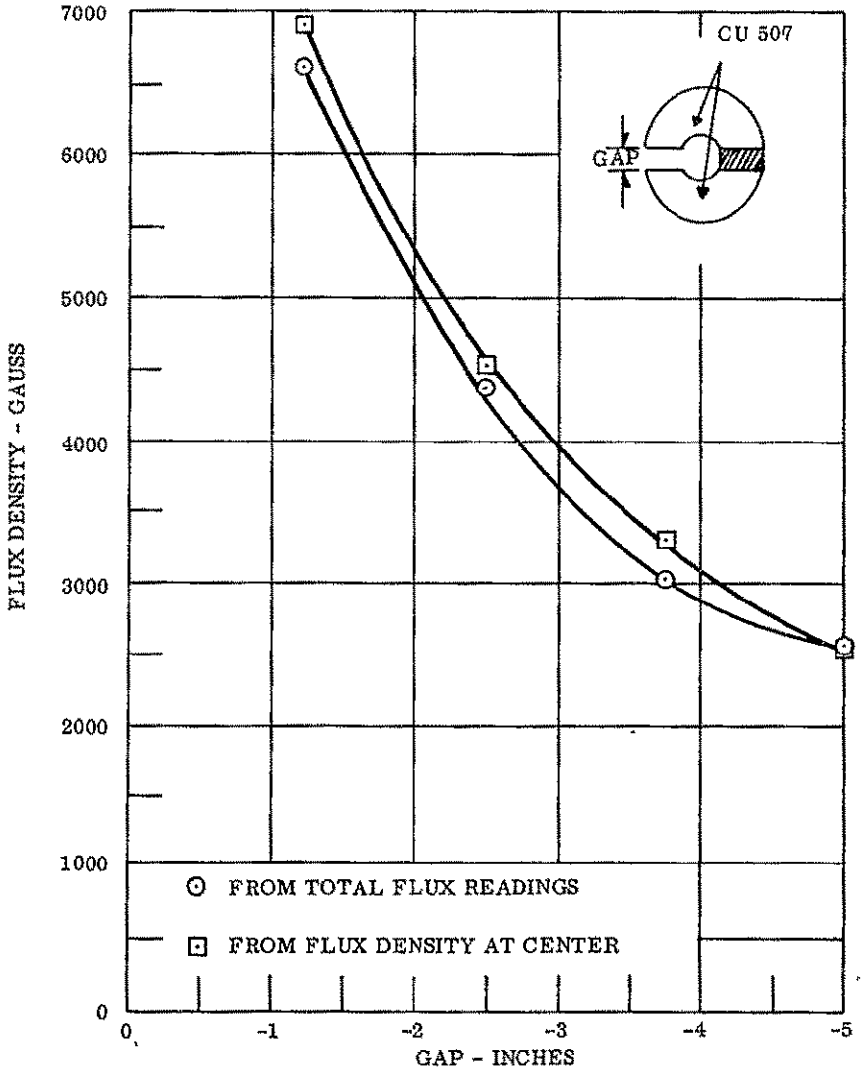

Figure 3-9. Flux Density Measurements

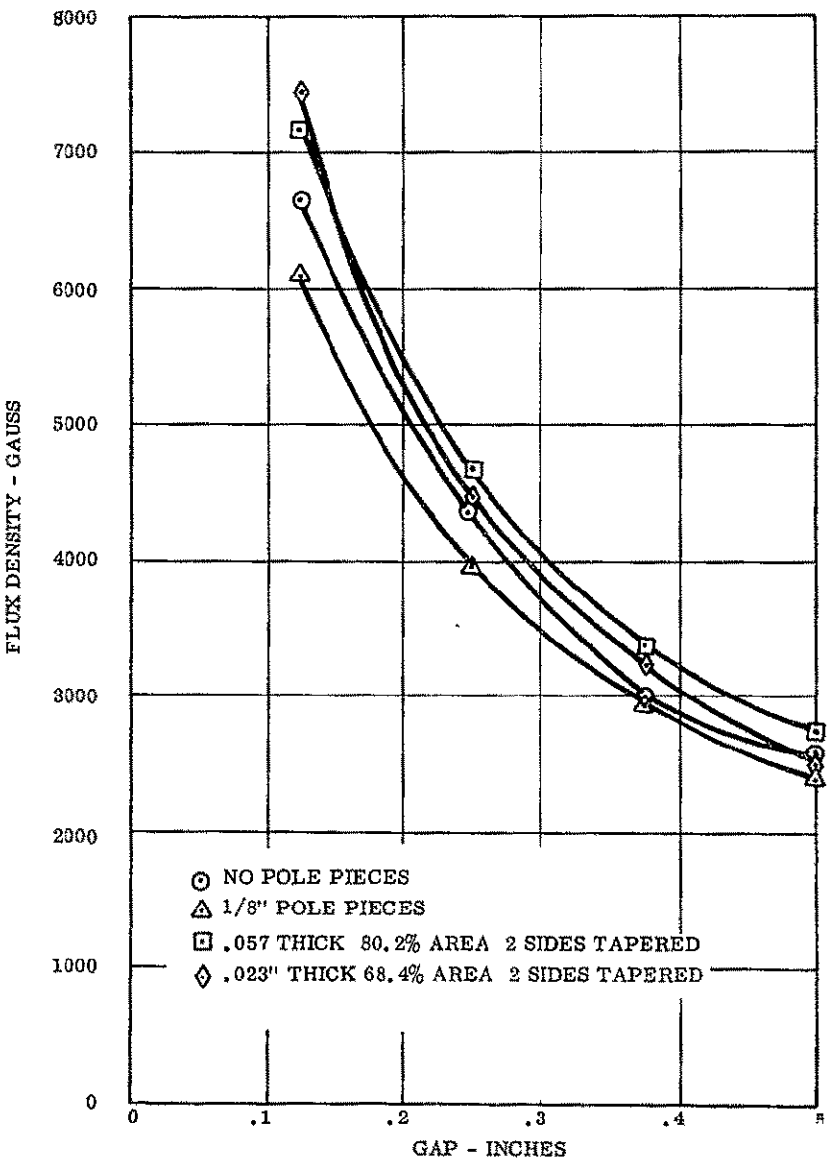

Figure 3-10. Flux Density Measurements Effect of Pole Pieces

to establish the general validity of the data, at least on a comparative basis. Flux density was determined for this plot both by measuring the total flux in the air gap and by using a different instrument which actually indicates flux density. It can be seen that although the curves are not coincidental they have the same general shape. It was found that the flux density increased inversely as the square root of the gap length. Measurements were also made of the effect of various types of pole pieces as shown in Figure 3-10. The flux density followed the same shape shown in Figure 3-9 and it was found that there is some increase in flux density due to tapered pole pieces.

The real measure of the value of various configurations is the change in damping torques obtained. A test was set up to evaluate the effects of various configurations with a copper disc approximately 6 inches in diameter. The results of these tests are tabulated in Table 3-1. A comparison of the tests: 1 and 2, 1 and 4, 5 and 6, and 5 and 7 is inconclusive as to the merit of pole pieces. Figure 3-11 depicts the arrangement of magnets used for the single penetrations and double penetration referred to in Table 3-1. A comparison of Tests 5 and 10 indicates the twofold increase obtained with the double penetration configuration. Tests 10 and 13 indicate the gain achievable by reducing the air gap.

The initial system requirement for damping torque from the eddy-current damper was approximately 1,560,000 dyne-cm-seconds. To achieve this value, various techniques were utilized to increase the torque obtained in Test 13. The basic equation given above for eddy-current damping was examined to determine the feasibility of reaching the design value.

In comparing the damping torque of the test damper (b_t) to that of the actual design (b_d), a slight modification of the basic damping equation is used:

$$b_d = b_t \left(\frac{D_d}{D_t}\right)^2 \left(\frac{B_d}{B_t}\right)^2 \left(\frac{p_t}{p_d}\right) \left(\frac{n_d}{n_t}\right) \left(\frac{t_d}{t_t}\right)$$

where:

subscript "d" refers to design values, subscript "t" refers to test values

p = resistivity of damper disc

t = thickness of damper disc

TABLE 3-1. DAMPING TORQUE OF EDDY CURRENT DAMPER

TEST CONSTANTS: 1. All Magnets CU 507
2. .125 in. Copper Disc, 5.85 in. dia.

Test No.	Magnet Arrangement	Air Gap (in.)	Pole Pieces	Radius (in.)	Damping Constant Dyne-cm-sec
1	2 single penetrations	.25	None	2.06	218,000
2	2 single penetrations	.25	1 Mag only 80%*	2.06	222,000
4	2 single penetrations	.25	2 Mags each 50%	2.06	209,000
5	1 single penetration	.25	None	2.06	105,400
6	1 single penetration	.25	Yes-56% area	2.06	98,000
7	1 single penetration	.25	Yes-80% area	2.06	110,000
8	1 single penetration	.25	Yes-80% area	2.31	111,000
9	1 single penetration	.25	Yes-80% area	2.56	89,500
10	1 double penetration	.25	None	2.00	228,000
11	1 single penetration	.195	None	2.31	171,000
12	1 single penetration	.195	None	2.31	142,000
13	1 double penetration	.195	None	2.31	336,000

*Percentage indicates ratio of area of pole piece face as compared to magnet face area.

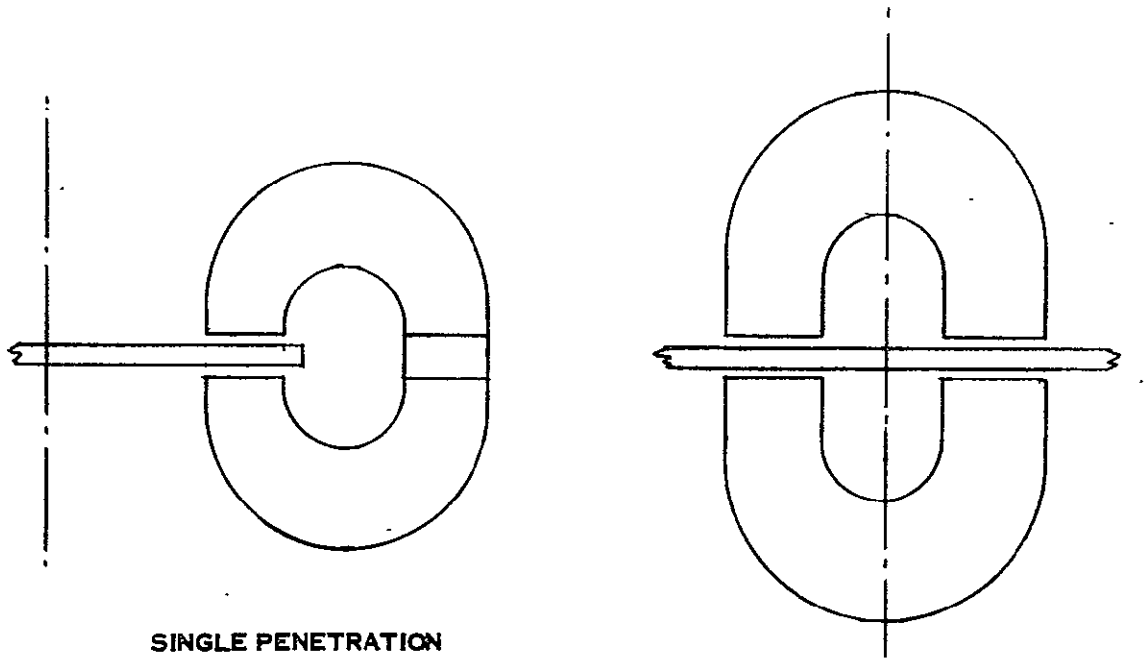

Figure 3-11. Magnetic Arrangement for Single and Double Penetration

and other symbols are as used previously. The following factors may then be used to determine how the required damping may be achieved in the design of the CPD:

$$\frac{D_d}{D_t} = \frac{4}{2} = 2 \qquad \text{(measurement of parts)}$$

$$\frac{B_d}{B_t} = \frac{5000}{4500} = 1.11 \qquad \text{(flux measurement indicates some improvement in design)}$$

$$\frac{p_t}{p_d} = .6 \qquad \text{(ratio of resistivity of copper to aluminum)}$$

$$\frac{n_d}{n_t} = \frac{4}{2} = 2 \qquad \text{(design)}$$

$$\frac{td}{t_t} = \frac{.100}{.125} = 0.8 \qquad \text{(measurement of discs used or to be used)}$$

$$b_d = 336,000 \times 2^2 \times 1.11^2 \times 0.6 \times 2.0 \times 0.8$$
$$= 1,600,000 \text{ dyne-cm-seconds}$$

Thus it can be seen that the calculated damping is only slightly higher than the actual damping required.

Actual tests using an aluminum disc and two pairs of magnets with double penetration (no pole pieces) gave a damping coefficient of about 20% low of the design value. A test was performed using a copper disc which gave results about 17% higher than required. An investigation was started to determine why the aluminum did not give the results predicted by the theory and tests and what could be done to increase the damping. The disc thickness was increased and the flux was increased by using longer magnets. Neither attempt proved adequate and copper was substituted for aluminum.

Before the substitution of copper for aluminum could be implemented, the system design requirements were reduced by 40% to 906,000 dy-cm-sec. for which the aluminum proved to be adequate.

3.2.3.2 Eddy Current Damper Suspension System

3.2.3.2.1 Background

1. Technical Memo TM 4176-007 Diamagnetic Shaft Support - Analytical Description
2. GE Document 64SD4326 Evaluation of/Suspension System for the Eddy Current Damper, CPD, ATS Program.

Reference 1 is a report on the analytical design of diamagnetic/suspensions. The analysis therein predicts the behavior of the CPD shaft under the influence of the worst combination of external cocking torques, radial forces, axial forces, and internal lateral force loads. The performance criterion employed is the amount of clearance remaining between the rotor and stator at their closest point of proximity for a given set of design parameters and a given set of loads. A positive value calculated for clearance implies successful performance for the suspension for the given conditions.

In Figures 12 through 24 of Memo TM 4176-007, values of the rotor clearance are plotted against the critical design parameter: lateral force load gradient. It may be seen from these curves that the external loads will be supported with positive clearance, provided the lateral force gradient produced by the magnetic torsional restraint does not exceed some critical value. This critical value depends upon the number of suspension magnets in each ring, the nominal air gap setting for these magnets, and upon certain dimensions in the CPD design.

Figure 3-13 is a schematic representation of the suspension system and shows the orbit loads that must be supported in addition to the lateral load introduced by the torsional restraint. (See Section 3.2.3.3 for a discussion of the torsional restraints.)

Figure 16 of Memo TM 4176-007 indicates that 8 magnets per ring set at a 0.050 inch air gap will support these loads for a lateral force gradient of less than about 11 dynes per mil.

However, as the expected lateral force gradient is 10 dynes per mil, it was decided to use 10 magnets per ring to provide some safety factor. In the CPD design the 10 suspension magnets are not uniformly spaced. In the direction of the lateral force, the suspension magnets are spaced at 30 degrees between centers, the equivalent of 12 magnets per ring. The expected performance, therefore, is better represented by Figure 13, of Memo TM 4176-007, which assumes 12 equally spaced magnets per ring. This curve shows satisfactory performance for lateral force gradients up to 16 dynes per mil, which gives an adequate margin of safety over the expected load of 10 dynes per mil. Thus, the non-uniform spacing of the suspension magnets gives additional safety margin without additional weight penalty.

Reference 2 is a comparative study of the two suspension systems considered for the CPD Eddy Current Damper. The conclusion from this study is presented below.

1. Test results and analysis demonstrate the feasibility of using a diamagnetic suspension system coupled with a ferromagnetic torsional restraint device on the eddy-current damper. Lateral forces, which are a characteristic of a magnetic torsional restraint system, are sufficiently low so as to pose no threat to the performance of a diamagnetic suspension system.

2. Analyses and test results showed that the torsion wire hysteresis effect on the eddy-current damper performance is negligible -- amounting to only 0.675 percent or less of total damping torque.

3. A comprehensive comparative analysis of torsion-wire suspension versus diamagnetic suspension for the eddy-current damper reveals that (although both systems adequately fulfill all requirements), the torsion wire suspension has some advantage over the diamagnetic suspension from the general standpoint of design, load carrying capability, least risk in area of schedule and cost, ease of manufacturing, and development testing.

   However, the diamagnetic suspension approach is very attractive from an experimental or state-of-the-art advance which is the purpose of the overall ATS program. Based on current data and past experience with the diamagnetic suspension system, the General Electric Co. feels confident that such a system, coupled with a magnetic torsional restraint, can be developed within schedule to fulfill all requirements of the ATS gravity gradient experiment.

From the above it was decided to use a diamagnetic suspension system in the CPD.

The following information is a brief discussion of the system, basic equations of the design, design parameters and materials considerations.

The cone angle was selected such that the suspension system is stiffer in the radial direction to support the 1200 dyne cm cocking torque and the added radial load due to the torsional restraint.

3.2.3.2.2 Analytical Approach

The following discussion is included as it is this basis from which the suspension system, as detailed in Memo TM-4176-007, was designed in order to determine the optimum suspension design, considering the type and quantity of magnets, material of diamagnetic rotor, cone angle and thickness of diamagnetic rotor, and air gap spacing, it is necessary to know the repulsion force versus air gap characteristic for a single magnet in combination with the diamagnetic material. These characteristics have been obtained for a variety of magnets in combination with both bismuth and pyrolytic graphite in a variety of thickness./ These results have been obtained experimentally by direct measurement of forces, and also analytically, based on measurement of the magnetic field pattern for a given magnet.

The force exerted on a diamagnetic specimen in a non-uniform field may be expressed as follows (see Figure 3-12):

$$dF = \frac{1}{2} K \frac{dH^2}{ds} dv \qquad (1)$$

where

F = force, dynes

K = volumetric susceptibility of the specimen, cgs units/cm^3

H = field strength, oersteds

v = volume of specimen, cm^3

s = distance from pole face, cm.

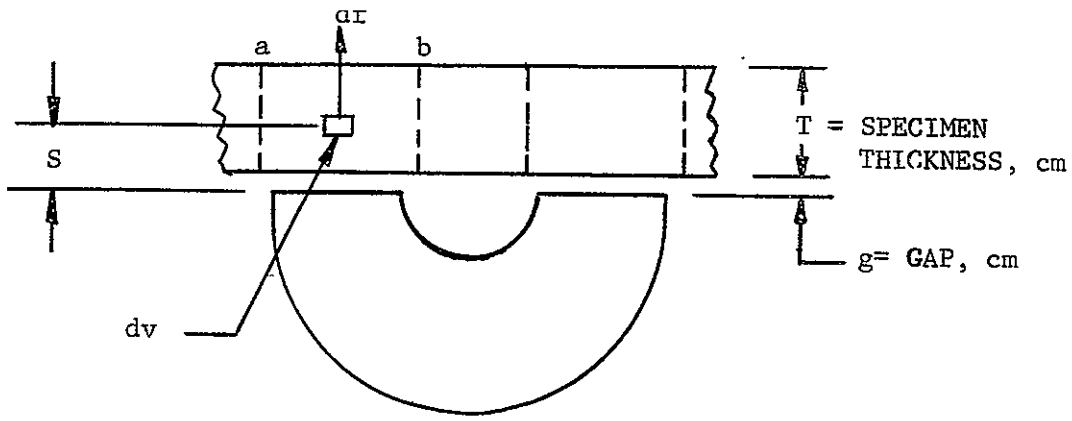

Figure 3-12. Force on Diamagnetic Specimen in Non-Uniform Field

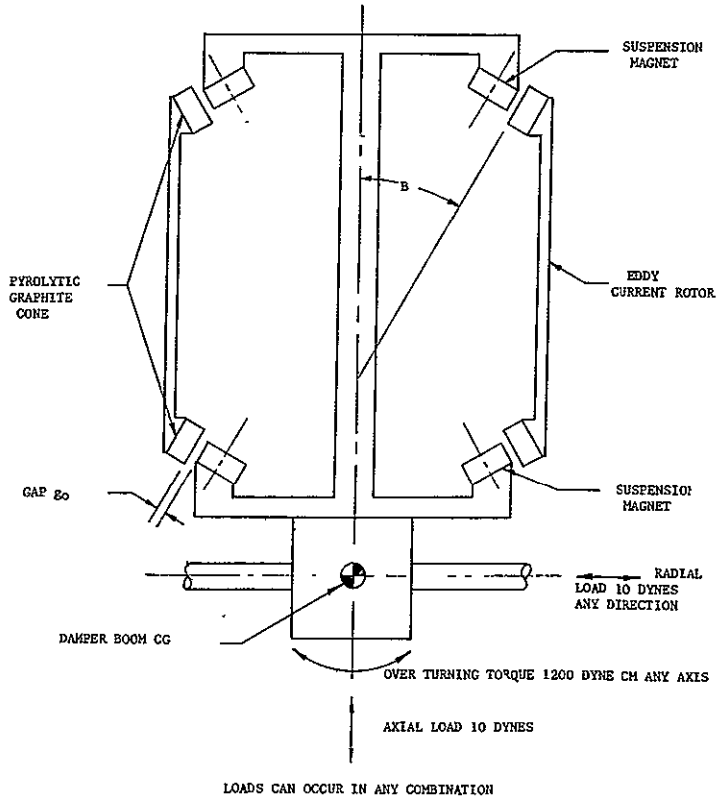

Figure 3-13. Eddy-Current Damper Suspension System Schematic

The field strength was measured as a function of distance from the pole face for several magnets. When values for H^2 were plotted against s, it was found that a decaying expotential curve gave a very close approximation of the measured data.

$$H = H_o^{\,2} e^{-ms} \tag{2}$$

$$\frac{dH^2}{ds} = -H_o^{\,2} \, m \, e^{-ms}$$

where

H_o = field strength at s = o

$-H_o^{\,2}m$ = initial slope, oersted^2 /cm

m = decay rate, cm^{-1}

A simplifying approximation was made by assuming that the same value of dH^2/ds exists for a given value of s, at points between a and b, which define the effective pole face area. It was further assumed (based on analysis of extensive test data) that the effective pole face area equals 1.8 times the actual pole face area. The differential volume for both poles, dv, may then be expressed as follows:

$$dv = 2 \times 1.8 \, A \, ds \tag{3}$$

where:

A = actual pole face area, sq cm

The total force on specimen, from both magnet poles, is obtained by combining Equations 1 and 3:

$$dF = \frac{1}{2} K \, (-H_o^{\,2} \, m \, e^{-ms}) \, (2 \times 1.8 \, A \, ds)$$

By integration,

$$F = \int dF = \frac{-1}{2} KH_o^2 \; m\,(2)\,(1.8)A \int_g^{g+T} e^{-ms}\, ds$$

$$= -1.8\,AK\,H_o^2 m \left[\frac{e^{-ms}}{m}\right]_g^{g+T}$$

$$= -1.8\,AK\,H_o^2 \left[e^{-m(g+T)} - e^{mg}\right]$$

$$= -1.8\,AK\,H_o^2 \left[e^{-mT} - 1\right] e^{-mg}$$

$$F = 1.8\,AK\,H_o^2 \,(1 - e^{-mT})\, e^{-mg} \qquad (4)$$

$$F = F_o e^{-mg}$$

Equation 4 expresses the force between one magnet and a specimen in a non-uniform field. If the specimen is diamagnetic, the susceptibility, K, is negative, and the force is repulsive. The factor $(1 - e^{-mT})$ shows the dependence of force on the thickness, T, of the specimen. The force is seen to decay exponentially with air gap, g.

3.2.3.2.3 Experimental Approach

For the many measurements which have been made of force versus air gap, it has been found possible to fit a decaying expotential characteristic to the measured data. This characteristic is of the following form.

$$F = a + F_o e^{-mg} \qquad (5)$$

This form differs from the analytical result only by the constant term, a.

3.2.3.2.4 Diamagnetic Suspension Design Equations

The diamagnetic suspension consists of a conical diamagnetic element located at each end of the rotor, and a ring of n magnets fixed to the stator, equally spaced around the diamagnetic cone, as shown schematically in Figure 3-13.

The diamagnetic forces tend to keep the rotor centered in the null position. The general shape of the force versus displacement characteristics of a diamagnetic suspension has been shown both analytically and experimentally to have the non-linear form of Figure 3-14.

For initial component design purposes, a linear approximation may be used as follows:

$$F = -K\,x$$

where

F = restoring force

x = displacement from null

K = slope of the actual characteristic at null point.

The value of K represents the force gradient, or stiffness, of the suspension at the null position. Since the stiffness actually increases with displacement, use of the linear approximation yields a properly conservative design.

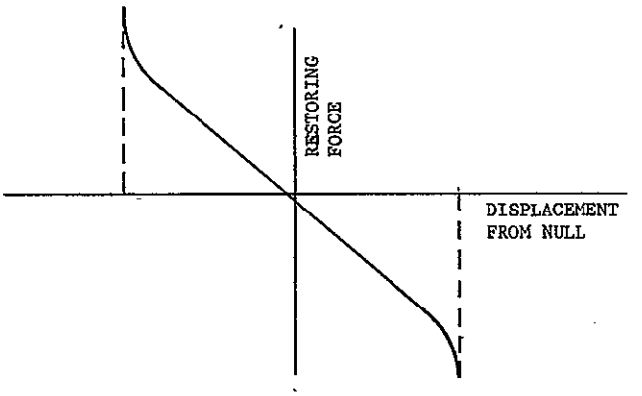

Figure 3-14. Diamagnetic Suspension Characteristic

The radial force gradient at the null point of a diamagnetic suspension has been found to be as follows:

$$K_r = \left.\frac{dPr}{dr}\right]_{r=o} = \frac{1}{2} F_o\, m\, e^{-mg_o}\, n\, \cos^2 B \qquad (6)$$

where $F_o\ e^{-mg}$ can be determined from the equation $F = a + F_o\ e^{-mg}$ which expresses the single magnet force versus gap characteristic, and the symbols are as previously defined. This expression represents the stiffness due to one diamagnetic cone and n magnets. The total force capacity at that end of the rotor is found by multiplying K_r by the radial displacement at that end.

Similarly, the axial force gradient at the null point of a diamagnetic suspension has been found to be as follows:

$$K_Z = \left.\frac{dP_Z}{dZ}\right]_{Z=0} = F_o\ me^{-mg_o}\ n\ \sin^2 p \qquad (7)$$

This expression represents the axial stiffness at each end of the suspension. The total axial force gradient due to both ends of the suspension is $2K_Z$. The total axial force capacity is found by multiplying $2K_Z$ by the axial displacement of the rotor.

3.2.3.2.4.1 Selection of Magnet Gap Setting. Values for the parameters F_o and m may be determined experimentally. The suspension capability, P_r, is found by multiplying K_r by the maximum radial displacement, r, where

$$r = g_o / \cos B$$

Therefore

$$P_r = \frac{1}{2}\ F_o\ n\ \cos B\ \left[mg_o\ e^{-m\ g_o}\right].$$

The function in the brackets has been normalized and plotted as Figure 3-15. This curve shows that the maximum load capacity is obtained when the initial air gap is set a 1/m where m is the decay rate of the single magnet force characteristic. This decay rate has been found experimentally to be $m = 15$ inches $^{-1}$ for the 5U41B magnet. The optimum air gap setting then would be 0.067 inches. A value 25 percent above or below this figure would result in a decrease in capacity of only about 3 percent, so the initial gap setting for the CPD is specified to be in the range from 0.050 to 0.083 inch in order to satisfy the

suspension capacity requirements. Other factors must determine the actual setting. The actual setting should be kept as small as possible within the specified range, in order to maximize the radial force gradient, or stiffness, K_r, Mechanical tolerances and launch environmental stresses also must be considered in finalizing the initial gap setting.

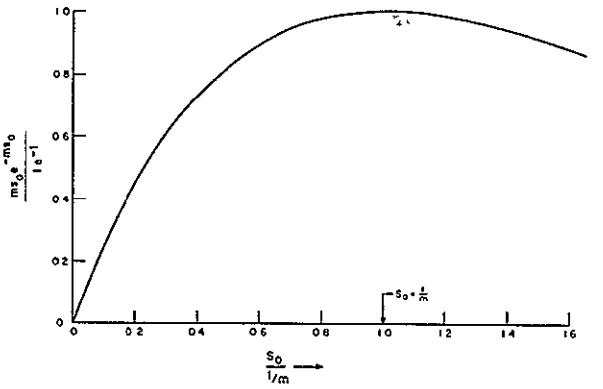

Figure 3-15. Suspension Load Capacity vs. Initial Air Gap Setting

3.2.3.2.5 Design Considerations

3.2.3.2.5.1 Material. The force acting on a body placed in a magnetic field is discussed under Analytical Approach. In these equations, it is shown that the force is directly proportional to the susceptibility of the material which is being acted upon. Diamagnetic materials with their negative susceptibility are repelled by a magnetic field. Many materials are slightly diamagnetic, but those having the largest negative susceptibilities (and thus capable of the largest repulsion forces) are bismuth and pyrolytic graphite. The volume susceptibility of bismuth is -13×10^{-6} and that of pyrolytic graphite perpendicular to the deposition plane is approximately -47×10^{-6}. Thus, the actual susceptibility realizable for support forces depends upon the configuration of the magnetic field and its relationship to the graphite in the field.

Bismuth was used in early experiments on diamagnetics and was subsequently used in the construction of the Passive Orientation and Damping System (PODS) damper in 1963 because of ready availability and ease of manufacture. Since that time, pyrolytic graphite has become more generally available and its various physical properties more accurately defined. Graphite has the advantage of a density which is only 22.5% of that for bismuth. Therefore, in the interest of obtaining maximum suspension capability with minimum weight, pyrolytic graphite was used in the suspension of the eddy current damper.

Several samples of pyrolytic graphite were tested for force characteristics. The results of typical data have been plotted on Figure 3-16. On this curve, it can be seen that there was a considerable increase in force available from the graphite, although it was not nearly as large as would have been expected based on a comparison of susceptibilities. For the 0.125-inch thick samples, there was only a change of 2.5:1 increase in force from the bismuth. The results of another test with a different magnet indicates an improvement of about 2:1 for the graphite. However, for both magnets, an increase of about 4.5 to 1 is possible by increasing the thickness of the graphite by about 3.1 to 1 so that a substantial increase in force is available with graphite which because of its much lower density, would represent a gain in force per unit weight. The actual thickness specified is 0.25 inches thick.

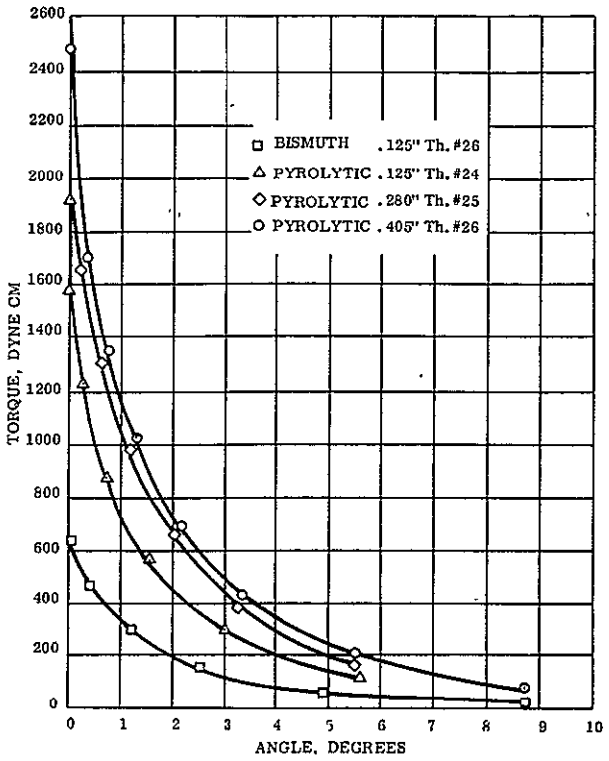

Figure 3-16. Torque Angle Characteristics for Bismuth and Various Thickness of Pyrolytic Graphite

The disparity between the theoretical and experimentally determined ratios of forces available from graphite as compared to bismuth must be due to differences in susceptibilities of the materials actually tested. Only one reference (Fishback) has given a value for the susceptibility of pyrolytic graphite and discussions with vendors indicate that there is a wide variation in some of the physical properties between samples.

During testing a significant difference was noted between pyrolytic graphite samples of the same thickness. Two 0.125 inch samples produced forces about 15 percent different, and two 0.250 inch samples produced forces about 10 percent different. This variation must be considered in the design.

The manufacturing process for the pyrolytic graphite cones requires the use of more than one cone, nested together to give the required 1/4 inch thickness. Tests were run with two 1/8-inch flat samples, and the results did not differ significantly from tests using one 1/4-inch flat sample. No harmful result is expected from use of nested cones in the CPD.

A series of tests were conducted to determine which portion of the pyrolytic graphite was useful in producing force. In these tests the magnet was located at various positions relative to the edge of the pyrolytic graphite. From these tests it was determined that the pyrolytic graphite surface should overlap the projected pole face by 0.1 inch on each side. "Side" of the magnet is defined as shown in Figure 3-17. No "overlap" is necessary on each end. That is, the magnet side leakage flux contributes force, but the end leakage flux does not.

Diamagnetic repulsion force measurements were made to determine the effect of high temperature. A 13 percent loss in force was suffered when the pyrolytic graphite temperature was elevated to 200°F, as compared to the force previously determined for room temperature conditions. When the pyrolytic graphite was returned to room temperature, the full force was recovered, showing that the change was reversible. It should be noted that the suspension design of the current CPD is sufficiently conservative to support the specified loads at the high temperatures.

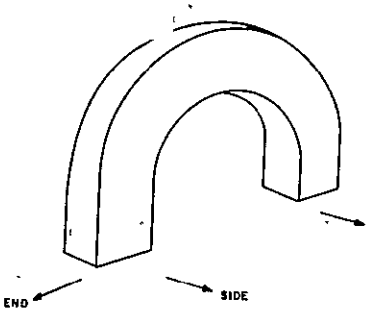

Figure 3-17. Definition of Magnet Side

Diamagnetic repulsion force measurements were made to determine the effect of pyrolytic graphite surface contaminants. The series of tests involved a pyrolytic graphite specimen subjected to various degrees of maltreatment, ranging from a

perfectly clean specimen to a specimen with iron filings rubbed into the graphite surface. The general conclusion from these tests was that normal laboratory and assembly procedures would not contaminate the pyrolytic graphite severely enough to cause a reduction in suspension forces. No measurable force degradation was observed, for example, after a magnet was forcibly rubbed against the front surface of the graphite for 30 seconds or more. The same result was obtained after a piece of low carbon steel was forcibly rubbed against the graphite, scratching its surface and leaving graphite shavings on the surface. In the next test, the surface was covered with iron filings which were rubbed into the surface using a piece of low carbon steel. The excess filings were removed by tapping the specimen. Only a 33 percent reduction in force was suffered after this severe treatment. Only if a significant portion of the pyrolytic graphite should become so contaminated would the suspension be significantly degraded. The probability of this occurring is considered extremely small, under normal handling conditions.

3.2.3.2.5.2 Selection of Permanent Magnet. The force characteristics were determined for five different type permanent magnets (all Alnico V). The GE Catalog No. 5U41B magnet was found to be superior to all others tested, in force per unit weight of magnet. All subsequent tests were conducted using this type magnet.

3.2.3.2.5.3 Consistency of 5U41B Magnets. Various 5U41B magnets produced the same forces when used in combination with a given pyrolytic graphite sample, and when charged to the same magnetic strength. To obtain the desired suspension characteristics, magnets used in the suspension will be charged to the same strength and checked prior to assembly.

3.2.3.2.5.4 Effect of Magnet Grouping. A series of tests were conducted with magnets in groups of two and three magnets, spaced about 0.4 inch apart, as in the CPD preliminary design. Force levels in these tests were found to be just two and three times the force measured for a single magnet. The tests were repeated for smaller spacings. Only when the spacing was reduced to 0.1 inch did a significant effect appear; at 0.1 inch the decrease in force was about 10 percent.

3.2.3.2.5.5 Effect of Magnet Polarity. The tests described immediately above were repeated with the relative polarities of the magnets reversed. The test results were approximately the same. The magnet polarity is immaterial for magnet spacings greater than 0.1 inch.

3.2.3.2.5.6 Effect of Mounting Surfaces. In the CPD two flats are ground on the curved parts of the horseshoe magnets to facilitate mounting. This was done to three of the magnets used in the series of tests. The depths of cut were 0.030 inch, 0.050 inch, and 0.070 inch, respectively. The magnets were recharged. Force characteristics were then measured and found to be identical with those measured prior to machining.

3.2.3.2.5.7 Effect of External Magnetic Fields. In accordance with a request from NASA, the CPD magnets were subjected to a 50-gauss field degaussing test with no apparent degradation. Speciments of three types of CPD magnets (ECD, TR and suspension) were subjected to magnetic fields of about 50 gauss dc, and 70 to 80 gauss peak ac at a frequency of 60 cps. The test was monitored for changes in flux density. Exposures were about 60 seconds in each case, and the magnets were rotated in the field to provide exposure in several directions. Flux was measured in the approximate center of the pole gap (pole face in the case of the suspension magnet) with the gaussmeter probe held firmly in place at all times.

Although a change of 10 to 20 gauss would have been discernible no change was observed. Therefore, it is GE's conclusion that an external field of 50 gauss, maximum, has no effect on the CPD magnets, and such exposure is quite possible.

3.2.3.3 Eddy Current Damper Torsional Restraint

Included in GE report Document No. 64SD4326 are initial calculations for a diamagentic suspension system using a ferromagnetic torsional restraint with its associated lateral force. Results of this study are included in Table 3-2 of this report.

As previously discussed a torsional restraint must be included to return the damper booms to a predetermined null with respect to the vehicle. The method used for the eddy current

damper consists of 2 elongated ferromagnetic cat eye patterns 180° apart wrapped around a cylinder. The patterns are approximately 120° long, .010 inch thick and .366 inch wide at the widest point. The design goals of the torsional restraint system were to provide a restoring torque to the booms while 1.) having a lateral force less than 10 dynes/mil, 2.) having a range of ± 45° from null 3.) having no hysteresis 4.) having a linearity of 6% of maximum torque. In light of these requirements considerable effort was spent on three different materials for the pattern. The results are presented below. Other materials were investigated but were discarded for various reasons.

Initial work was done using patterns manufactured from .001 inch thick 302 stainless steel. Although 302 stainless is normally non-magnetic, this material was cold reduced from .002 inch thick which caused a change in the magnetic properties making it slightly magnetic. Test results are presented in Table 3-2.

In these tests, the desired torsional restraint (i.e., the apparent spring constant) obtained from the ferromagnetic torquing member as well as the accompanying (but undesired) lateral force were determined. These characteristics were measured as a function of:

1. Presence or absence of pole pieces
2. Gap length
3. Flux density
4. Misalignment (tilting) of torsional restraint element.

It was concluded from the results of these tests that:

1. Torsional and lateral forces are roughly proportional to flux density
2. Ratio of the lateral force to torsional force is independent of flux density
3. Pole pieces reduce the ratio of lateral force to torsional force.
4. Larger air gaps produce less lateral force and a smaller ratio of lateral force to torsional force.

TABLE 3-2. RESULTS OF FERROMAGNETIC TORSIONAL RESTRAINT TESTS

Line No.	Gap (in.)	Flux Density (Gauss)	Pole Pieces	Torsional Force			Lateral Force		Lateral Force / Torsional Force = dynes/.001 in. / dynes/degree
				(dyne cm) / (degree)	(dynes) (degree)	*Plotted in Figure	(dynes) (.001 in)	*Plotted in Figure	
1	0.50	2400	Without	10.5	1.50	A.2-1	4.3	A.2-7	2.83
2	0.25	4200	With	22.0	3.14	A.2-2	11.0	A.2-8	3.50
3	0.25	4800	Without	24.0	3.43	A.2-3	13.0	A.2-9	3.79
4	0.25	2400	With	11.0	1.57	A.2-4	5.0	A.2-10	3.18
5	0.25	4300	Without	20.0	2.86	A.2-5	12.0	A.2-11	4.21
6	0.25	2400	Without	8.0	1.14	A.2-6	5.0	A.2-12	4.37
7	0.50	2400	Without	10.0	1.43	A.2-13	Special Test: Magnet Tilted 17 degrees with Respect to Crescent.		

*See Appendix A.2 of GE Document No. 645D4326 for Figures

5. Tilting the torsional member with respect to the imposed magnetic field had little effect on the torsional force.

This initial testing proved that a magnetic torsional restraint was feasible to construct within the confines of the CPD and laid the ground work for further development effort. However 302 stainless provided too much lateral force for the suspension system to handle; effort was therefore directed to magnetic recording tapes.

Test results using Eastman Sound Recording Tape, Type A303 determined that satisfactory torque vs. angle characteristics were obtainable and that lateral forces of approximately one half that of the stainless steel were obtainable. However, as shown in Figure 3-18, that for oscillation amplitudes below 15 degrees, more energy is dissipated by hysteresis in the torsional restraint pattern than by eddy currents in the eddy-current damper. From these results investigation was terminated on magnetic tapes and directed towards magnetic powder dispersions in epoxy resin.

The investigation of low-hysteresis materials for the eddy-current damper magnetic torsional restraint device was concentrated in the area of testing laboratory samples of magnetic powder dispersions in epoxy resin. This type of material provides the most flexibility in design because specimen thickness and the concentration of magnetic power can be varied as well as the type of powder to provide the desired performance characteristics.

The main difficulty to be overcome with the dispersion-type materials was non-linearity due to voids and non-uniformity of the dispersion. The formulation technique was improved with successive laboratory samples such that acceptable linearity is now being obtained.

Samples of nickel, cobalt, electrolytic-grade iron and carbonyl-iron-powder dispersion were formulated. Of these, only the iron powders produced less hysteresis than the specified magnetic tape. Carbonyl iron was vastly superior because it produced negligible hysteresis.

Initial tests of carbonyl-iron powder dispersions indicated a characteristic of relatively strong lateral force but subsequent tests with variations in thickness of specimen,

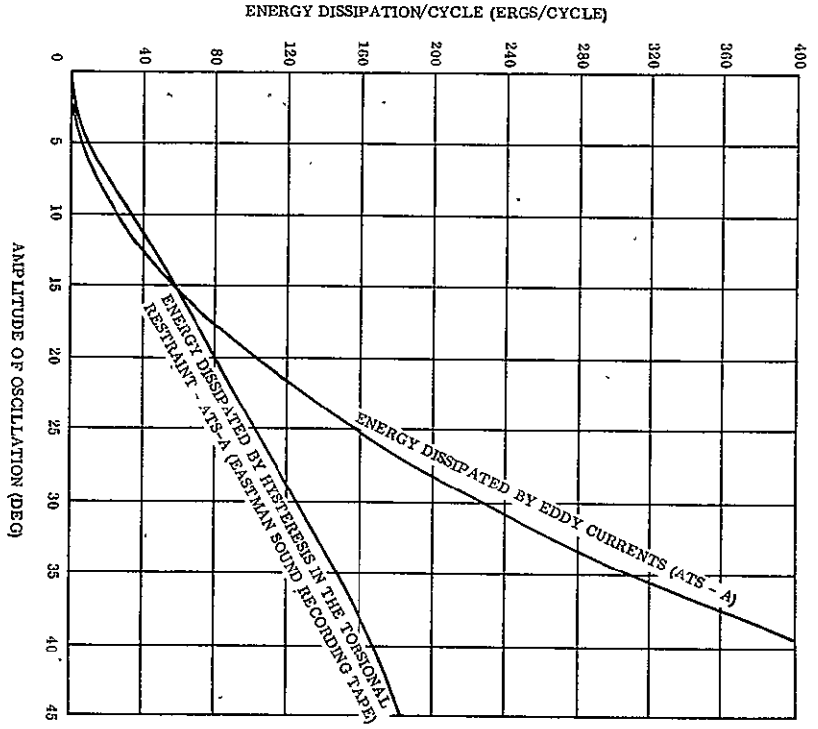

Figure 3-18. Energy Dissipated by Eddy Currents and Hysteresis in Torsional Restraint Versus Amplitude of Oscillation (ATS-A Eddy-Current Damper)

percentage of iron, and magnetic flux have produced sufficient data so that it is now possible to hold the lateral force to an acceptable level.

Improvements in the formulation technique resulted in the production of uniform magnetic dispersions which were essentially free of voids and other imperfections. The effect of material thickness, magnet flux, air gap, and percentage of iron were investigated to arrive at a near optimum pattern configuration for both the ATS-A and ATS-D/E applications. A final configuration was selected which met all performance requirements and which had no measurable hysteresis loss when tested on equipment capable of measuring as little as 1 dyne-cm of hysteresis torque.

Consequently the previously selected Eastman sound recording tape, Tape A303 was replaced by this new material on all CPD units. Engineering Unit 1 has a 20% carbonyl iron magnetic dispersion material, 0.015 inch thick. Engineering Unit 2 has a 5% carbonyl iron

magnetic dispersion material 0.0075 inch thick. Further development of the material and pattern configuration led to the selection of one pattern design for all prototype and flight units. This pattern contained 5% carbonyl iron by volume and is 0.010 inch thick. The desired magnetic torque for either ATS-A or ATS-D/E is obtained by adjusting the magnet flux.

With the 5% carbonyl iron pattern 0.010 inch thick, nominal performance was obtained as shown in Table 3-3.

TABLE 3-3. TORSIONAL RESTRAINT MATERIAL NOMINAL PERFORMANCE

	ATS-A	ATS-D/E
Torque, dyne cm/deg (2 patterns)	23.1 ± 10%	3.85 ± 10%
Lateral Force, dynes/mil (2 patterns)	9 max	1.5 max
Hysteresis, dyne cm	None	None
Linearity, % of max torque	6% Max Variation	6% Max Variation
Angular Magnetic Travel, deg	± 48° min	± 48° min
Nominal Magnet Flux, gauss	1350	550

Tests were conducted with the carbonyl iron patterns over a range of oscillation amplitudes from ± 50 degrees down to ± 2 degrees of angular travel. No hysteresis was measurable at any of these amplitudes.

Elevated temperature testing of the carbonyl iron patterns indicate a variation in torque of less than 0.4% between room ambient and 150°F. Therefore, a maximum variation in torque less than 1% is anticipated due to thermal effects over the operating temperature range of the CPD.

Material specification 171A4411 for the carbonyl iron-epoxy magnetic dispersion was prepared and issued.

The other materials investigated included paramagnetic and feebly magnetic metallic materials (such as Hastelloy F, 65-30 CuNi, 10-8 MnNi, and 17-7 PH) antiferromagnetic compounds (including $MnC1_2 . 4H_2O$ and MnO) and plastic materials with a magnetic filler (including PR1422 polymer and iron powder dispersed in epoxy resin). Of the materials listed, all exhibited lower hysteresis loss than either 302 stainless steel or A303 sound tape, except the 10-8 Mn-Ni steel. Hastelloy F exhibited almost immeasureable hysteresis loss but the torsional restraint varies excessively with temperature and lateral force is relatively high. PR1422 polymer was found to have unacceptable outgassing characteristics and 65-30 CuNi exhibited high lateral force. Testing of antiferromagnetic compounds was discontinued due to the difficulties forseen in adapting this type of material to the design. 17-7PH had a low hysteresis loss and low lateral force but the design flexibility of the expoxy/iron dispersion was a considerable advantage.

3.2.3.4 Passive Hysteresis Damper (PHD)

The hysteresis damper was an amplitude dependent device. This particular damper had a constant damping torque over the entire range of ± 45°. Damping torque is developed by passing a vane of magnetic material such as 3.5% chrome steel, approximately .010 inches thick, between two sets of permanent magnets circuits spaced 180° apart. As the vane moved between the magnetic fields of the circuits, the magnetic domains in the vane were first oriented and then reversed. During this reversal energy was dissipated in proportion to the area of the hysteresis loop of the vane material. The fact that the vane was a magnetic material which was attracted to the permanent magnets with a relatively high force level, precludes the use of a diamagnetic suspension system of a reasonable size for a magnetic hysteresis damper. Although GE had developed a hysteresis damper, the PHD used in the CPD was subcontracted by NASA direction to TRW Inc. (Thompson Ramo-Woolrige Inc.) Therefore the information presented is primarily a discussion of the testing and mechanical design in which GE was involved.

Figures 3-19 and 3-20 show the basic design of the PHD and is typical for all units with the exception of the wire suspension system shown in Detail C of Figure 3-20 which was used for ATS-A type units only. A redesigned suspension system was needed on ATS-D & -E type units and is shown in Figure 3-21.

Functionally the PHD has had a minimum of problems. Test data was well within specification and eddy current damping has been below 4% of the total damping.

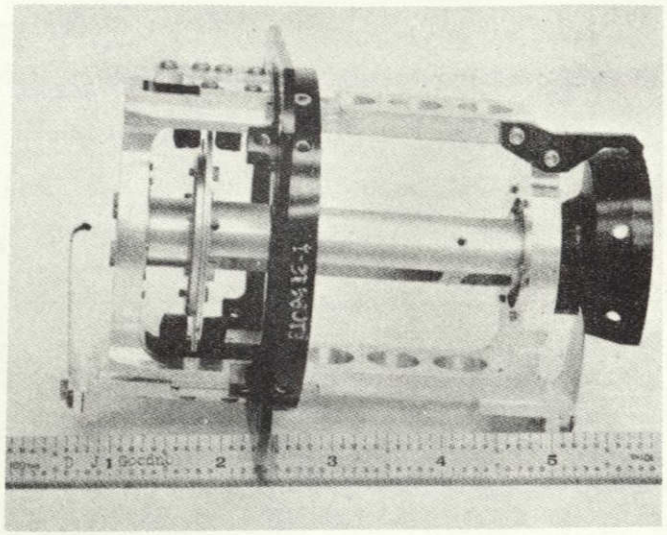

Figure 3-19. Passive Hysteresis Damper for ATS-D/E Configuration (Engineering Unit No. 2)

It was initially intended to cage the PHD rotor during launch and to provide magnetic shielding to prevent distortions of the magnetic circuits from other magnetic fields. After engineering tests it was decided that the shielding was not necessarily due to lower than anticipated extraneous fields in PHD area. Also engineering vibration tests determined that caging was not necessary for ATS-A type units. However, ATS-D & -E units, with their necessary reduced diameter wires, (length could not be reduced due to envelope considerations) could not withstand the vibration uncaged using the same suspension system as used on ATS-A and rather than having one unit caged and the other uncaged it was decided to redesign the ATS-D & -E suspension system to eliminate caging which obviously presents a simplier design and cleaner interface.

The following is a discussion of the suspension system. The basic difference between the ATS-A & -D designs are in the wire attachment method and the suspension method. The ATS-A version used the double cantilever flexure system and wire attachment method shown in Figure 3-20. This method produced a spring-mass system that could not be tolerated in the ATS- D & -E System. Therefore, a development test program was undertaken out of which evolved the single cantilever flexure design shown in Figure 3-21 & 3-22. A further requirement of the suspension system was that the null position shift due to vibration not exceed ± 1°. This was required because the clutching system in the CPD has no nulling

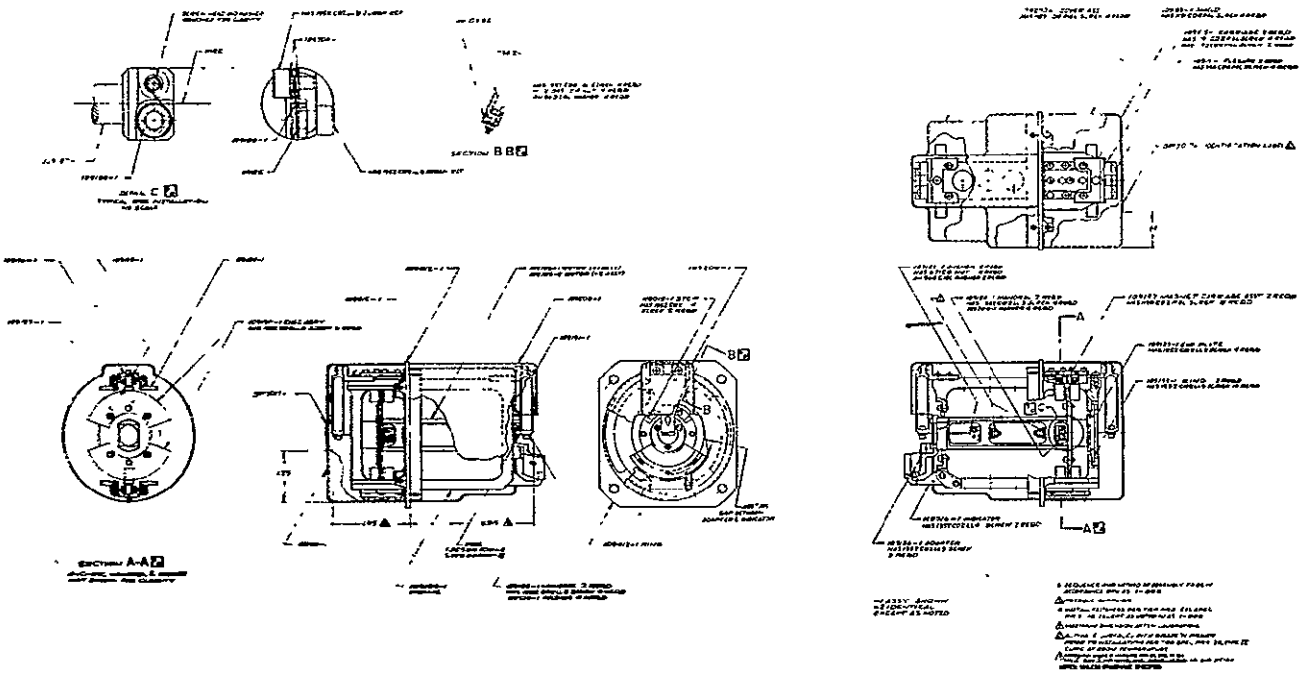

Figure 3-20. Passive Hysteresis Damper Details

technique to prevent the dampers from being picked up off of null which if done will produce a pointing error in the vehicle.

The development tests were conducted on the PHD Development Model and Engineering Unit 2. The test procedure used was that specified in Reference 2*, with minor changes due to intermediate results. The standard air-melted, 0.003-inch 302 cres wire was used throughout the tests. Most of the wire had been qualified per Reference 3* but samples were also used that came both before and after the qualified section of wire on the spool.

3.2.3.4.1 Variable Torque Hysteresis Damper (VTHD)

The Passive Hysteresis Damper (PHD) produces a constant torque of 50 dyne-cm and uses a torsional restraint of 3.5 dyne-cm/deg. This damping constant could result in a hang-off angle from the null of as much as 14.3 degrees at times of low vehicle oscillations. The Variable Torque Hysteresis Damper (or bow-tie damper as it is sometimes called) is

*See Paragraph 3.2.2.4.4

designed to have a constant torque of only 7 dyne-cm about the null position. (± 10 degrees from null as shown in Figure 3-23), producing a maximum hang off of 2 degrees using the same torsional restraint. In addition, the damping value is increased from 7 dyne-cm (between +10 and -10 degrees) at a slope of 29 dyne-cm/deg to the limits of +45 and -45 degrees. Thus, a maximum torque of 108 dyne-cm is produced at the extremes. The relationship between the original PHD and the VTHD is illustrated in Figure 3-23; torsional restraint effects have been omitted from the curves for clarity.

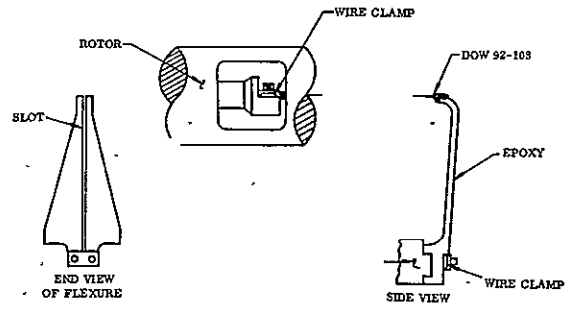

Figure 3-21. Passive Hysteresis Damper Suspension System, ATS-D/E Configuration

This damping characteristic has the desirable effect of reducing the required damping time. It would not be possible to produce a constant torque damping with the higher torque because the hang-off angle would increase. Therefore, GE proposed a change to crescent shaped magnets in the PHD and NASA authorized the change in the ATS-D/E systems through Modification 21 (dated January 18, 1967) to the contract.

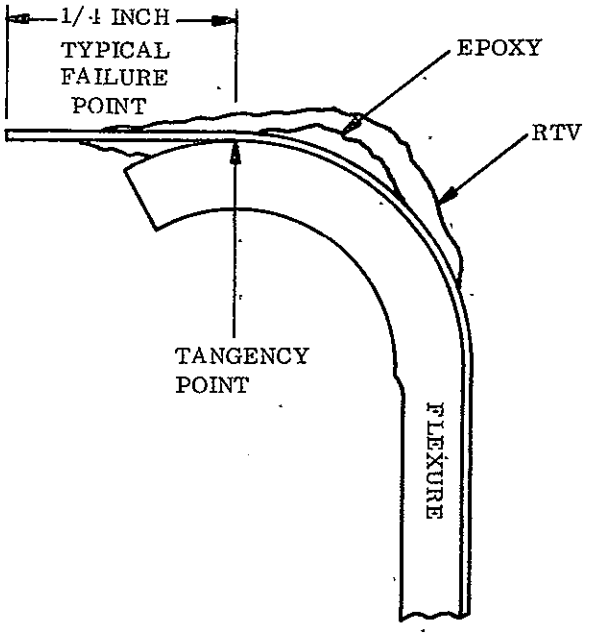

Figure 3-22. Attachment of Wire to End Flexure

3.2.3.4.2 Summary of Results, Passive Hysteresis Damper

Thirty-three vibration tests were performed on the two units. The input used was the worst axis (Z-Z) of the Qualification Sinusoidal Vibration Schedule per Specification SVS-7331

at a one-octave-per-second sweep rate instead of the two-octaves-per-second-prescribed in Reference 1*. The results of the tests are tabulated in Table 3-4.

All broken wires were examined (discussed in detail in Reference* 4) to determine the nature or cause of the failure. These results are summarized in Table 3-4. Their conclusion was that, for all but one of the failures, the wire failed in a brittle manner. Several failures were identified as resulting from fatigue, but no conclusion could be reached as to whether a material defect in the wire was the cause of any of the failures.

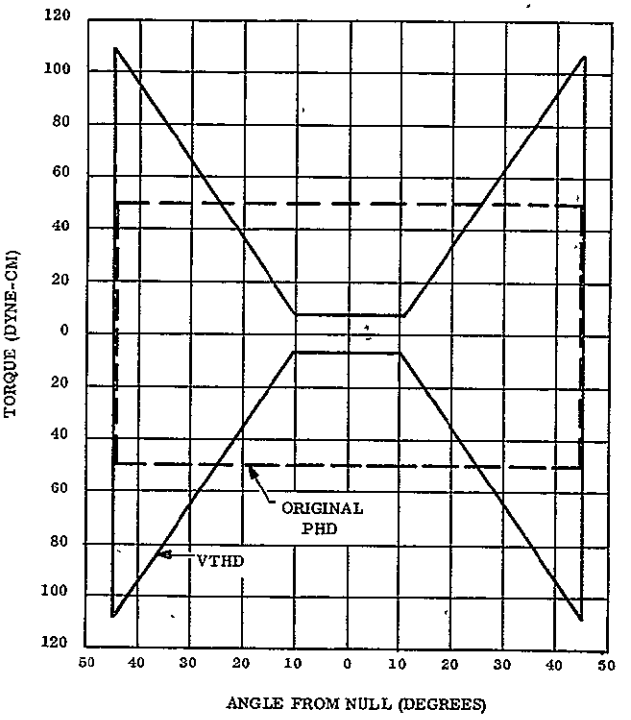

Figure 3-23. Idealized Damping Curves for Original PHD and VTHD (Torsional Restraint Omitted)

Various means of reducing the stress levels in the wires were investigated that would also help minimize the rotational null shifts. Items that were investigated included: soft rotor stops, flexure end stops, reduced wire tension, reduced rotor stop distances, a revised flexure design with reduced tip mass, epoxy attachment of the wire, Silastic attachment of the wire, and clamps instead of mandrels on the rotor.

The results of the early tests on the Development Model and Engineering Unit 2 are shown as Tests 1 through 3 in Table 3-4. The development program started with Test 4. Most of the early configurations explored resulted in either wire failures or excessive null position shift. As seen in Table 3-4, failures occurred in Tests 4 through 8 as some of the previously mentioned items were investigated.

*See Paragraph 3.2.3.4.4

When the hook flexures were installed (Test 9 to 32) the wire was able to survive the qualification test environment. One set of wires successfully passed through qualification levels four times (Tests 10, 10A, 11, and 12) without failure but had null shifts on the order of 10 to 15 degrees. A test-to-failure was run on this configuration and the wire failed at 40g and 350 cps (the prescribed input at this frequency is 18.5g). An apparent correlation was found between the direction in which the rotor was oriented during the latter stages of the vibration test and the direction of the null position shift. When the rotor was rotated clockwise onto the stop it nearly always resulted in a shift to the left on the chart and vice-versa for a counter-clockwise rotation.

Since the magnitude of the null shifts with this configuration was unacceptable, means holding the wire more securely at its end were explored. The first thing tried, epoxy bond, was apparently too rigid and caused the wires to break (Test 14). Removal of the epoxy and reducing the wire tension also resulted in wire failure (Test 15).

Starting with Test 16 the most successful configuration was examined. This configuration, which has been incorporated into Engineering Unit 2 is shown in Figures 3-21 and 3-22. It consists of:

1. Single-blade hook-end flexures with the wire restrained by clamps at the base and by epoxy on the back of flexures. A small amount of viscoelastic sealing material, Dow 92-018, is located near the tip of the flexure for cushioning.

2. Clamps of 302 CRES to hold the wire on the rotor, with additional Dow 92-018 for cushioning at the edge of the clamp.

Engineering Unit 2 was subjected to repeated qualification level tests in this configuration with null shifts less than 1 degree. In Tests 16 through 21 Silastic was used as the viscoelastic material but this is an unacceptable material for flight units due to outgassing. The results of these tests were so promising, however, that a similar viscoelastic material which does not outgas (Dow 92-018) was obtained. With Silastic on the tip of the flexure and clamp, the unit successfully passed three tests with 0.55 pound tension and another two after the tension has been increased to 0.7 pound (Tests 16-20). Test 21 was a test at

TABLE 3-4. PASSIVE HYSTERESIS DAMPER VIBRATION TEST DATA

Test No.	Date	Time	Model	Location	Item investigated	Number Failures	Wire Tension (lb)	Adapter	Wire Source	Type Flexure	Flexure Spring Rate (lb/in.)	Rotor Attachment	Flexure Attachment	Point of Failure	Frequency at Failure (cps)	Type of Failure	Null Shift & Direction (deg)	Remarks
1	2 June	4:00p	Development Model	FIT	-	0	0.7+	Dummy	Before Qualified Section	Double	10	Steel mandrel	Steel mandrel	-	-	-	-	
2	16 July	4:00p	Model	EML	-	2	0.7	Dummy	After Qualified Section	Double	10	Steel mandrel	Steel mandrel	Flexure (1) Rotor (1)	60-80	7	-	
3	17 July	9:00a	EU 2	FIT	-	1	0.7	Actual	Qualified	Double	20	Titanium mandrel	Titanium mandrel	Flexure (v-end)	< 800	5	-	FHD adapter only
4	17 July	3:00p	EU 2	EML	Teflon rotor stops	1	0.7	Actual	Qualified	Double	20	Titanium mandrel	Titanium mandrel	Rotor	320	1	-	
5	19 July	3:30p	Development Model	EML	End stops on flexures	1	0.7	Dummy	After Qualified	Double	10	Steel mandrel	Steel mandrel	Rotor (anodized end)	320	7	- -	One stop bent out during test
6	19 July	4:30p	EU 2	EML	Repeat of 5	1	0.7	Actual	Qualified	Double	20	Titanium mandrel	Titanium mandrel	Rotor (v-end)	210	2a	-	
7	19 July	8:15p	EU 2	EML	Repeat of 6, reduced tension	1	0.6	Dummy	Qualified	Double	20	Titanium mandrel	Titanium mandrel	Rotor (v-end)	110	2a	-	
8	21 July	10:00a	EU 2	EML	Same as 6, reduced rotor stop distribution	1	0.7	Dummy	Qualified	Double	20	Titanium mandrel	Titanium mandrel	Rotor (v-end)	250	2b	-	Rotor stops 0.006-in. axial & 0.008-in. radial
9	21 July	2:30p	EU 2	EML	Hook flexure(1) (no end stops)	0	0.7	Actual	Qualified	Single(1) Double(1)	12 20	Titanium mandrel	Hook (1) Titanium mandrel(4)	-	-	-	-	Double flexure with Titanium mandrel & 0.005-in. wire on other end (no stop)
10	22 July	2:00p	EU 2	EML	Hook flexure(2) (no end stops)	0	0.7	Actual	Qualified	Single	12	Titanium mandrel	Hook	-	-	-	-	Filter installed for input. Used for remaining tests
10A	22 July	2:10p	EU 2	EML	Repeat of 10, same wire	0	0.7	Actual	Qualified	Single	12	Titanium mandrel	Hook	-	-	-	15 (R)	Null shift due to both 10 & 10A, Mechanical hysteresis 2% before & after 10 & 10A. Rotor ccw
11	22 July	3:40p	EU 2	EML	Repeat of 10, & 10A, same wire	0	0.7	Actual	Qualified	Single	12	Titanium mandrel	Hook	-	-	-	13 (L)	Rotor cw
12	22 July	4:30p	EU 2	EML	Repeat of 10, 10A, & 11, same wire	0	0.7	Actual	Qualified	Single	12	Titanium mandrel	Hook	-	-	-	11 (R)	Rotor ccw
13	22 July	5:30p	EU 2	EML	Same wire as 10 & 12, high level input	1	0.7	Actual	Qualified	Single	12	Titanium mandrel	Hook	Rotor (v-end)	350	5b	-	40g input at failure
14	24 July	9:30a	EU 2	EML	Wire clamps on rotor, epoxy on flexure	3	0.65	Actual	Qualified	Single	12	Steel clamp	Hook	Flexure(2) Rotor (v-end)	180	Rotor(2a) Flexure (4c) Flexure (3a)	-	Mechanical hysteresis 1% before test
15	24 July	2:30p	EU 2	EML	No epoxy on flexure reduced tension	1	0.55	Actual	Qualified	Single	12	Steel clamp	Hook	Rotor anodized end	200	2b	-	
16	25 July	9:15a	EU 2	EML	Silastic on flexure tip, epoxy on back	0	0.55	Actual	Qualified	Single	12	Steel clamp	Hook	-	-	-	2.2 (R)	
17	25 July	10:00a	EU 2	EML	Repeat of 16 same wire	0	0.55	Actual	Qualified	Single	12	Steel clamp	Hook	-	-	-	8 (L)	
18	26 July	10:30a	EU 2	EML	Repeat of 16, & 17, same wire	0	0.55	Actual	Qualified	Single	12	Steel clamp	Hook	-	-	-	2.5 (L)	Rotor cw
19	26 July	1:30p	EU 2	EML	Increased tension same wire	0	0.7	Actual	Qualified	Single	12	Steel clamp	Hook	-	-	-	2.2 (R)	Rotor cw
20	26 July	2:00p	EU 2	EML	Repeat of 19, same wire	0	0.7	Actual	Qualified	Single	12	Steel clamp	Hook	-	-	-	12.3 (R)	Rotor ccw
21	26 July	2:30p	EU 2	EML	Same wire at 18 & 18, high level input	2	0.7	Actual	Qualified	Single	12	Steel clamp	Hook	Middle of wire (2)	50	v-end (3b) anodized end (3c)	-	38g input at failure
22	27 July	11:00a	EU 2	EML	Dow 92-018 on flexure tip & clamp	0	0.5	Actual	Qualified	Single	12	Steel clamp	Hook	-	-	-	1.0 (R)	Rotor cw, epoxy on back of flexure,
23	27 July	11:40a	EU 2	EML	Repeat of 22, same wire	1	0.5	Actual	Qualified	Single	12	Steel clamp	Hook	Rotor anodized end	50	?	-	
24	28 July	10:20a	FU 2	FML	New hook flexure	0	0.5	Actual	Qualified	Single	6.4 & 12.8	Steel clamp	Hook	-	-	-	-	Rotor ccw, null shift unkown, nut slipped
25	28 July	11:10a	EU 2	EML	Repeat of 24, same wire	0	0.5	Actual	Qualified	Single	6.4 & 12.8	Steel clamp	Hook	-	-	-	2 (L)	Rotor cw
26	28 July	1:15p	EU 2	EML	Repeat of 24 & 25, same wire	0	0.5	Actual	Qualified	Single	6.4 & 12.8	Steel clamp	Hook	-	-	-	0	Rotor ccw, slight reduction in torsional restraint
27	28 July	2:30p	EU 2	EML	Repeat of 24 & 26, same wire	1	0.5	Actual	Qualified	Single	6.4 & 12.8	Steel clamp	Hook	Middle of wire (v-end)	50	2a	-	(Reduced torsional restraint observed before test)
28	28 July	10:20p	EU 2	EML	Same configuration as 24-27, new wire, proof loaded -	0	0.5	Actual	Qualified	Single	6.4 & 12.8	Steel clamp	Hook	-	-	-	-	Went down to 135g at 220 cps, rotor ccw, slight reduction in torsional restraint
29	29 July	11:10a	EU 2	EML	Repeat of 28, same wire	0	0.5	Actual	Qualified	Single	6.4 & 12.8	Steel clamp	Hook	-	-	-	0.5 (L)	Rotor cw, proof loaded before and after test
30	29 July	11:45a	EU 2	EML	Repeat of 28 & 29, same wire	0	0.5	Actual	Qualified	Single	6.4 & 12.8	Steel clamp	Hook	-	-	-	-	Null shift not measured, proof loaded before test
31	29 July	11:55a	EU 2	EML	Same wire as 28-30, high level input	1	0.5	Actual	Qualified	Single	6.4 & 12.8	Steel clamp	Hook	Middle of wire (v-end)	50	6	-	40g input at failure
32	31 July	3:30p	FU 2	FIT	Fully assembled, full qualification test	0	0.5	Actual	Qualified	Single	6.4 & 12.8	Steel clamp	Hook	-	-	-	1	Tape on rotational stops, proof loaded before and after test

NOTES

(1) All wire from same spool of .002 grey. Part of this spool has been qualified per Spec PT-1-12, Revision A. During qualification approximately 50 feet of wire was discarded due to failures during static loading tests.
(2) All tests but 1 and 32 conducted to qualification levels along x-axis only. Tests 1 and 32 conducted through full 3-axis sine and random qualification test schedule.
(3) All tests but 3 and 32 conducted with magnet circuit and both covers removed.
(4) All tests but 4 conducted with hard-anodized rotor stops.
(5) Types of failure

PREFIX

1. "Cup-cone" - ductile
2. Brittle "A"
3. Brittle "B"
4. Brittle "C"
5. Brittle - No observation recorded as to A,B,C
6. Brittle "B" - No observation recorded as to A,B,C.
7. Wire not examined

SUFFIX

a - Fatigue progression lines
b - Vague indication of fatigue progression lines
c - No indication of fatigue progression lines

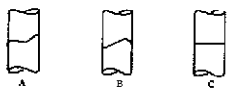

increased levels and each of the two wires broke in its middle. This was an encouraging result since it indicated that the ends were no longer the most critical points. All previous failures had occurred on the mandrels or clamps.

The model was then reassembled in the final configuration with Dow 92-018. The first time the model was assembled in this configuration it passed one such test (Test 22) but failed on a second test (Test 23). The model was then restrung in the same configuration and survived three qualification level runs (Tests 24-26). After Test 26 a small reduction was observed in the torsional restraint of the damper. During Test 27 one of the wires broke in the middle. It is felt that the reduction in torsional restraint was due to a local failure of the wire and that this is the spot where it broke on the next test.

Engineering Unit 2 was restrung again in the same configuration and successfully passed through three more qualification-level tests (Test 28-30). A proof load of 0.5 pound was added to each flexure before each of these tests to check the wire condition. This doubled the design preload of 0.5 pound. A slight reduction in torsional restraint was noted after Test 28 but no failures occurred during Tests 29 and 30. Any local failure that caused the reduction in torsional restraint was apparently not large enough to cause a failure. test-to-failure was then conducted on this model (Test 31) and failure occurred at 40g and 50 cps, (the prescribed qualification test level at this frequency is 34. g).

The final vibration test of this configuration was a full qualification-level run along all three axes conducted on the fully-assembled Engineering Unit 2 before delivery (Test 32). This test showed no breaks in the wire or decrease in the torsional restraint.

3.2.3.4.3 Conclusions and Design Changes to PHD

From the results of these tests it was concluded that the new suspension system configuration was adequate to survive the worst input vibration environment prescribed and limit the

null position shift to 1 degree or less. The following changes were implemented into the PHD (ATS-D/E) design, assembly, and test procedures:

1. The ATS-D/E configuration was modified to include the new flexures and clamping devices.

2. Epoxy and Dow 92-018 are applied as part of the assembly procedure.

3. A more thorough examination is made of the wire samples during wire qualification.

4. Certain samples of the wire are subjected to repeated qualification-level vibration tests in a damper model before their cyclic fatigue testing.

5. A proof load of 0.5 pound is applied to each flexure after each vibration test.

The ATS-A configuration is not affected by these changes. It had the double flexures and mandrels.

3.2.3.4.4 References, PHD

1. General Electric Specification SVS-7331, "Passive Hysteresis Damper'

2. Memo 65-9711-27, "Development-Test Plan, Torsional Restraint Characteristics, PHD," J.J. Conway, 18 June 1965.

3. Specification PT-1-12, Revision A, "Lot Qualification of Wire, Passive Hysteresis Damper Suspension," 18 June 1965.

4. Memo 9714.2-3, "PHD Wire Failure Analysis, "Materials Engineering Department, 6 August 1965.

5. Memo 65-9711-39, "Vibration Test Report, Development Model PHD, Revised ATS-D and E Configuration," J.J. Conway, dated 18 June 1965.

References 1 to 5 are contained in the Hysteresis Damper Component History Document CLIV Volume 1 to 3.

Two other tests of interest are:

1. A radial force test to determine radial stiffness. Results were 1288 dynes for .002 displacement. Spec. limit is 100 dynes minimum to bottom against stops (approximately ± .010 from neutral position)

2. 100 mode changes were made on the development model using the solenoid and Belleville washer spring in a fixture that simulates the CPD without any degradation. This test was run to determine the effect of impact during clutching between dampers.

3.2.3.5 Clutch Belleville Washer

A mechanism was required within the CPD to allow engagement of one damper to the Damper Boom while allowing the other damper to be disengaged entirely from the system. Closely tied in with the clutch was the actuation device to change positions of the clutch. This is discussed in Section 3.2.3.6.

Some of the critical design considerations were: Must be non-magnetic as it must rotate with the Damper Boom, holding force during engagement must be great enough to withstand torque during operation without slippage and also strong enough to permit testing in a lg field, must be bi-stable to minimize any possibility of hangup in the neutral position which would prevent engagement of either damper, must be free of external forces in all axes (including rotational) because of the very small damping forces involved, and also, because of the very weak axial forces produced by the diamagnetic suspension, must be non debrie producing to prevent contamination of CPD, must be able to positively align dampers such that the damper axis is perpendicular to Damper Boom axis and concentric to the Damper Boom shaft. Initially it was also attemped to align the damper null to the boom null during shifting but the mechanism became too complex and the reliability was greatly affected. Null alignment was controlled by shifting when the angle indicator read 0 degrees. The angle indicator sensed the Damper Boom position and the unengaged Damper was at its null position due to the torsional restraint of the damper.

Many different designs were studied until the final design was established as described below.

The coned diaphragm spring (Figure 3-24) was mounted within a ring (2) centrally located within an integral housing of the output shaft (3). The ring (2) provided a surface about which the spring pivoted during "snap through." The integral housing formed an upper clutch face (4) and a lower clutch face (5). Shaft one (6) contains a circular V-groove (7) which matches the lower clutch face (5). Shaft two (8) contains a circular V-groove (9) which matches the upper clutch face (4). The actuator shaft (10) was positioned through the open center of the diaphragm spring (1) and faces (11) and (12) formed a spool on the end of the actuator shaft which contact the surface of the diaphragm spring during actuation only.

The coned diaphragm spring (1) had two stable positions, and was used as an over-center toggle. The diaphragm spring was coned so that it exerts a force on shaft one (6) such that V-groove (7) contacted the lower clutch face (5) of the output shaft (3). The mating of these surfaces under the compressive load provided by the diaphragm spring (1) produced a friction coupling torque which allowed shaft one (6) to drive the output shaft (3) rotationally with no restraining external force present. The V-shape of the engaging surfaces ensured that the mating shafts would be properly aligned axially and radially.

In transferring the output shaft (4) to shaft two (8), the actuator (10) was displaced linearly upward. This displacement causes spool face (11) to contact the surface of the diaphragm spring, driving it flat and then over-center so that the diaphragm spring (1) assumed a conical shape in the other direction as shown in Figure 3-23-C. The actuator (10) was further displaced such that the upper face (12) and the lower face (11) of the spool were clear of the spring, thereby eliminating any external forces which would retard rotation of the output shaft (3). With the diaphragm spring (1) coned in the position shown in Figure 3-23-C, it forces clutch surfaces (4) and (9) together, which coupled shaft two (8) to the output shaft (3) and resulting in the CPD being changed to the hysteresis damper mode.

Reversing the direction of linear displacement of actuator (10) shifted the diaphragm spring (1) back to the position shown in Figure 3-24(g) where shaft one (6) was again coupled to the output shaft (3). Note in Figure 3-24(b) and (c), that the inoperative shaft had a nominal

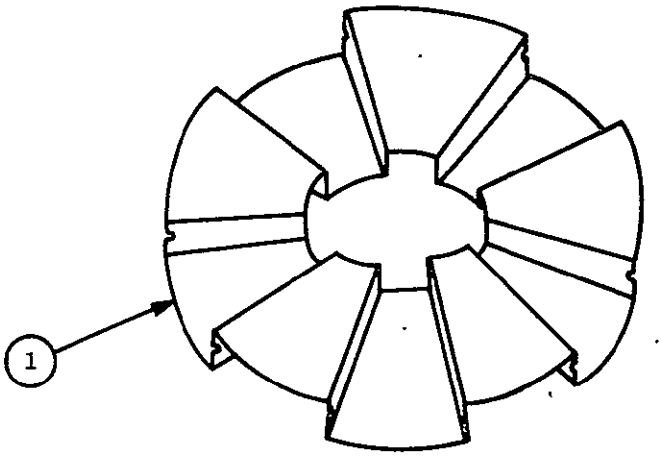

(a) DIAPHRAGM SPRING

1. Diaphram spring
2. Ring
3. Output shaft
4. Upper clutch face
5. Lower clutch face
6. Shaft one
7. Circular V-groove
8. Shaft two
9. Circular V-groove
10. Actuator
11. Lower spool face
12. Upper spool face

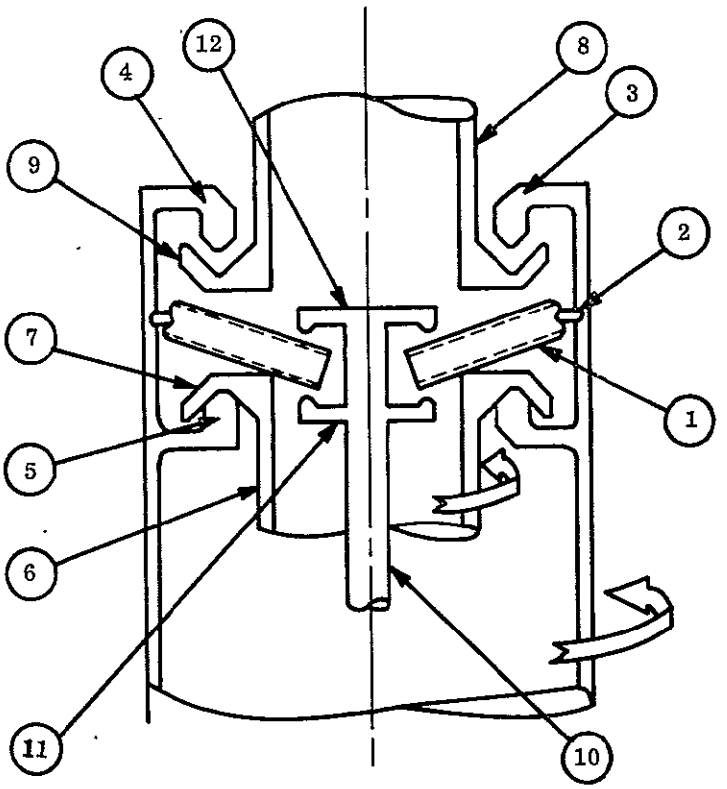

(b) EDDY-CURRENT DAMPER MODE

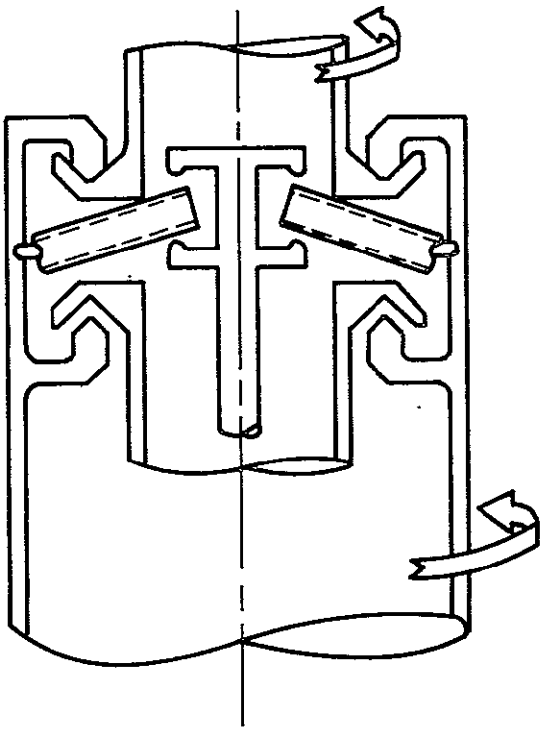

(c) HYSTERESIS DAMPER MODE

Figure 3-24. CPD Clutch Mechanism

clearance to the output shaft V-surface. Because of this clearance which was necessary to isolate the inoperative shaft, the output shaft ⑨ was displaced axially this same distance switchover.

3.2.3.5.1 Design Features

a. The overall clutch mechanism provided in a compact package a dual coupling method which eliminated all external forces that would tend to retard rotation or cause axial displacement. When the clutch was engaged in one direction, it was essentially floating and completely free from the actuator and the disengaged component parts.

b. The fluted configuration (Figure 3-24(a)) of the diaphragm spring lent itself to a wide range of load-deflection combinations which were readily predictable. The spring, in combination with the pivot ring, had the properties of an over-center toggle device but with fewer parts. The spring had a larger "throw" than a plain Belleville washer plus the advantage of having essentially equal force/deflection characteristics in each of the two operating directions. It also occupies less space than other similar over-center devices. The spring was formed in a flat (on-center) position, and was coned at assembly by the fact that the diameter of the holding rings was smaller than the free diameter of the flat spring. The deformation of the spring during coning and during subsequent over-center actuations was accounted for through simple bending of the sides and faces of the flutes. Stresses and loads resulting from such bending was readily calculable and any desired load-deflection characteristics easily obtained. Load-deflection characteristics of other similar devices (i.e., Belleville washer and variations thereof) were more restrictive and less amenable to accurate prediction. Another advantage of the fluted configuration of the spring was that it could be manufactured without resorting to exotic manufacturing techniques.

c. The self-centering feature of the V-groove clutch surfaces as forced together by the spring was an integral advantage of the overall design. The V-groove arrangement ensures that the mating parts will repeatedly engage in the concentric position and with parallel faces for any location of clamping force within the engagement circle.

Once the design approach was established several models were fabricated to determine load-deflection characteristics. Several problem areas developed such as high stresses in the diaphragm, lower or higher than desired forces, etc. From the results of tests on these models, a design was established which met all requirements. Briefly, these are: approximately 8-pound holding force against the clutch face, a neutral dead band of 0.040 inch maximum either side of center (flat position), a maximum force at any point in the deflection curve of 18 pounds and lowering of stresses to tolerable levels for the design life.

The diaphragm used is a 12-segment, fluted washer similar to that shown in Figure 3-24(a). (only 10 segments shown) formed from 0.013 inch thick beryllium copper then heat treated to 1/4 hard. A typical force deflection curve is shown in Figure 3-25. This was from one of the first models.

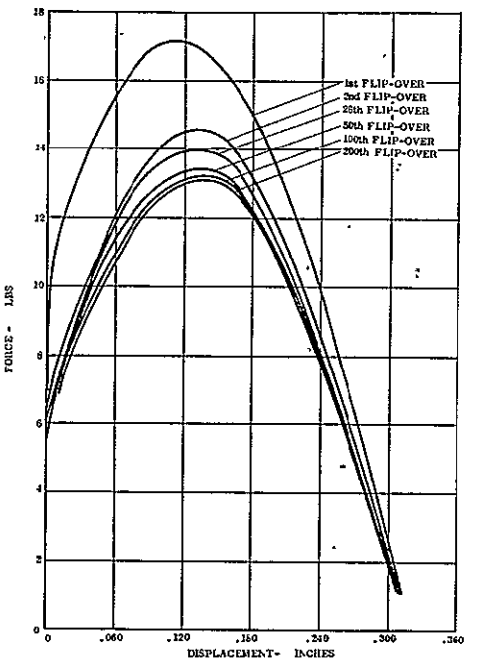

Figure 3-25. Force vs. Displacement for Square Fluted Diaphragm (.014 in. beryllium copper)

3.2.3.6 Solenoid

As mentioned in the preceding section the clutch actuator was closely tied in with the clutch design. The selection of the diaphragm clutch and solenoid actuator was based on studies of various combinations of components that would meet the desired functional requirements and offered the most advantageous use of power, weight and space while maintaining a high degree of reliability.

The solenoid was a push-pull design having a total stroke of 0.460 ± .005 inch with detents at either end of the stroke to prevent the armature from moving axially so that the spool faces shown in Figure 3-24 attached to the armature could not contact the diaphragm after clutching. Figure 3-26 is the front sheet of the solenoid specification and shows the envelope of the solenoid. The 0.125 inch diameter hole shown in section A-A was for a caging pin that was part of the CPD and was retracted in orbit when the CPD was uncaged. It was hoped that the caging pin would not be required but vibration tests on an uncaged engineering unit showed that unit must be caged. Figure 3-27 is a section view of the solenoid.

Several design iterations had to be made due to changes in available power to operate the solenoid. Design voltage was 22.3 to 30.0 vdc with a maximum current draw of 15 amps.

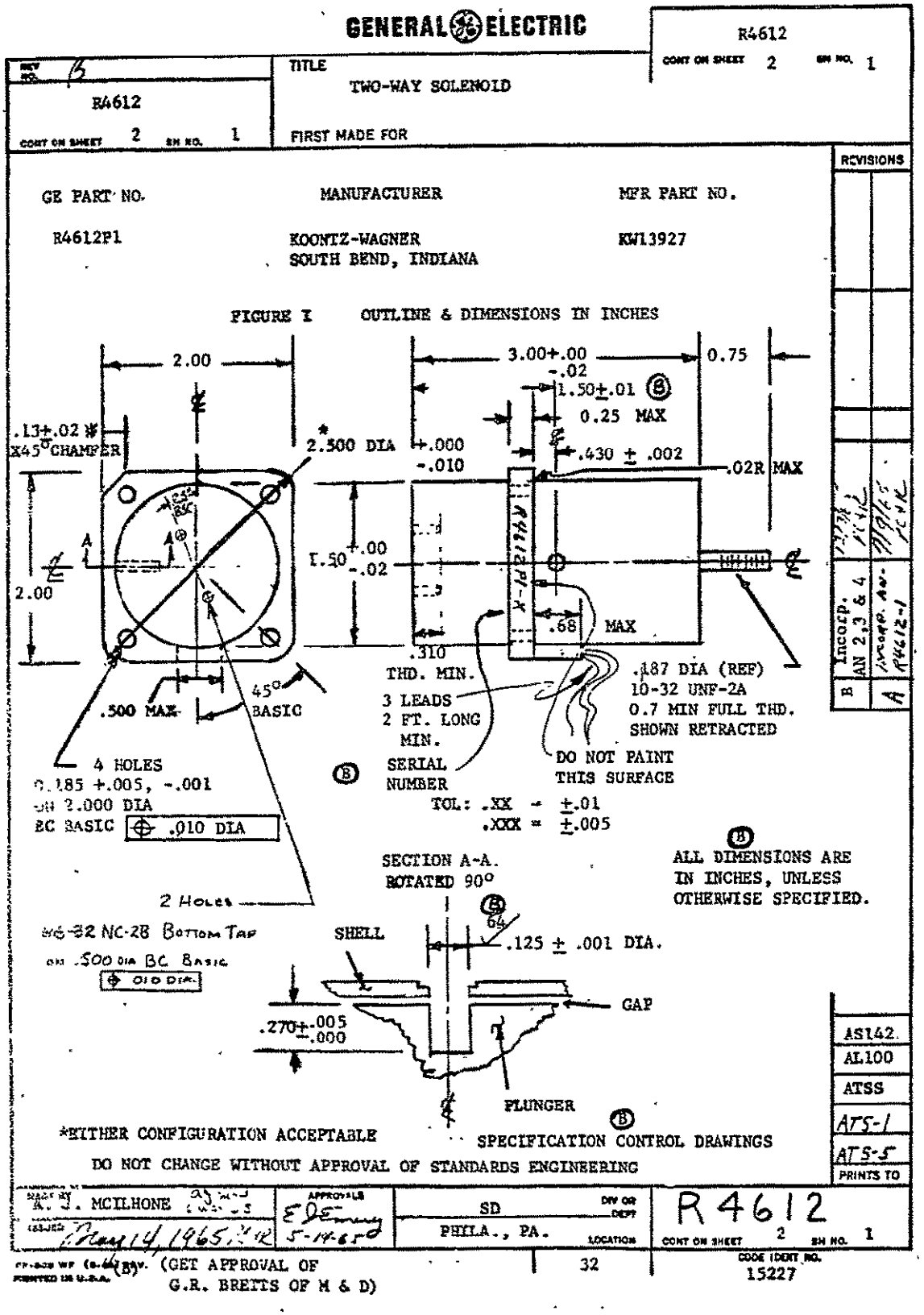

Figure 3-26. Two-Way Clutch Solenoid Specification Sheet

Testing of the unit was accomplished in accordance with the engineering test plan except that the spring actuation test was omitted (no springs were available) and vibration and dipole tests were added. Figure 3-28 shows the force versus travel characteristics for the solenoid with temperature and voltages at the extremes. All functional testing was done at room temperature. The voltage and temperature extremes were simulated by controlling the coil current in the solenoid.

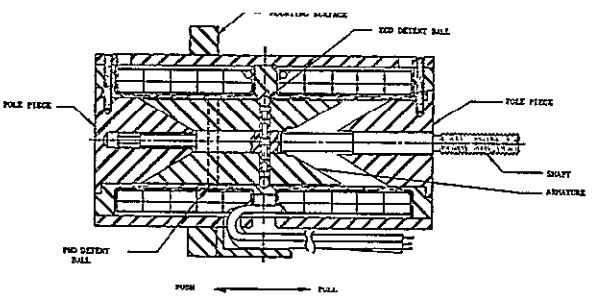

Figure 3-27. CPD Solenoid Section

Figure 3-28 also shows a curve for an input to the solenoid of 18.6 volts at a temperature of 66°C. It failed, by a very slight margin, to meet the force required at 0.2 inch of travel (16-pounds required, 15.5 pounds measured.) This test was performed to determine the minimum voltage the solenoid could tolerate at its maximum temperature and still meet the force versus travel requirements. Note the solenoid has successfully operated the clutch within the CPD at 16 vdc at room ambient.

Component History Document CLIII contains a section (PIR4176-684) on the engineering testing performed on the solenoid. In addition to this testing a complete qualification test program of 6 units was conducted on the solenoids in accordance with R4612. The results of these tests were also in the component History Document CLIII. The only failure that occurred during these tests was a shaft fracture at the thread termination on the armature shaft. This was due to the thread being put on by machine and the tool dwelling at the termination causing a sharp notch. A radius was put in and no further problems occurred. Engineering units had been hand threaded and therefore the problem did not exist.

Briefly summarized there were two groups of solenoids, Group I contained two solenoids that were subjected to functional tests to verify operating characteristics and verify that the design was met. These tests included detent force, force vs. displacement, response time, etc. In addition this group was also subjected to qualification level environmental tests such as, thermal shock, vibration, acceleration, humidity, insulation strength, etc. Group II contained 4 solenoids.

This group was the life test group in addition to a vibration test and armature motion test, these units were subjected to thousands of strokes at high and low temperature.

Table 3-5 gives the results of the life tests and indicates the areas where rework of the pole pieces took place. Initially the tests called for 5000 strokes at -23°C and 5000 strokes at +66°C. However, due to a misinterpretation by the vendor, the initial cold test was run for 10,000 strokes. It should be noted that the flight solenoids are required to be capable of 100 strokes strokes maximum. This includes ground testing.

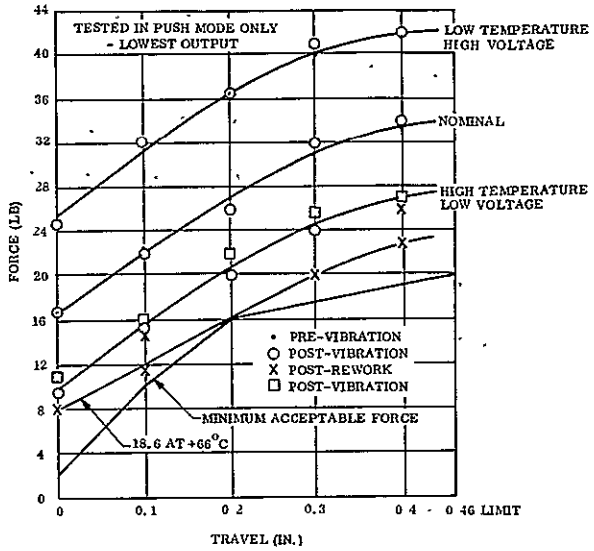

Figure 3-28. Force Versus Travel Test Results for Engineering Unit 1 Solenoid.

3.2.3.6.1 Qualification as Part of the CPD. Although this report is to cover only work up through the engineering units, a significant failure of the solenoid occurred during prototype testing that warrants mention.

This failure happened during the vibration testing of Prototype 1 and manifest itself in that the solenoid would not change modes. A careful disassembly was performed in which it was noted that the spring loaded detent balls used to hold the armature of the solenoid in the retracted position-ECD mode (flight caged condition)- had severely deformed the detent groove - See Figure 3-29. One ball (2 balls per mode) was jammed in its groove. An exhaustive dimensional check showed nothing to be abnormal other than the wear areas. Hardness checks were made on the materials and nothing unusual was found. Six units had passed the solenoid qualification tests which include a vibration test of an approximate amplification of 2.5 over the CPD qualification test levels (1.5 over solenoid qualification level). Two of these units were previously dissected by the vendor and a comparison to the failed unit did not reveal the same condition or any evidence of the same condition.

TABLE 3-5. LIFE TEST HISTORY OF THE CPD SOLENOID EXTEND TO RETRACT FORCE, (LB)

Strokes	Environment	S/N 103	S/N 104	S/N 108	S/N 109
0	cold	2.0	1.58	2.08	1.8
1000	cold	2.0	1.58	1.9	1.8
5000	cold	2.1	1.66	2.1	2.0
10,000	cold	2.6	1.6	2.1	2.0
10,000		rework pole pieces			
10,000	hot	2.1	1.68		
11,000	hot	2.0	2.0		
12,850				Rework	Rework
15,000	hot	stuck	2.8	Pole Pieces	Pole Pieces
		Disassemble and return to GE for inspection			
17,000					2.0
17,850				2.3	
18,000					2.3
18,850				2.4	
19,500					2.6
20,350				2.76	
22,000					4.25
22,850				4.75	

Two additional units were revibrated in an attempt to repeat the failure with no success. The acceleration level was pushed up to 50g's in the 36 to 400 cps range (as compared to 11.5g's from 25 to 250 cps and 18.5g's from 250 to 400 cps for the CPD qualification tests). One of these units and Engineering Unit 1 solenoid were dissected with no repeat of the failure condition noted. In addition to these solenoid tests, the solenoid in Engineering Unit 1 passed the same environmental tests as the failed unit; engineering tests have been performed with no problems.

The only significant observation noted about the test during which the failure occurred was that the unit was vibrated 90° out of phase, i.e., the highest g loading was put into the weakest structural axis; whether or not this caused the failure is not known.

A flight spare solenoid was installed in the unit and revibrated with no problems. The solenoid was removed and performed as required during bench test.

On the Engineering Unit 2 CPD, a solenoid was used which had been vibrated to two solenoid qual level vibration tests and one partial vibration test uncaged which was stopped

when the pole pieces came loose and re-pinned - not disassembled-plus 600 strokes. This overtested unit finally failed during the second CPD qualification vibration test. This solenoid had been instrumented with a tri-axial accelerometer in an attempt to check for high amplifications. However due to equipment problems the data received was meaningless. The failure mode was the same, i.e., the ball deformed the groove and wedged the armature. This type failure was due to the travel of the armature during vibration. Even though there was a caging pin in the armature there was sufficient movement to allow the armature to drive the ball into the groove under certain conditions. A redesign was attempted but due to schedules and state of assembly (Flight No. 1 had just about finished final acceptance tests) and in light of all the successful test results it was decided not to incorporate the new design. This new design would have added a hardened steel vee groove and hardened steel ball guides and a more obtuse vee angle. Also the design would have been modified such that disassemble of the solenoid could be accomplished without destroying the unit as is now the case. These changes would have resulted in lower forces but the present design has enough margin to allow this.

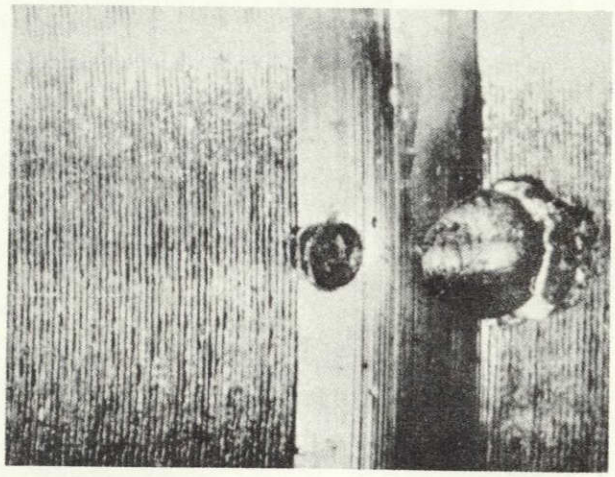

Figure 3-29. Deep Indentation at Edge of V-Groove Caused By Dentent Ball in ECD Mode

3.2.3.7 Angle Indicator

There were two primary functions of the angle indicator. The first was to provide diagnostic information on the movement of the damper boom. The second was to indicate the null position so that shifting from one damper to the other could be done with minimum bias introduced into the system.

Initially, the second function was not a requirement of the system as the clutch mechanism was to have aligned the dampers to the boom "Zero" during shifting. However, as previously explained, this became too complex for the clutch to reliably handle.

The angle indicator was required to have the following accuracy: ±2° from +20° to -20°

±(0.5 + 10%) from +20° to +45° & -20° to -45).

Position sensing accuracy was maintained regardless of boom shaft excursions which were ±0.040 inch radially and a total range of 0.220 inch axially.

Initially the tolerance was tighter in the 0° to 20° ranges (±1.0° from 0° to 4° and 1.5° from 4° to 20°) but due to several problems that occurred during development it was decided to relax the accuracy as the information is basically for diagnostic purposes and the rework effort to meet the original tolerances was not compatible with costs and schedules. It should be pointed out that the error at null (shifting position) is ±1°; this tighter spread is due to different technique in interpreting the data.

At the beginning of the program it was intended to subcontract the angle indicator; however, of the 23 vendors contacted, only three vendors bid and only one was satisfactory. This vendor's design was an analog system which eventually was terminated due to accuracy problems under temperature extremes, complexity of circuits and reliability. In addition to correcting the above problems, the in-house design turned out to be lighter and consume less power. However, this design was not without its own problems.

Basically, the device was a simple expanded Gray-code encoder which has a slot pattern on a thin disc. The disc was attached to the rotating member (damper boom) that was to be monitored. The disc is shown in Figure 3-30. A beam of light either passed through or was interrupted by pattern lines on the disc; the light was detected by photodetectors which were located below the disc. Use of the Gray code pattern provided a digitized readout while minimizing error at the code change point.

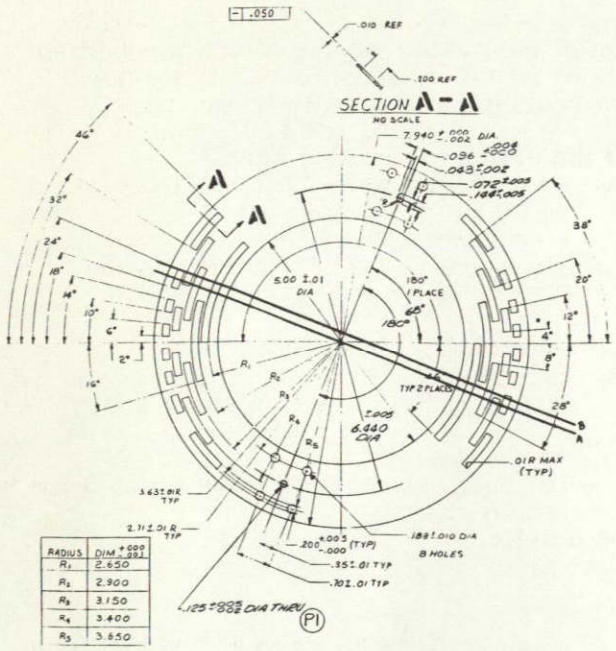

Figure 3-30. Encoder Disc for Angle Indicator

The Gray-code encoder was a simple, digital device which inherently met the reliability and temperature specifications easier than a typical analog device. Ordinarily the code pattern was designed to provide equal accuracy over the entire range, however the pattern could be readily modified so that the lower accuracy was provided at larger angles in accordance with the requirements of the ATS application. The advantage gained as compared with the ±2 degree accuracy over the entire range was a decreased number of digital bits and the associated detector channels to provide them.

Nonrational relative motion can be divided into three types: axial, lateral (or radial) and tilt. In the design application the axial shift could be relatively large, up to 0.22 inch. However, with a fairly well collimated slit light beam, the encoder was inherently insensitive to this shift. Tilt was confined to about 1 degree of arc, since this error projected into the plane of the disc was proportional to the cosine of the tilt angle, it had negligible effect on accuracy.

Lateral or radial motions were significant. The design application permitted up to ±0.04 inch lateral motion. With the encoder disc size proposed this could result in a readout error greater than 2 degrees. However, by providing a second, identical code pattern and reading this out as well, the necessary information for lateral shift compensation was provided. This was effectively an averaging technique.

With pure rotational motion about the center of the disc, the light slit and detectors were along line A. In this case, the coded word on one side of the disc was identical to the word on the other side. Line B represented the detector line with the same rotation plus a small lateral displacement. In this case there was one bit different in the two words as read out from opposite sides of the disc.

If now the descrete different angles that each side reads are averaged, the error will be within 1 degree of the true position. This is also true at the larger angles. Note that there were several different ways to read the codes, i.e., have the code correspond to the actual change point or when a code change was made read it as a point half way between adjacent points. The latter was the actual way it is done in the CPD. This was required to meet the initial tolerances and it was decided not to change the technique when the tolerance was changed. Also it should be noted that the system was read dynamically, i.e., readings were made and were accurate to the tolerance at the instant of change. An attempt was made to calibrate each unit for exact readings at code changes, i.e., if the code changed a 4.3 degrees it would be recorded as such and not a nominal value of 4 degrees. This did not work out due to the effects of shaft excursions and long term degradation.

The second head in addition to compensating for the transilatory motions of the shaft, also added redundancy into the system in that if one head was completely lost due to both filaments in one lamp failing, or if any individual channels fail, information was still available obviously at reduced accuracy but still the information will be valid and valuable.

Figure 3-31 is a partial section of the angle indicator top assembly (GE Drawing 47E207350) and shows the general arrangement of the angle indicator sensing head. Each sensing head was a complete unit itself, i.e., the light source, fiber optics assembly and all electronics for one head were integral in one package; no electrical or mechanical interconnections were required between the heads. No point-to-point wiring was required within the CPD because there was a connector mounted directly on the sensing head.

The double filament lamp assembly (1) is potted in the lamp housing (2) which positions the lamp adjacent to the entrance end of the fiber optics (3). The fiber optics are potted into a shell which is separable from the head assembly. The single fiber optics pipe is divided into five equal diameter pipes. These pipes project the light onto lenses (4) which, in turn, focus the light through the coded disc onto the detectors (5). The detectors are phototransistors. The detectors and lamps are wired directly to the electronics module (6). All components are mounted to the head (7) which makes an integral package. The simple electronic circuit required for each phototransistor to supply one bit of data is

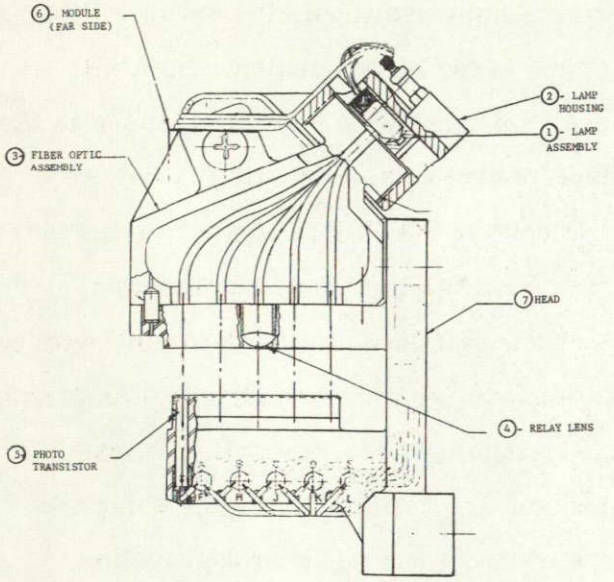

Figure 3-31. Angle Indicator Head Assembly

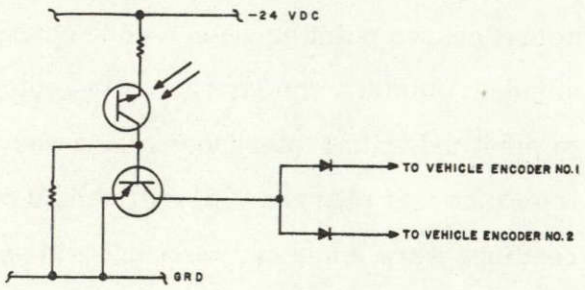

Figure 3-32. Typical Angle Indicator Bit Circuit

shown in Figure 3-32. There are five of these circuits for each angle indicator head. The voltage requirements for the lamp is 5.7 vdc and 24.0 vdc for the phototransistors. Total power consumed is 0.43 watts per head including the lamps which consume 0.39 watts. The system works satisfactorily with 3.19 vdc on the lamps and 16.0 vdc on the phototransistors at room ambient.

Figure 3-33 shows an assembled Engineering Unit in the test fixture. The left head has the lamp assembly removed to show the fiber optic input end. Figure 3-34 is an exploded parts view of the same parts. As shown in the figure the encoder disc is in two halves, however it is initially one piece and is bonded to the support rings which are aligned by pins and body bound screws and then the disc is separated. This ensures proper registration and alignment of the patterns.

Texas Instrument phototransistors type LS 443 (GE Specification R4615) were selected for the detectors. Initially the phototransistor was investigated and put aside because of the lack of test data and field data; the reliability data showed reason for concern to use the

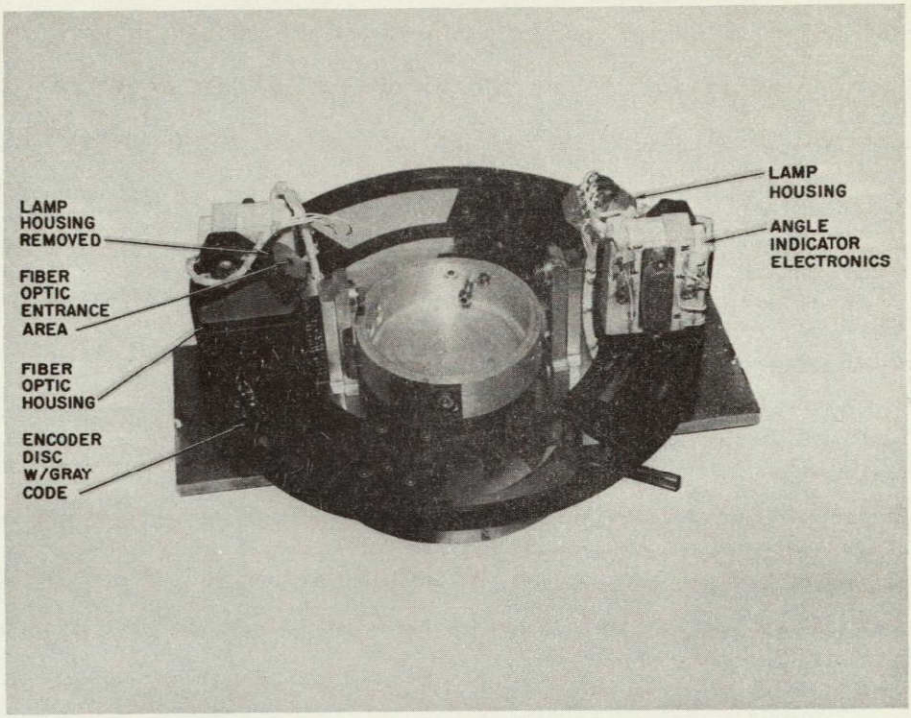

Figure 3-33. Angle Indicator Assembly in Test Fixture

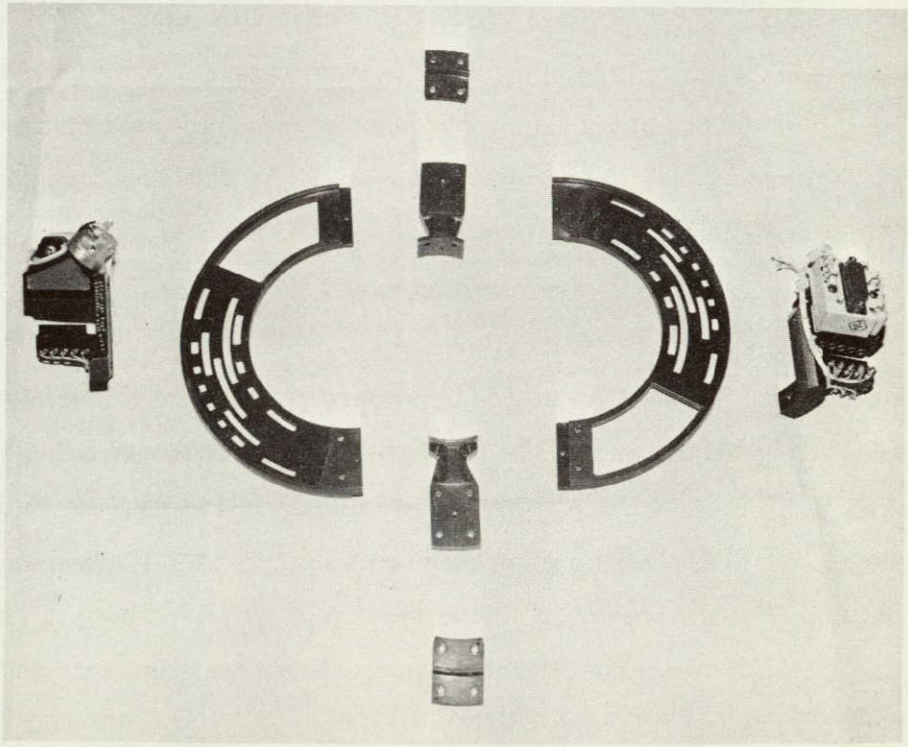

Figure 3-34. Angle Indicator Assembly Exploded View

device in the circuit then proposed which was to have the output go directly to the encoders without amplification. The failures described in this initial data were based on the light current falling below a level which was then intolerable. With the present circuits, lower light currents can be handled due to increased design margins. Also, the reliability information and the test reports presently available indicate that these devices are acceptable using the present design. For these reasons, it was initially felt that a different type detector should be investigated in parallel with the phototransistor investigations. Solar cells seemed to offer the best choice because of the large usage of these devices on space vehicles. Initial designs were based on information available for power cells and also vendor information. This information proved unsatisfactory when designing cells for use as low-level light sensors. It became evident that the type cell required was non-standard and would have to be developed and tailored to the specific needs of the system. The major problems encountered with the solar cells was in the ratio of signal-to-noise. With the low level illumination available, the signal level is so low as to require extensive amplification which would result in increased weight and complexity circuits. The narrow anticipated margin 5:1 between minimum light current (signal) to maximum leakage (noise is so small as to reduce confidence in performance. The margin anticipated with the phototransistors is 120:1. Both of these ratios are worst case analysis. It would be possible to increase the light current by using an individual lamp for each cell, but this is not feasible because the method would consume too much power and would be less reliable than the present scheme. Other light sources were investigated (neon and galium arsenide) but proved fruitless. The lamps used are similar to the T1 1/4 type except for the double filament and operate at 5.7 vdc. A double filament was selected to increase the probability of having at least one filament operating after 3 years. The lamps are wired such that each filament of one lamp is paralled to its corresponding filament of the other lamp. If one filament fails, a ground command will trip a relay which will turn off one set of lamps and light the other set. If and when one of these filaments fails switching will not be done until the other filament fails. This plan of course can be changed if say detectors in the head which is still operating have failed. This system of switching does not give as much flexability as say having a switching circuit for each of the four filaments but there was a limitation of the number of switching circuits available.

The lamps successfully passed several qualification vibration levels with only one failure. This failure occurred at the same time the solenoid failed. No valid cause for the failure was found.

Lamp life was an area of major concern and how to determine life was an area of disagreement in industry. In general the life at the operating voltage (L_1) is given by

$$L_1 = \frac{(V1)}{(V2)}^{12} L_2$$

where the subscript 2 is the vendor design life and voltage. Based on this equation the average life for each filament should be about 25,000 hours. A test program was set up to verify this but was stopped due to lack of funds.

The fiber optics presented three problem areas. The two most important were percent transmission and uniform scrambling. Transmission varies from 50 to 60 percent of the incident light available at the input end. This has proved adequate. Closely tied in with transmission is the scrambling of the individual fibers of which there are approximately 10,000. Good uniform scrambling was required to evenly distribute the light among the five output pipes. This proved difficult but was eventually accomplished to a level that was satisfactory. The association with transmission is that for good scrambling more and consequently smaller fibers are required. This increases breakage and also increase the ratio of cladding to core area which reduces light output. If fiber cladding is reduced cross talk (leakage) is increased with increased transmission loss.

Many tests were performed on the unit both as a component and on sub-component parts. One of the most important ones was the ability of the detector circuit to remain stable over the temperature range. The results of the test, as plotted in Figure 3-35, show that the "0" threshold of the module is well below the nominal design maximum for this threshold. It should be noted that these nominal threshold values have been chosen so that a considerable degradation can occur in the threshold (i.e., current required can increase significantly) without affecting the performance of the angle indicator. The data also show that the "1" threshold is considerably higher than the minimum design value at all temperatures.

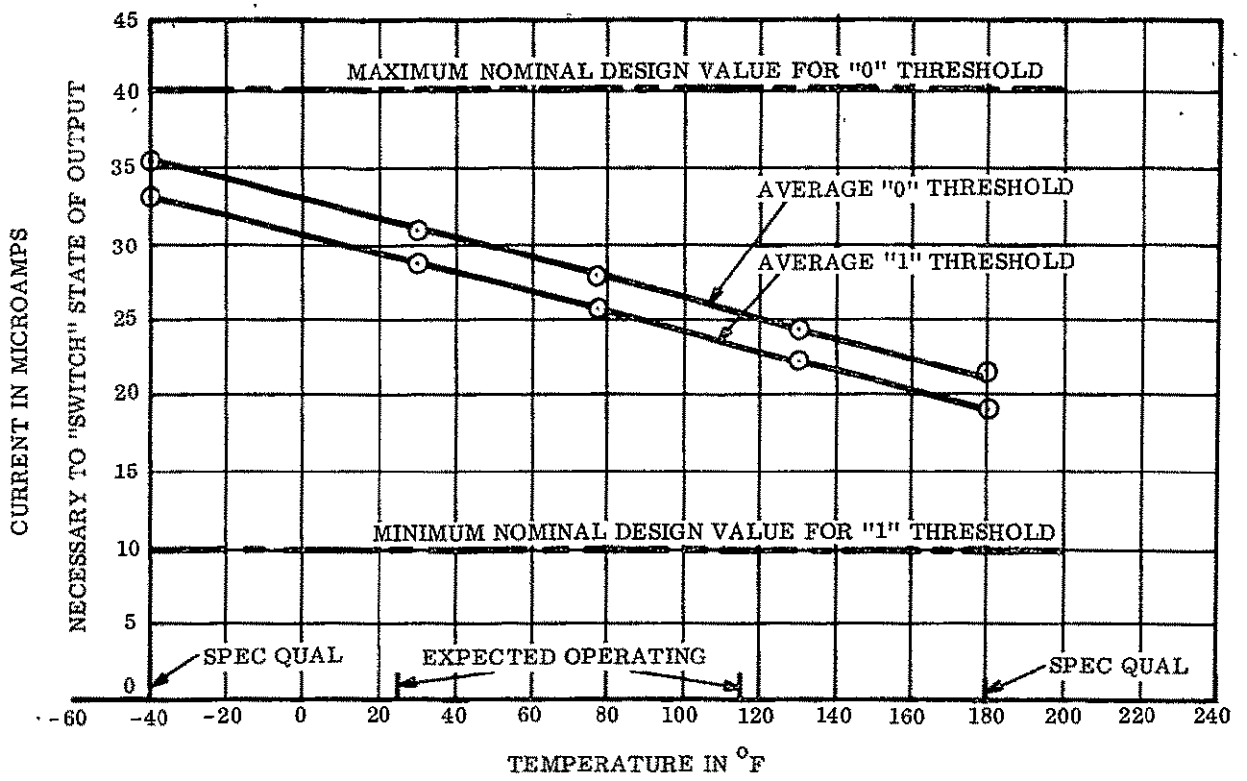

Figure 3-35. Angle Indicator Thermal Test Results (Average of Two Modules)

Testing done on prototype units revealed out-of-spec conditions occuring in the 0 to ±10 degree regions. Analysis of the data indicated that the higher sensitivity phototransistors (as compared to those on engineering units) are the basic cause of the problem. As an average, individual bits were changing 40 arc minutes too soon and too late. A 0.025-inch wide mask was placed over the phototransistors which reduced the too-soon, too-late conditions to approximately 30 arc minutes, respectively. A further reduction of the slot to 0.010 inch changed this to approximately 25 arc minutes with the disadvantage of reducing the design margin of the electronics circuit. A reduction of the lamp voltage from 5.7 volts down to 4.5 volts using the 0.025-inch slot did not significantly change the error. Combining the lower voltage with the 0.010-inch slot was not adequate and, as noted before, the design margin was compromised. The significance of the lower voltage and smaller slot is that there is ample design margin in the system such that severe degradation can take place and not affect the accuracy appreciably. This led to a possible solution to the inaccuracy in that the slots in the code disc can be shortened by about 30 arc minutes on both ends to bring the accuracy within tolerance and still have ample design margin.

However, due to the time and cost factors and seeing as the angle indicator information is primarily diagnostic, except for clutching which still can be done to within ±1 degree, it was decided not to make the disc change.

During vibration of Engineering Unit 1 the encoder failed as shown in Figure 3-36. The possibility of this happening had been considered and a new disc was being designed. However, it was not possible to incorporate it into the unit prior to testing. Figure 3-37 shows the redesigned disc.

The design was changed as follows:

1. The pattern was repositioned to eliminate inadequately supported section.
2. Corner radii were increased to reduce stress concentrations.
3. Material was changed to improve fatigue strength.

The original disc was made of 0.005-inch copper and the pattern was arranged as shown in Figure 3-36 and failed during vibration tests on the CPD. To provide a point of reference, an encoder disc identical to the one in the CPD was hard-mounted to a vibration table. The failure condition for the 0.005-inch copper disc was duplicated in this test. A 0.010-inch copper disc with larger corner radii was then subjected to vibration in a second test, and this disc also failed. In a third test, a 0.010-inch thick beryllium-copper disc with 0.050-inch radii and an aluminum disc of the same dimensions both successfully passed a vibration test. The encoder disc configuration for these tests was that shown in Figure 3-37. Based on these test results, the design was changed to use 0.010-inch beryllium-copper and the new pattern as shown in Figure 3-37 was used to further increase the structural integrity of the disc.

To establish that an adequate design margin was incorporated into the encoder disc design, another vibration test was run using the 0.010-inch thick beryllium-copper and incorporating the new encoder disc pattern Figure 3-37. The disc was subjected to a random test (three times qualification level) without any deterioration. It is of interest to note that the

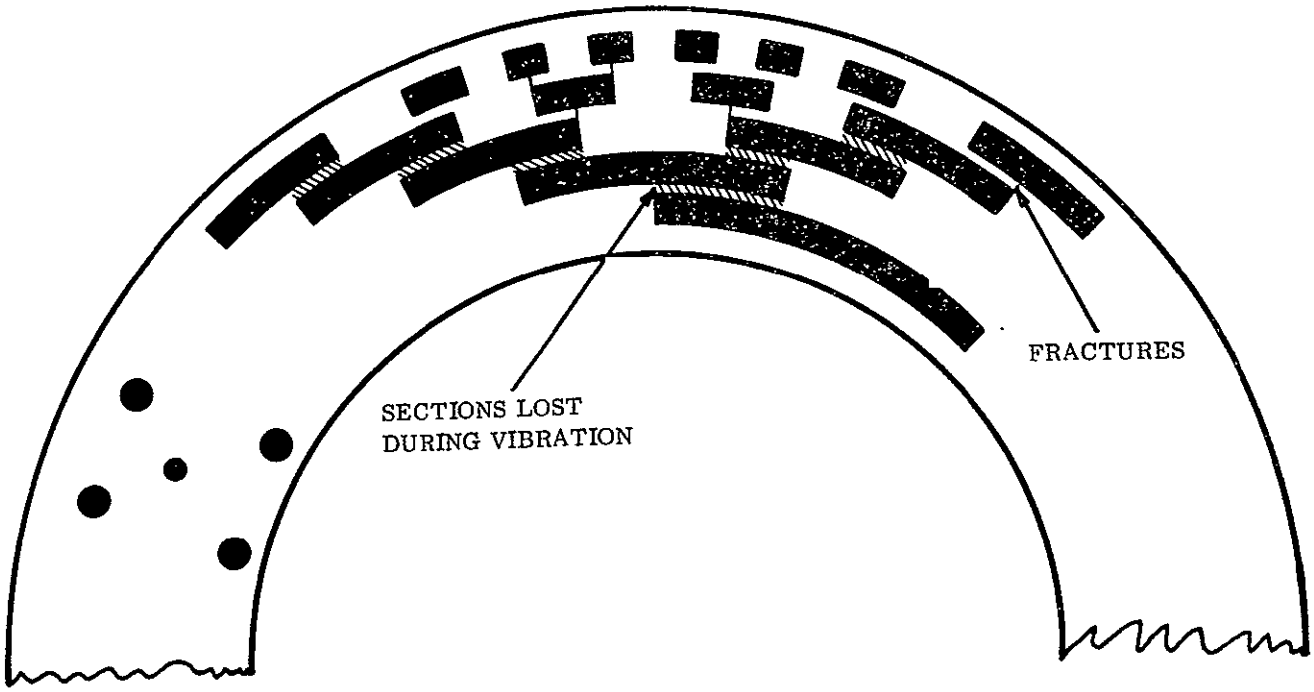

Figure 3-36. Original Encoder Disc Design

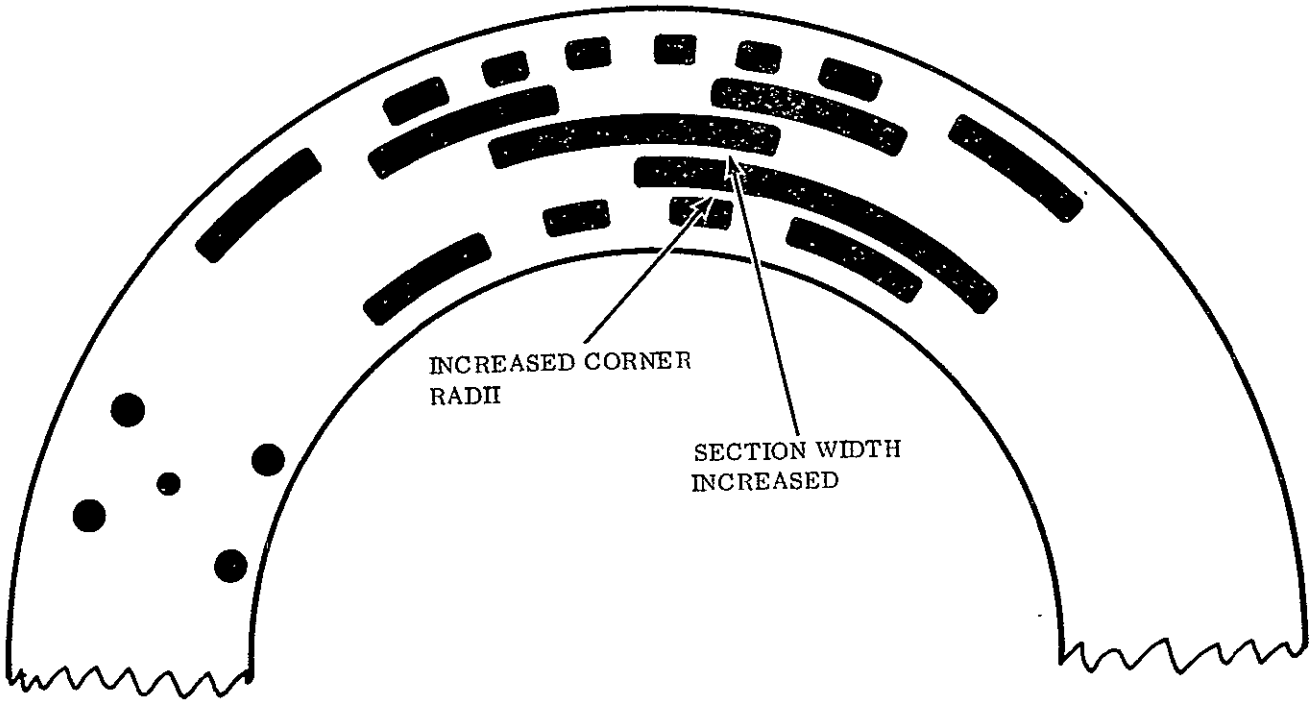

Figure 3-37. New Encoder Disc Design

encoder disc support ring and brackets successfully pased six qualification sine vibration levels and one random vibration test (at three times qualification level) with no indication of failure.

3.2.3.8 Caging Mechanism

The caging mechanism, as described in Paragraph 3.2.3.8 and shown in Section C-C of Figure 3-4, was the result of many conceptual studies and tests (See GE Document 65SD4266). The reasons for the amount of effort required are due to the following rigid design requirements.

1. Must be highly reliable.
2. Must be capable of many operations during test cycle without degrading either itself or any other parts.
3. Must not produce any debris that could contaminate the CPD.
4. Must not depend on using any magnetic materials on the rotor.
5. Must allow complete freedom of the rotor for axial and radial exersions as well as rotation.
6. Must be able to be recaged readily without major disassembly of the CPD.
7. Must have minimum height to limit Damper Boom cantilever.
8. Design must be made to avoid the problems of dirt contamination, misalignment, cocking, brinelling, friction, and thermally induced binding.

The system used meets all these requirements. Initially there was a good deal of resistance from NASA to the system used. Primarily this was focused on the fear of the pins hanging up in the caged condition and thereby aborting the mission. Straight tipped pins were first used but changed to the taper tips. This greatly decreases the possibility of a pin hang up but it does increase the axial loading in the pins during vibration and also makes the system sensitive to axial displacements of the pins; however, many tests were performed both on a caging model and actual CPD's and there has never been any trouble with this system.

The cable is tensioned to about 800 pounds and is released by either one of the guillotine cable cutters thereby providing a redundant system for release. It should be noted that although the main caging system also picks up the eddy current rotor caging mechanism, it is essentially independent of it, i.e., when the main pins retract, the eddy current rotor pins are now free to retract; however, they are not mechanically locked to the main pins. This was done to increase the reliability of caging system by assuring that if a eddy-current caging pin is restricted it will not restrain the main pins thereby assuring that at least the PHD can be made operature by operating the solenoid (caging pin on solenoid is retracted by the main pins).

Tests were run on Buna-S rubber cushions to be used to absorb the caging pin energy when the damper is uncaged. The cushions prevent the pin bracket plates from yielding particularly under repeated operations during testing. The tests are reported in PIR 4371-0063. Load vs. compression tests and a 300-cycle impact test were run. The load corresponding to the required design energy of 12-inch pounds is about 220 pounds from the load vs. compression curve. The bracket is adequate to take this load. The cushion satisfactorily withstood the 300-cycle test. The cushion is considered satisfactory for flight and also for repeated testing on the ground.

The cable (GE Drawing 47C207134 G2) used in caging the dynamic model (vibrated prior to Engineering Units) of the CPD was calibrated prior to installation. The cable is of 1/8-inch diameter, made of stainless steel with seven bundles of 19 strands each. The length was measured with a vernier caliper over reference blocks which were clamped to the cable. The distance over the blocks was set at approximately 4.25 inches, the length which was to be used to adjust the cable on the damper. The design load of the cable is 800 pounds. As a result of the test, the cable on the Dynamic Model was stretched 0.032 inch over the initial 4.25-inch measurement, by the design load. The cable performed satisfactorily in the test; Figure 3-38 is the calibration curve obtained from the test.

Prior to this a test was made to determine the torque required for setting the eddy current caging pins. The test fixture was set up in the testing machine with an actual caging pin, adjusting nut, and guide installed. A sketch of the test arrangement is shown in Figure 3-39 together with the torque versus load results.

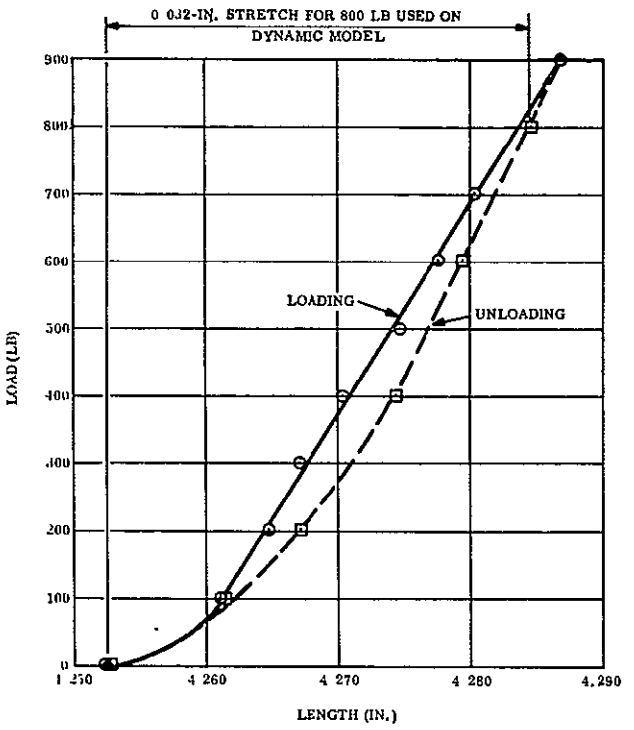

Figure 3-38. Caging Cable Calibration Results

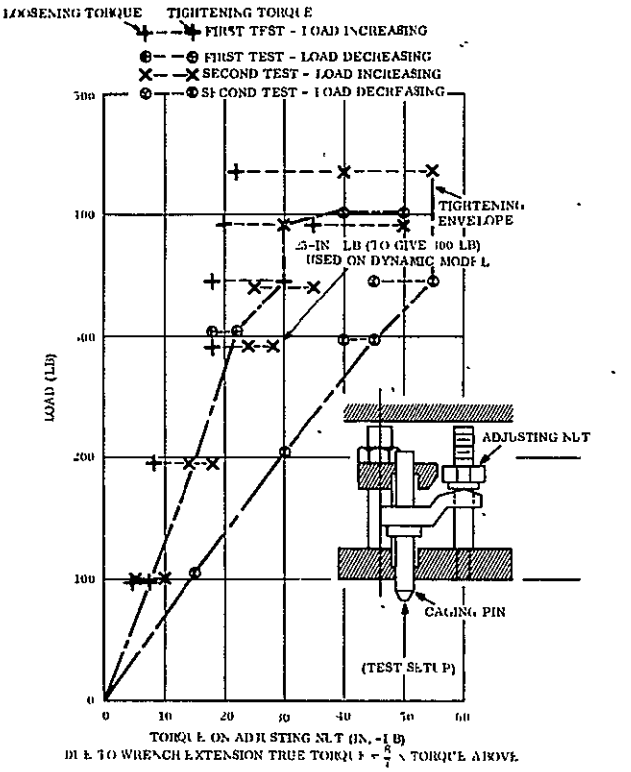

Figure 3-39. Eddy Current Caging Torque Test Results

The end of the three studs rested against a steel plate which was, in turn, cushioned by a thick piece of foam material resting on the platen of the universal load testing machine. The foam was used to produce more "give" in the system so that the load would not change appreciably with slight changes in adjustment of the nut. The holes in the plates of the test fixture had the same diameter and tolerance, and the bearing length of the holes was the same as in the actual parts of the CPD which were being simulated. The holes were anodized, as in the actual parts. The torque action was rather erratic and is plotted as a range rather than a single value. Two tests were run with the nut turned 90 degrees between tests to present a new surface to the guide. Both the nut and guide showed some local deformation at the higher loads. The design load on the eddy current caging pin is 300 pounds. To give this load, the adjusting nuts on the Dynamic Model were tightened to 25-inch pound reading on the wrench. They performed satisfactorily on the vibration tests. The nuts showed less local deformation than in the test (the load was less). The local deformation probably helps prevent loss of adjustment.

3.2.3.9 General Areas

The major components within the CPD have been discussed in the preceeding sections. Obviously there was much effort spent in other areas. These include the basic structures, harnessing, instrumentation (temperature sensors, cable release monitor, mode change indicators, boom tip release monitors) with each area having its specific problems. However seeing as these areas are not of the importance as the major components no discussion will be made here. For more information on these areas it is suggested that use be made of the reference lists. Particularly the Component History Documents.

3.2.3.10 Other Development Areas

The following topics are briefly presented as a fair amount of effort was spent in developing these components and they may be of some interest to the reader. These devices were eliminated from the design either due to change in requirements or by being replaced with a similarly functioning device.

1. Soft Stop - This was intended to act as an energy absorbing device to prevent the damper boom shaft from stopping abruptly against a rigid structural member at the limit of rotation (+ or -45 degrees) which would impart too great a bending moment in the Damper Booms due to the tip weights out at 45 feet from the axis of the CPD. This of course depends on the rate of rotation of the Booms.

   The Soft Stop consisted of a torsion wire of which one end was attached to the rotor. The other end contained a cross bar of the same diameter wire as the torion wire, mounted at right angles forming a tee. The arms of the cross bar would engage two pairs of pins placed at ±40 degrees from null. The Soft Stop was to be active from 40 degrees to 45 degrees. Typical values were 1000 dyne-cm/degree for ATS-A and 250 dyne-cm/degree for ATS-D/E. The problems associated with this device as with just about every device in the CPD was the low torque levels and the relative motions of the rotor with the stator. Also obtaining uniformity between units was difficult as the torsion constant was greatly affected by wire imperfections (wire diameter was 0.016 inches for ATS-A and 0.011 inches for ATS D/E) and by attachment variations. Subsequent analysis determined that the Soft Stop was not required. (See PIR 4T45-ATS-1 in Component History Document CXL VIII Vol. 1 under design). Consequently it was removed from all flight units.

2. Diamagnetic Torsional Restraint - This system for the torsional restraint was proposed and preliminary tests started because if this system would work it would eliminate the lateral forces present with the system now used. This would then eliminate several magnets from the suspension system and thereby reduce the weight of the CPD.

Two approaches were taken one of which proved to be unstable at null and the other appeared to be suitable for ATS-D/E only thereby creating major differences between ATS-A which was not desirable.

The first approach was to make use of the anisotropic character of the negative magnetic susceptibility of pyrolytic graphite; i.e., this material would experience a much stronger repulsion force in the direction perpendicular to its laminations than in a direction parallel to its laminations. This ratio was reported to be 10:1 in the literature. However, test showed a ratio less than 2:1. Similar problems were found with the suspension system. The second concept utilized a varying volume of diamagnetic material placed in a magnetic field. (See GE Document 655D4201 Page 2-132 for a description of the systems.)

3. GE developed Passive Hysteresis Dampers - Considerable effort was put into the development of these dampers and an actual Engineering Unit was fabricated of one of these concepts prior to NASA's direction to subcontract the PHD. NASA's reason for discontinuing GE's work was a desire to evaluate a second vendor's hardware.

   The first PHD concept studied was similar to the TRW type used in CPD. This Damper was developed using the basic design of Bell Telephone Labs and is a constant torque damper. An Engineering Unit of this design was fabricated but testing was stopped due to NASA direction. Additional information on this development is contained in 64SD4361, Page 2-136, 65SD4201, Page 2-142, and 65SD4266, Page 2-3-17.

   The second system that was worked on was a "Bow Tie" Damper so named because the damping torque vs. angle curve looks like a bow tie. This is done to provide high damping towards the rotation extremes with lower damping about null. The advantage of this type of system is that it would reduce damping time as a Hysteresis Damper is not rate sensitive and therefore for large amplitudes it takes longer for a constant torque Damper to dampen than does an eddy current Damper or "Bow Tie" Hysteresis Damper. Work on this damper was also terminated by NASA prior to full development. Information pertaining to work on this Damper as part of the CPD effort is contained in GE Documents 65SD4381, Page 4-16 and 65SD4464, Page 4-27.

   Additional work, separate from the CPD effort was made on this system and is contained in Component History Document CLXXIX-Optimized Passive Hysteresis Damper.

3.2.4 TEST EQUIPMENT

See Section 3.7 for a list of test equipment drawings.

Several pieces of special test equipment were required to test the CPD. A discussion of the major ones follows:

3.2.4.1 ADTF (Advanced Damping Test Fixture)

This equipment is used for testing the torsional restraint and damping characteristics of both dampers.

The ADTF consists of a spherical air bearing, with an electromagnetic null seeking device, for supporting the weight of the CPD Rotor and providing a frictionless bearing (less than 1 dyne-cm static frictional torques), and a rate table. The air bearing is mounted over and concentric with the rate table. In operation the CPD Rotor is attached to the air bearing adapter shaft and the stator is mounted to the rate table. As the stator is rotated, either manually for static tests of torsional restraint or dynamically for damping tests, the air bearing is rotated off of null by either the torsional restraint or the damping magnets. The torquer pick-off in the null seeking device senses the off null position and supplies a voltage to torquer coils which drives the bearing back to null. The torquer voltage is measured and this multiplied by the torquer constant gives the torque produced by the CPD. For eddy current damping this torque is divided by the rate of the table to give the damping coefficient. Typically the air bearing constant is 770 dyne-cm/volt and torques as low as 1.0 dyne-cm are measured. The ADTF is also used for inprocess testing of various subassemblies. Figure 3-40 shows the ADTF being used for the inporcess test of the eddy current damper. The manometers in the background indicate air bearing unbalance.

3.2.4.2 LOFF (Low Order Force Fixture)

This equipment is used to measure the radial and axial suspension forces of the CPD. The LOFF also uses a spherical air bearing for supporting the weight of the rotor and providing at the same time a frictionless bearing. The air bearing is mounted above an eight inch thick leveled stone slab which is supported by an angle iron frame. Mounted on the air bearing shaft is an arm which is perpendicular to the bearing shaft and can support the CPD rotor either vertically for radial force tests or horizontally for axial force tests. The stator of the CPD is mounted to a cross feed table which is mounted on the stone slab. One end of a calibrated torsion wire is attached to, and concentric with the bearing shaft. The

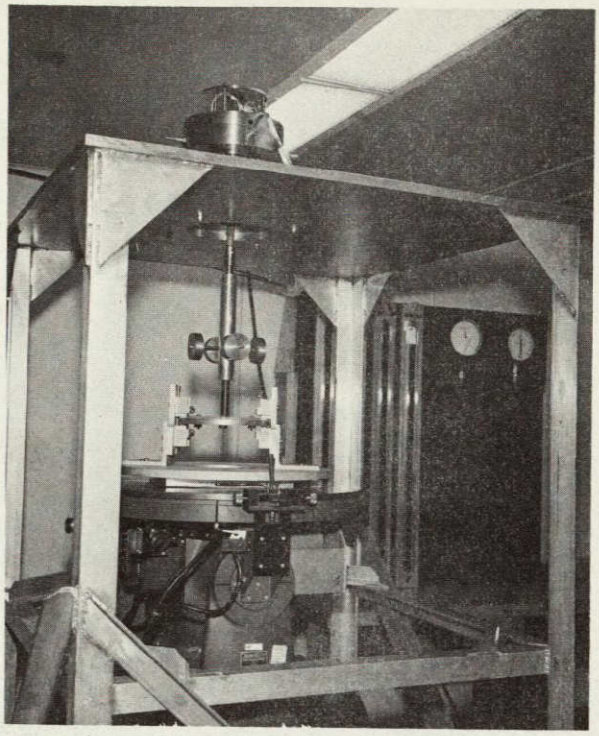

Figure 3-40. Advanced Damping Test Fixture (ADTF)

other end is passed through the stone table and mounted in a precision dividing head. A theodolite is positioned to read either lateral motions of the end of the arm by looking in radially at the arm, or is used to indicate the bearing null by looking at a mirror on the bearing shaft.

In operation the CPD rotor is attached to the arm and the stator is displaced a known amount perpendicular to the arm. The suspension forces cause the bearing to move off null. Then by twisting the wire with the dividing head until the bearing is at null again the suspension force for a given displacement can be determined by multiplying the wire constant by the dividing head rotation and dividing by the moment arm. This force is plotted against displacement and thus knowing the total displacement of the CPD the suspension forces can be computed. Over a two-year period this equipment has been repeatable within 0.25 dynes.

Figure 3-41 shows the basic LOFF. Both the ADTF and the LOFF have thermal panels which may be installed for high and low temperature testing.

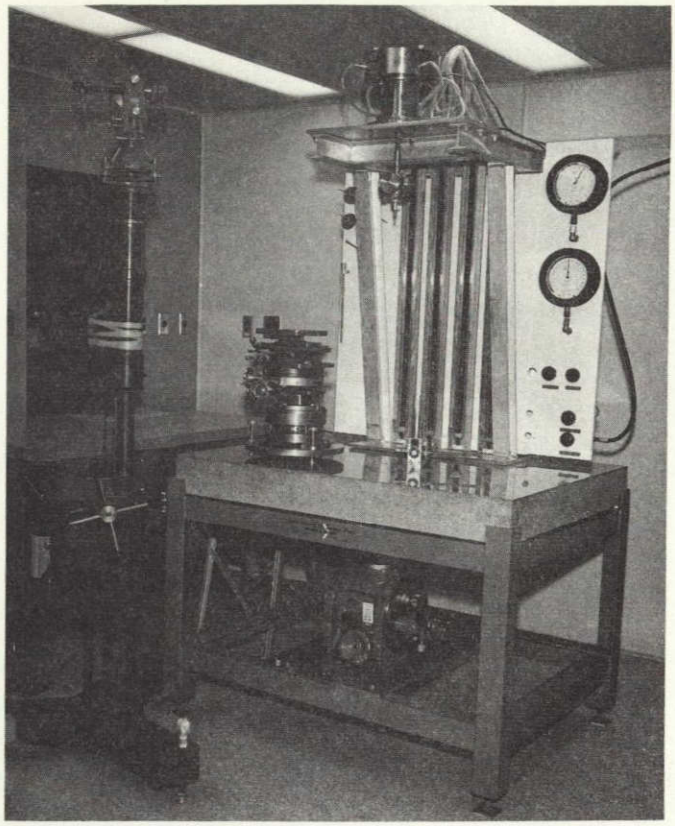

Figure 3-41. Low Order Force Fixture (LOFF)

3.2.4.3 Test Rack

This console is used for all electrical testing including; the firing of the cable cutters; activating the solenoid; reading the angle indicator codes; monitoring mode switch, boom tip release, and uncaging functions; and monitoring the two temperature sensors. The circuits used represent the vehicle circuits and power supplies can be adjusted to simulate low vehicle voltages for degradation testing.

3.2.4.4 Angle Indicator Test Fixture

A special fixture was required to test the angle indicator as a separate unit. This was required for two reasons, the first is for inprocess testing to insure proper operation prior to installing into the CPD, the second is that it is virtually impossible to accurately put in all of the possible rotor excursions to the CPD when it is mounted on the ADTF. This device is simply a rotary table which has a cross feed mounted on it to which the disc is mounted, and a table to which the heads are mounted. The heads can be adjusted vertically

while the rotary table cross feed set up gives the rotation and radical excursions. Figure 3-33 shows the angle indicator mounted in the fixture.

3.2.5 TEST RESULTS

3.2.5.1 Engineering Unit 1

Tests were conducted in accordance with the engineering test plan (PIR 4176-085, Rev. A) and GE Specification SVS-7314.

Weight and center of gravity were measured and were within specification limits. Weight was 22.89 pounds.

The circuit impedances were checked as well as the insulation resistance and dielectric strength. All results were within the specification limits. Electrical performance was checked by applying power to the instrumentation and mode switching (solenoid) circuits. All circuits worked properly. The CPD boom and Eddy-Current Damper (ECD) were decaged by cutting the caging cable in one place at a time (two cutters are included in the design). The firing of the first cable cutter successfully decaged the boom, ECD, and solenoid. The damping mode was changed by switching the solenoid. Instrumentation read-out and visual inspection noted the proper changes.

The CPD was placed in the ADTF for evaluation of the angle indicator, eddy-current damping and torsional restraint, and hysteresis damping and torsional restraint. With the CPD in the ECD mode, the tests on the angle indicator and ECD were performed. The performance of the angle indicator was as anticipated. One head was not functioning properly due to a miswired internal connecting cable. The ECD torsional restraint constant was 23 dyne-cm/deg (specified as 21.0 to 25.2 dyne-cm/deg). The soft stop torsional restraint constant was found to be 700 dyne-cm/deg. It was determined that an error in manufacturing caused this constant to be lower than the specified value of 1000. Soft stop has since been deleted from the design.

The eddy-current damping coefficient was found to be 730,500 dyne-cm-sec (spec is 905,000 nominal) or 18 percent low. An investigation showed that the use of a "master" disc to set the flux level in the damping magnets resulted in the flux being set too low, hence a low damping coefficient. Future adjustments of the flux levels in the damping magnets were performed with the actual damping disc to be installed into the particular CPD rather than with a "master" disc. Thus, a matched set is used for each damper.

Tests performed on the hysteresis damper (installed in the CPD) indicated high values of damping and torsional restraint torques. Investigation into the cause of this out-of-spec data revealed that problem was due to an inadequate alignment procedure during assembly, and to the inability to perfectly align the CPD to the air bearing during testing. In process alignment has been improved and set up of test equipment has improved to the point where damping tests agree perfectly with in-process tests and torsional restraint nearly agrees though slightly high. High torsional restraint is still due to misalignments in test setup.

The CPD was installed on the force fixture for suspension system tests. The ECD radial forces measured were 7.93 dynes/0.001 inch (as compared to 6.2 predicted) in the direction of the torsional restraint magnets and 13.6 dynes/0.001 inch (13.0 predicted) in the direction perpendicular to the torsional restraint magnets. The ECD axial suspension forces were measured at 1.6 dynes/0.001 inch (4.1 predicted). Since this axial force data varied significantly from the predicted value, an investigation was made into the cause. It was determined that by reducing the height of the pyrolytic cones the axial force component could be increased. Present values are 3.0 dynes/0.001 inch.

The magnetic dipole of the CPD was measured both with and without electrical power applied to the unit. It was found that no difference in the dipole exists between the powered or unpowered condition. The measurements indicate a fundamental and a strong second harmonic. The dipole of this unit and other units is about 500 pole-cm (design goal is 100 pole-cm). No effort was made to compensate for this high value as it was decided to correct the dipole of the total spacecraft.

The CPD was next subjected to vibration, acceleration and humidity tests. Prior to and after each of these tests, the CPD and boom were decaged and the instrumentation and mode changing capabilities checked. All of these tests were performed successfully with no damaging effects upon the functional performance of the unit except the following. The angle indicator encoder disc fractured in the vibration environment (see Section 2.3.7) and the unpainted magnesium parts in the humidity test. The magnesium parts had been given the Dow 9 surface treatment. Finish has been changed to either Dow 17 or Dow 17 with an epoxy paint.

The CPD and damper boom were then subjected to a 3-part solar-vacuum test. All functions, caging, solenoid switching, etc., were successfully performed. Based on calculations, the temperature distributions throughout the unit were very close to the predicted values. PIR 4730-220 is a complete report on the test and test results.

Final functional tests were performed on the CPD following environmental testing. The final functional tests included: damper and force testing at ambient temperatures and qualification temperature extremes, angle indicator checks, and other instrumentation and actuator checks.

The CPD performed the same during the ambient tests made after environmental testing as it had performed during similar tests made prior to environmental testing. No significant changes were noted in the operating characteristics of either the eddy-current damper, the passive hysteresis damper, or any other component sections of the CPD.

The angle indicator continued to operate properly despite a damaged encoder disc. The encoder disc was damaged during the vibration test.

In addition to the miswired cable to angle indicator head No. 1 threshold detector No. 5 in head No. 1 did not operate properly prior to the vibration test, but it did operate satisfactorily after the vibration test. This indicates that an intermittent short was loosened during the test. The circuit has continued to operate properly ever since. The insulation of phototransistor leads has been improved in an effort to prevent a recurrence of the problem.

A post-environmental dipole test was performed and the results were essentially the same as those recorded during the pre-environmental dipole test.

The temperature test data of suspension, damping, and torsional restraint characteristics confirmed calculations for the predicted performance at qualification temperature levels (see Table 3-6).

TABLE 3-6. THERMAL DATA FOR EDDY-CURRENT DAMPER

Radial Force		Damping Coefficient		Torsional Restraint	
Temp (°F)	(dyne/0.001 in.)	Temp (°F)	(dyne-cm-sec)	Temp (°F)	(dyne-cm/deg)
+ 75	9.13	+ 77	774,500	+ 77	22.2
+175	8.60	+177	621,500	+177	21.6
-2	9.81	- 40	1,107,500	- 40	22.85
- 31	10.40	+ 80	766,000	+ 80	22.2
+ 75	9.13	-	-	-	-

The engineering testing program revealed the following information which led to redesign, modification, and/or different processing methods as noted:

1. Redesign angle indicator encoder disc for greater mechanical strength.
2. Protect magnesium parts with a surface treatment other than Dow-9.
3. Perform in-process damping magnet tests on actual magnets and disc to be used in a particular assembly rather than using a master damping disc.
4. Change configuration of the eddy-current damper pyrolytic graphite rings for greater axial suspension stiffness when the damper is in the eddy-current damper mode.
5. Use slightly different setups and data measuring techniques to obtain more accurate data and to obtain the equivalent information with the expenditure of much less time.

Table 3-7 is a summary of a portion of the data obtained during the initial function testing (pre-environmental) and during the final functional testing (post-environmental). The differences in the data can be attributed in part to improved techniques used to obtain the post-environmental data, and in part, to normal measuring errors. The post-environmental data was more repeatable than the initial data obtained.

All solenoid actuations (mode changes) and all decaging at ambient and temperature extremes were 100% successful.

3.2.6 OTHER SIGNIFICANT TEST RESULTS — IN ORDER OF UNIT TESTED

3.2.6.1 Prototype Unit 2

This unit was tested to flight acceptance levels only. During the testing of this unit, the out of tolerance conditions on the angle indicator were found (see Section 3.2.3.7).

3.2.6.2 Prototype Unit 1

This unit was the qualification unit and as such was put through the full qual test program. This unit experienced its greatest difficulties during the vibration testing. All functional testing (damping and torsional restraint) was performed satisfactorily except in the case where a structural failure prevented proper operation. Discussion is therefore limited only to these problem areas.

The first vibration test resulted in two CPD part failures, the solenoid and a lamp failed (see Section 3.2.3.6 and 3.2.3.7) and the damper boom failed. This was the vibration test in which the highest g load was put into the weakest CPD axis by error. Whether or not this was the actual cause of the failures is not known. Subsequent testing of the solenoid failed to reproduce the failure except for EU 2 which was overtested. The lamp failure could not be duplicated. A total of 20 lamps were vibrated to qual levels representing 80 binding posts - area of failure - no failures occurred.

After the failures, this CPD was outfitted with a new solenoid and lamp and revibrated. The lamps and solenoid passed; however, the torsional restraint magnet mounting bracket fractured. This failure was due to a sharp corner in the bracket. An inspection of Engineering

TABLE 3-7. COMPARISON OF PRE-ENVIRONMENTAL AND POST-ENVIRONMENTAL FUNCTIONAL PERFORMANCE CHARACTERISTICS

Characteristics	Pre-Environmental	Post-Environmental
Electric Circuit Functions	Okay(1)	Okay(1)
Dipole	Recorded Data	Recorded Data-no change
Eddy-Current Damper		
Damping Torque (dyne-cm-sec)	730,500	774,500
Torsional Restraint (dyne-cm/deg)	21.7	22.2
Axial Force (dyne/0.001 in.)	1.6	1.72
Radial Force 1 (2) (dyne/0.001 in.)	7.93	8.80
Radial Force 2, (3) (dyne/0.001 in.)	13.60	14.40
Passive Hysteresis Damper		
Suspension	(1) Okay	(1) Okay
Damping Torque(4) (dyne-cm)	212	200
Torsional Restraint(4)(dyne-cm/deg.)	64.4	36.9 to 78.8
Angle Indicator(5)		
Primary Circuit	(1) Okay	(1) Okay
Redundant Circuit	(1) Okay	(1) Okay

Notes:
1. Where "Okay" appears, the function is meeting specification and no change occurs.
2. Against torsional restraint magnets.
3. Perpendicular to torsional restraint magnets.
4. Data varied because of problems in test setup alignment and/or passive hysteresis damper alignment in the CPD. The passive hysteresis damper has no apparent degradation in performance because of the environmental exposure.
5. Threshold detector No. 5 in head No. 1 did not function properly before vibration. It worked properly after vibrations.
6. Total solenoid actuations - 71
   Total decagings - 5

Unit 1 revealed a hairline crack in the same area. At this time it was decided not to continue testing with this unit because the damage had incurred as a result of the fracture and because the unit had seen two full qual tests. All major parts were removed and Zyglo and x-ray inspection were made. No problem areas appeared.

3.2.6.3 Engineering Unit 2

This unit was used as a structural qual unit in light of the failures incurred on Prototype 1. The unit was fitted with new torsional restraint magnet mounting brackets. A tri-axial accelerometer was put on the outboard end of the solenoid and 2 accelerometers were placed on the angle indicator head (data from the accelerometers was invalid due to equipment troubles). The unit was vibrated and the solenoid, lamp, and bracket all passed. The brackets were dye-penetrant inspected in place and showed no degradation. Extreme difficulty was encountered during the functional test. Inspection revealed that the retaining ring used as a backup to the bonding to hold the pyrolytic graphite cones in place had come out of its groove. The upper ring was bonded in place and the unit was revibrated. The ring held. An inspection was made of all other units and indications were that the rings had come out on these also. This would explain the difficulty sometimes experienced in testing the eddy-current damping. All flight units were reworked to include the new brackets and bonded rings.

3.2.7 TESTING, GENERAL

Testing of the CPD is generally straightforward. However, it takes considerable care in setting up the tests to avoid misalignments. Internal contamination has caused problems on several occasions. The contamination is mainly from the manufacturing stage. Procedures have continually been updated to eliminate problems.

Table 3-8 is a matrix of all testing to date and also shows the basic differences between units. Tests are listed in order of normal sequence. However, some changes have been made in later units in order to identify problems early. Functional testing at high and low temperature has been discontinued due to excellent correlation of Engineering Unit 1 and Prototype 1 test data with theoretical data.

TABLE 3-8. CPD TEST RESULT MATRIX

Tests per SI 237, 018	EU 1 Qual	Proto 2-Accept	Proto 1-Qual	Proto 1 Qual-Retest (Refitted with New Lamp and Solenoid)	EU 2-Qual	EU 2 Qual-Retest (Reworked with Bonded Upper Ret. Ring)	Flight 1 Accept
Visual and Mechanical Inspection	Failed: Harness Mis-routed Limiting Travel to +45° -32°	Failed: Minor External Discrepancies-Burned Insulation Loose Screw, Frayed Tie Cord (All Corrected Prior to Continuing Test)	Passed	Passed	Passed	Passed	Passed
Electrical Circuit Impedance	Failed: Improperly Wired	Passed	Passed	N/C	N/C	Passed	Passed
Insulation Resistance	Passed	Passed	Passed	N/C	N/C	Passed	Passed
Dielectric Strength	Passed	Passed	Passed	N/C	N/C	Passed	Passed
Electric Circuit Power	Passed	Passed	Failed: Microswitch ramp rotated, Set screw change required	Passed	N/C	N/C	Passed
Radial Force, Ambient	Passed	Passed	Passed	Passed: Test run in one direction, Worst Case	Passed: Test run in one direction, Worst Case	N/C	Passed
Axial Force, Ambient	Passed	*N/C	Passed	Passed	Passed	N/C	Passed
Radial Force High Temperature	Passed	N/C	Passed	N/C	N/C	N/C	N/R
Radial Force Low Temperature	Passed	N/C	Passed	N/C	N/C	N/C	N/R
Torsional Restraint and Damping AMB	Passed	Failed: Soft Stop Since Removed	Passed: PHD misaligned-re-worked	Passed: Difficulty due to loose retain ring 3	Passed: Tested ECD only	Passed: Tested ECD only	Passed
Torsional Restraint and Damping Temperature	Passed	N/C	Passed	N/C	N/C	N/C	N/R
Modified, Electrical Circuit Power	Passed	Passed	Passed	Passed	Passed	Passed	Passed
Humidity	Failed-Various parts corroded-New finish now used	*N/R	Passed	Passed	N/C-Installed New TOR Restraint Bkts.	N/C	N/R
Mod Electrical Circuit Power	Passed	Passed	N/R	Passed	N/C	N/C	N/R
Vibration	Failed: Loose SCR and Washer, Angle Indicator Disc (1)	Passed: 2 axes sine and random	Failed: Sol and Lamp	Failed: Ramp rotated-Set SCR not changed	Failed: Retaining ring loose	Failed: Solenoid (2)	Passed
Mod Electrical Circuit Power	Passed	Passed	Passed	Passed	Passed	Passed	Passed
Accelaration	Passed	N/R	Passed	Passed	Passed	N/C	N/R
Mod Electrical Circuit Power	Passed	N/R	Passed	Passed	Passed	N/C	N/R
Thermal Vacuum	Passed-Also Ran Solar Vacuum	Passed	Passed	N/C	N/C	N/C	Passed
Electrical Circuit Impedance	Passed	N/C	Passed	N/C	N/C	Passed	Passed
Insulation Resistance Dielectric Strength	Passed	N/C	Passed	N/C	N/C	Passed	Passed
Electrical Circuit Power	Passed	Passed	Failed: Sol. and Lamp	Passed	Passed	Failed: Solenoid (2)	Passed
Radial Force	Passed	N/C	Passed: Test run in one direction-Worst Case. Other Direction could not be run due to retaining (3) ring being loose-discontinued testing due to Solenoid and lamp failure.	Could not test due to torsional restraint bracket failure	N/C	N/C	Passed
Axial Force	Passed	N/C			N/C	N/C	Passed
Torsional Restraint and Damping, Ambient	Passed	Passed: Angle Indicator Indicator out of Spec. Spec Revised: Unit modified			Passed: With Retaining ring removed. Tested ECD only	Passed tested ECD only	Passed
Magnetic Dipole	Measured	N/R			N/C	N/C	Measured
Modified Electrical Power	Passed	Passed			N/C	N/C	Passed
Visual and Mechanical Inspection	Failed: As Noted Above	Passed			N/C	N/C	Passed

(1) Disassembly of EU 1 verified loose snap ring and a hairline crack in torsional restraint mounting bracket.

(2) All previous problems resolved this solenoid had been through 1 qual CPD vibration test +2 solenoid qual vibration tests +1 uncaged partial vibration test +600 strokes.

(3) Discovered on retest of EU 2.

(4) Unit was torn down to bond retaining rings. Temperature sensor replaced due to probable damage by over voltage in hi-pot test.

*N/C = Not conducted either because of customer by-off, previously performed or not necessary due to intent of test such as retest of structural integrity only.

N/R = Not required

Major Differences Between Engineering and Prototype and Flight Units

EU 1	EU 2	PROTO 2	PROTO 1
Has Soft Stop	Potting on one retaining ring	Has Old Tor Rest Bkts.	Has Old Tor Rest Bkts.
Has Old Tor Rest Bkt.	Has old thermal shield	No Masks on Angle Ind	No potting on Retain. Rings.
Has Old Disc	No diodes on solenoid	No Potting on Rot. Rings	
Has Old Mag Finish	Has accelerometers on angle ind	Has Soft Stop	
No Diodes on Solenoid	Lamps from two vendors		
No Masks on Angle Ind			
No Potting on Rot. Rings			
Old Thermal Shield			

FOLDOUT FRAME 1

FOLDOUT FRAME

FOLDOUT FRAME 2

3.2.8 CONCLUSIONS AND RECOMMANDATIONS OF ENGINEERING DEVELOPMENT

Comprehensive testing both in the early engineering test and through component test verified the ability of the CPD to perform to the requirements of the component specification.

The major problem area was mechanical. This can be broken down into two general areas. The first are those problems that can be considered structural or mechanical design weaknesses. Almost all of the failures or problems were in this area. All of these problem areas have been corrected on flight units. The second is also mechanical and is due to the necessary complexity of the CPD by having two completely independent damping systems within one housing.

Analysis of the test results indicate that the unit will successfully survive launch and should perform for the required three years in orbit. The only question concerning in-orbit life would be the possibility of contamination of the CPD during ground handling and possibly launch, and whether or not the angle indicator lamps will survive for the full three years. According to theory and vendor test data, they should; however, the life test to verify this was terminated.

It is recommended that no changes be made to the CPD as now manufactured. If, however, new units are to be fabricated the following areas bear investigation.

1. The solenoid should be redesigned to incorporate a detent system that has a greater margin of safety, and the design of the stator modified to permit non-destructive disassembly.

2. Change the wiring of the angle indicator lamps to provide independent selection of all four filaments.

3. Rework the encoder disc to provide more accuracy.

4. Reduce the lamp voltage if possible to provide more life margin.

5. Redesign the structure to allow easier access to the internal parts and to avoid blind areas where contamination can be trapped.

3.2.9 CHRONOLOGICAL SUMMARY OF CPD DESIGN (THROUGH PROTOTYPE UNIT 2 — 2nd UNIT FABRICATED)

15 Oct. 1964 - Presentation of CPD design concept (2 lever)* to NASA representative at GE. As a result of this meeting, an all-out effort was made to simplify the design by deleting the boom/damper alignment feature and working on the assumption that clutching could occur only at the boom null position.

15-30 Oct. 1964 - Intensive redesign activity investigating various methods of clutching at null only, plus overall simplification of the entire concept. Reviewed resulting designs with NASA on 30 October at GE but no single concept was satisfactory.

6 Nov. 1964 - Presented working model of 2-lever concept of the CPD at a meeting at NASA Goddard. Model demonstrated smooth operation and stability of 2-lever concept; however, it still was considered too complex.

13 Nov. 1964 - Presented the "Diaphragm Clutch" concept at NASA meeting. This concept contained only one moving part plus the actuator, and agreement to proceed with this design concept was reached.

17 Nov. 1964 - The CPD to Spacecraft mounting arrangement concept was agreed upon during the NASA/Hughes/GE Interface Meeting at GE.

2 Dec. 1964 - GE was requested by NASA to obtain a proposal from TRW for the development and delivery of the Hysteresis Damper portion of the CPD. GE would continue to be responsible for the entire CPD package including the eddy-current damper.

21 Jan. 1965 - Dynamics Research Corporation presented their proposal and cost for the Angle Indicator. GE contracted with them for a 3-week study effort to definitize the problems.

---

* 2-Level concept was the initial method for activating either of the two dampers of the CPD.

2 Feb. 1965 - GE presented results of evaluation of TRW proposal to NASA Goddard. An engineering evaluation model of the GE Hysteresis Damper was displayed and discussed at the meeting.

12 Feb. 1965 - A Design Review of the Combination Passive Damper was held at GE with GE personnel in attendance. Attendees included two consultants from GE Advanced Technology Labs, Schenectady, N. Y.

17 Feb. 1965 - Received NASA direction to "buy" the Hysteresis Damper. GE made preparations to obtain competitive bids.

25 Feb. 1965 - Dynamics Research Corporation presented to GE the results of their preliminary study for the Angle Indicator and submitted a fixed price cost which was considerably higher than the previous CPFF cost.

5 March 1965 - Requested by NASA to redesign the boom caging mechanism for the CPD.

16 March 1965 - Interface meeting at NASA Goddard. Hughes presented the new vehicle configuration which required various modifications to the CPD package to meet vehicle interface requirements. A major change was an extension of the damper boom shaft.

17-19 March 1965 - Hughes personnel at GE to coordinate component locations and arrangements of the new vehicle structure. Systems optimization studies required study of several mounting positions. No final agreement reached.

19 March 1965 - An in-house Angle Detector, utilizing a digital output, was conceived and costed at GE. A decision was made to use the GE angle detector in lieu of the proposed DRC design.

19-31 March 1965 - Conceptual redesign effort on the CPD package to incorporate the GE angle detector, changes to accommodate the new HAC vehicle (including boom shaft extension), and a redesigned caging mechanism.

2 April 1965 - Final negotiations were held with TRW Inc. relative to the PHD contract.

5 April 1965 - Agreement on the CPD caging mechanism design concept was reached with NASA.

14 April 1965 - A design summary presentation on the overall CPD design concept was made to NASA management personnel at GE.

22 April 1965 - First indication of performance problems with the "constant torque" hysteresis damper as a result of preliminary systems analysis at GE.

12 May 1965 - Problems in the Quality Control System of a potential vendor for the solenoids required re-evaluation of other vendors and subsequent award of the job to another company.

26 May 1965 - GE and TRW Inc. personnel attended a meeting at NASA to discuss the variable torque requirement to produce hysteresis damper performance. Methods of developing and incorporating a "bow tie" disc into the prototype damper with no schedule slippage and minimum costs were discussed. TRW Inc. was asked to submit cost and schedule estimates.

7 June 1965 - Final Design Review of the PHD was held at TRW Inc. The deletion of the caging mechanism simplifies the PHD design and reduces the weight of the damper. The "bow tie" torque requirements were also discussed.

15 June 1965 - GE received an overall cost estimate from TRW Inc. which traded off various cost reductions in the PHD effort against the potential costs to perform a feasibility study of the "bow tie" torque requirement.

16 June 1965 - Adverse vendor information relative to the utilization of solar cells as sensors in the damper boom angle indicator application resulted in a reevaluation and the decision to search for a more suitable detector. Phototransistors were the most likely candidates for this application.

17 June 1965 - First "bow tie" test performed at GE on a test fixture which utilized magnets furnished by TRW Inc.

25 June 1965 - GE Systems Analysis personnel visited TRW Inc. to discuss unofficial TRW Inc. systems analysis efforts which had disagreed with the analysis performed at GE. The discussions revealed that an error had been made in the TRW Inc. computer programming and that there was, in fact, agreement between the two analytical efforts.

17 July 1965 - TRW Inc. reported problems during vibration tests with the ATS-D/E torsion wire.

30 July 1965 - Vibration tests at GE on the CPD Solenoid proved conclusively that the solenoid must be caged to withstand the launch environment.

11 August 1965 - Completed assembly of the CPD Thermal Unit except for the revised resistors (heaters) which were installed 18 August.

9 Sept. 1965 - CPD Dynamic Unit assembled and delivered to be tested on the MB-210 Shaker Facility at GE.

9 Sept. 1965 - CPD Thermal Unit shipped to BAC

12 Sept. 1965 - Successfully completed vibration tests on CPD Dynamic Unit with no failures.

16 Sept. 1965 - Delivered corrected and signed CPD Interface Drawing to NASA for further coordination with HAC. This drawing included a revised thermal shield envelope as verbally requested by NASA and HAC.

25 October 1965 - Final assembly of Combination Passive Damper (CPD) Engineering Unit 1 started.

5 November 1965 - CPD Thermal Unit returned from HAC to GE because vehicle thermal tests were deleted.

22 November 1965 - CPD Engineering Unit 1 was delivered to test area from final assembly. First firing of pyrotechnic devices was successfully accomplished.

23 November 1965 - CPD Dynamic Unit shipped to (HAC) per NASA request.

10 December 1965 - CPD Engineering Unit 1 completed vibration test. Fired squibs.

14 December 1965 - CPD Engineering Unit 1 completed acceleration test successfully. Fired squibs.

16 December 1965 - CPD Engineering Unit 1 completed humidity test with slight corrosion of magnesium parts. Fired squibs.

18-19 December 1965 - CPD Engineering Unit 1 in solar vacuum test. Test setup unsatisfactory.

28 December 1965 - CPD Engineering Unit 1 re-entered solar vacuum chamber with improved test setup.

2 January 1966 - CPD Engineering Unit 1 was subjected to a solar vacuum test using an improved test setup which more nearly simulated actual vehicle environment in orbit.

7 January 1966 - Solar Vacuum test completed on CPD Engineering Unit 1. Test results were in excellent agreement with the thermal analysis.

25 January 1966 - All major tests were successfully completed on the CPD Engineering Unit 1.

29 January 1966 - Completed planned functional and environmental tests of CPD Engineering Unit 1.

2 February 1966 - Meeting held at NASA/GSFC on alignment procedures. Several changes to the planned fixtures for use during CPD alignment to the ATS vehicle are being evaluated.

14 March 1966 - CPD Prototype 2 (S/N 5962028) abbreviated acceptance test begun.

24 March 1966 - NASA representatives visited GE for a discussion of the qualification test instructions (SI 237016) for the CPD. A summary of all waivers and proposed specification changes was presented and discussed.

28 March 1966 - Abbreviated acceptance of CPD Prototype 2 completed. Minor discrepancies noted during testing not series enough to prevent shipment of the unit on schedule.

3.2.10 DRAWING AND SPECIFICATION LIST - ONLY THOSE DRAWINGS AND SPECIFICATIONS ARE LISTED WHICH ARE OF MAJOR IMPORTANCE.

3.2.10.1 CPD Drawings

47E207098	CPD Envelope
47E207100	CPD Assembly
47J207277	CPD Schematic
47D207083	PHD Source Control
47E207350	Angle Indicator Head Assembly
47C207272	Angle Indicator Encoder Disc
47C207354	Torsional Restraint Pattern
47D207165	Pyrolytic Graphite Ring
47D207283	Belleville Washer
R4612	Solenoid
R4615	Phototransistor

3.2.10.2 Test Equipment

The following list is given because it is not officially recorded any place and would be difficult to locate.

3.2.10.2.1 Test Equipment Drawings

Air Bearing Work Statement	9744-WS-004
Support Stand	47J207030G1
Mtg. Plate (Modified for Fecker Table A.D.T.F.)	47C 031P1
Tachometer Generator Assy.	47E 03AG1
Air Bearing Support Stand	47D 037G1&P9
Vertical Jack Assembly	47D 039G1
Stand Surface Plate	47E 040G1
Helmholtz Test Stand	47E 041G1
Leveling Device	47C 046P1&P2
Arm, Axial & Radial	47C 075P1
Inserts, Balance Weights	47B 078P1,2,3,4
Inertia Disc (2)	47C 079G1&G2
Cross Feed Device	47E 080G1
Mounting Plate, Air Bearing A.D.T.F.	47B 086P1
Air Bearing (Spec. Cont.)	47D 088P1
Adapter, Horizontal L.O.F.F.	47E 089G1
Balance Weights	47B 090P1,2,3,4,5,6
Adapter Assy., Bearing Test	47D 150G1&G2
Hysteresis Damper Test Fixture	47E 371G1
Hysteresis Damper Stator Test Fixture	47D 381
Weldment Overturning Torque Test	47E 398G1
L.O.F.F. Fixture Details (Weldment CPD)	47E 399G1
Support Bracket Weldment	47E 479G1
Thermal Panels (Details) (A.D.T.F.)	47D 946P1 thru P13
Thermal Panels (Details) (L.O.F.F.)	47D207949P1 thru P6
Test Set Up, Overturning Torque (L.O.F.F.)	17E209550G1
Test Set Up, Axial Force (L.O.F.F.)	551G1
Test Set Up, Radial Force (L.O.F.F.)	552G1
Test Set Up, Eddy-Current Damper (A.D.T.F.)	553
Test Set Up, Hysteresis Damper (A.D.T.F.)	47E209554
Thermal Chamber Assy. (L.O.F.F.)	47J209562
Thermal Chamber Assy. (A.D.T.F.)	47J209563
Heater Mtg. Panels	47C209565P1&P2

3.2.10.2.2 CPD Test Console

Schematic, Angle Detector Panel	47J209568
Schematic, CPD Panel	47J209569
Wiring Diagram, Test Console CPD	47C209570
Outline, Test Console CPD	47D209571
Outline, Cable Assy, Angle Detector	47C209572
Outline, Cable Assy, CPD	47C209573
Outline, Cable Assy, CPD Thermal Vac.	47C20957
Angle Indicator Test Fixture	47R205601

3.2.10.2.3 Specifications

SVS-7312	ATS Gravity-Gradient Systems Requirements
SVS-7314	CPD
SVS-7331	PHD
SVS-7325	Use of Standard Parts Materials, and Processes
SVS-7338	Engineering Requirements Standards
SVS-5992	Electroexplosive Pressure Cartridge and Cable Cutter
171A4211	Pyrolytic Graphite
171A4411	Carbonyl Iron Epoxy Dispersion

Test Specifications

S2-0102	NASA Environmental Qualification and Acceptance Test Specification
PIR 4176-085 Rev. A	CPD Engineering Test Plan
S.I. 237, 016	CPD Acceptance and Qualification Test Instructions
CPD T.I. #1 thru #10	CPD In-Process Test Instructions

3.3 QUALIFICATION TESTS

Two prototype Combination Passive Damper units (designated as component and system qual) were subjected to similar environments at more severe levels than the anticipated operating environments in order to establish confidence that the design was valid under extreme operating conditions. Following tests, the component qualification unit was not further dispositioned, but the system qualification unit was included in the spacecraft qualification tests conducted by the vehicle contractor following the GE tests. A summary of these environments and references to the appropriate test reports are listed below. These documents are on file at GE and will be made available on request of the Contract Administrator for NASA programs.

3.3.1 COMPONENT QUALIFICATION

Serial No. 5962027

Part No. 47E207100

Part No. 4315-QC-008(8/9/66)

Test Sequence

1. Visual Inspection
2. Electrical Circuit Impedence
3. Incubation Resistance
4. Dielectric Strength
5. Electrical Circuit Check
6. Radial Force, Ambient
7. Axial Force, Ambient
8. Radial Force, High Temperature
9. Radial Force, Low Temperature
10. Centering Force & Damping Test, Ambient
11. Centering Force & Damping, High Temperature
12. Modified Electrical Circuit Check
13. Humidity
14. Modified Electrical Circuit Check
15. Vibration
16. Modified Electrical Circuit Check
17. Acceleration
18. Electrical Check
19. Thermal - Vacuum
20. Electrical Circuit Check
21. Dielectric Strength Measurement
22. Electrical Check
23. Radial Force Check
24. Axial Force Measurement
25. Centering Force & Damping, Ambient
26. Magnetic Dipole
27. Electrical Check
28. Visual Inspection

NOTE: Also see Paragraph 3.2.3.6.1

3.3.2 SYSTEM QUALIFICATION

Serial No. 5962028

Part No. 47E207100

Test Report 4315-QC-008(8/9/66)
4315-QC-026(3/20/67)

Test Sequence

1. Visual Inspection
2. Impedance
3. Insulation Resistance
4. Dielectric Strength
5. Electric Power
6. Thermal - Vacuum
7. Vibration
8. Electric Power
9. Radial Force, Ambient
10. Torsional Restraint (Eddy Current Damper)
11. Soft Stop Torsion CW and CCW, Ambient
12. Eddy Current Damper

13. Hysteresis Damper
14. Torsional Restraint
15. Hysteresis Damper Torque
16. Angle Indicator
17. Electric Power
18. Magnetic Dipole

3.4 FLIGHT ACCEPTANCE

Each of the Combination Passive Damper flight units was exposed to vibration and thermal-vacuum environments at levels anticipated during flight to verify that the design had not degraded during manufacture. A summary of their environments and reference to the applicable test reports are listed below. These documents are on file at GE and will be made available on request of the Contract Administrator for NASA programs.

3.4.1 ATS-A

Serial No. 5962029

Part No. 47E207100

Test Report: Final Acceptance Report for ATS-A, March 15, 1967

Test Sequence

1. Visual Inspection
2. Electrical Characteristics
3. Electrical Circuit Power Tests
4. Magnetic Suspension Forces
5. Damper Performance Characteristics
6. Angle Indicator Checkout
7. Enviromental Tests
8. Check and Calibration

3.4.2 ATS-D

Serial No. 5962030

Part No. 47E207100

Test Report: Final Acceptance Report for ATS-D, December 5, 1967

Test Sequence

1. Visual Inspection
2. Impedance
3. Insulation Resistance
4. Dielectric Strength
5. Electric Power
6. Centering Force and Damping, Ambient
7. Radial Force, Ambient
8. Axial Force
9. Visual Inspection
10. Electrical Circuit Power
11. Vibration
12. Thermal-Vacuum
13. Impedance
14. Insulation
15. Centering Force and Damping, Ambient
16. Radial Force
17. Axial Force
18. Magnetic Dipole
19. Electric Power Check
20. Weight and CG (34.67 lbs.)

3.4.3 ATS-E

Serial No. 5962031

Part No. 47E207100

Test Report 1315-QC-002 (4/9/68)

Test Sequence

Test Sequence for the ATS-E Flight System was essentially the same as for ATS-D (See paragraph 3.9.2)

3.5 REFERENCE LIST

3.5.1 COMPONENT HISTORY DOCUMENTS

CXLVII	Vol 1, 2, 3 Angle Indicator
CLXVIII	Vol 1, 2 CPD
CXLIX	Vol 1 Magnetic Suspension
CL	Vol 1 Eddy-Current Damper
CLI	Vol 1 Torsional Restraint
CLII	Vol 1, 2, 3 Mechanical Design including Thermal & Dynamic Models
CLIII	Vol 1, 2 Solenoid
CLIV	Vol 1, 2, 3 Hysteresis Damper
CLXXIX	Vol 1 Optimized Passive Hysteresis Damper - Not Part of CPD System

3.5.2 QUARTERLY PROGRESS REPORTS TO NASA

64SD4361	1st
65SD4201	2nd
65SD4266	3rd
65SD4381	4th
65SD4464	5th
66SD4201	6th
66SD4318	7th
66SD4388	8th
66SD4505	9th

3.5.3 OTHER PERTINENT DOCUMENTS

64SD4326	Evaluation of Suspension System for the Eddy-Current Damper
TM4176-007	Diamagnetic Shaft Support Analytical Description
TSI66SD301	Development of a Passive Damper System for Gravity Gradient Stabilized Spacecraft
PIR4176-684	Solenoid Engineering Report
PIR4730-220	Engineering Unit #1 Solar Vacuum Test Results
4598.00	TRW Proposal for PHD RFQ 80-3031
EU1-1 thru EU1-4	Engineering Unit #1 Log Books
EU2-1 thru EU2-2	Engineering Unit #2 Log Books

APPENDIX TO

SECTION 3

APPENDIX 3A

PHD WIRE VIBRATION AND FATIGUE QUALIFICATION TEST RESULTS FOR ATS D&E SYSTEM TESTS PERFORMED BY TRW, INC.

A.1 SUMMARY

The 0.003-diameter PHD Wire (ATS-D&E) successfully passed qualification vibration and fatigue testing as specified in Paragraph 7.1.5 of Reference A-1. PHD sinusoidal vibration qualification levels are shown in Table A-1. Vibration sweep schedules and a summary of the series of nine tests performed are shown in Tables A-2 and A-3, respectively. All tests after the first sweep at qualification levels for each wire sample exceed the qualification requirement and the results from these tests are to be used for reliability purposes only. Some of the wire samples survived vibration levels of up to 60g in the 60 to 250 cps frequency range. One wire sample survived over 800,000 cycles of oscillation during the fatigue tests after vibration.

A.2 DISCUSSION

The PHD developmental model of the flight configuration damper was used as the vibration test fixture. Two 0.003 inch diameter 302 stainless steel wires, 0.86 inch in length between the rotor clamp and flexure tangency point, were installed for each test. In addition to the vibration tests summarized in Table A-3, fatigue tests were performed on three wire samples as shown in Table A-4 and as specified in Paragraph 7.1.5.2 of Reference A-1. Two of the three fatigue tests were performed on the same wire samples which had previously undergone vibration testing.

The wire failure during Vibration Test 2 is discussed in Reference A-2. Failure occurred at approximately 1/4 inch from the flexure tangency point (Figure 3-22) during the second sweep at qualification levels. Failure occurred somewhere between 10 and 400 cps. Following Test 2 the qualification specification was revised (Revision C) so that more samples would be tested to higher levels. Previously the specification required fewer wire samples but more severe test conditions.

Failure of the special clutch adapter during Test 4 is not considered a significant factor in the wire qualification tests. The adapter, being free to rotate, continuously impacted the damper housing stops during vibration, causing a fatigue failure in the adapter flange. This is not the same adapter that is on the unit as it is delivered to GE. This is a special adapter used for vibration tests that simulates both the actual adapter and the mating piece in the GE clutch. The adapter was used in approximately 60 high level vibration tests prior to failure. Failure occurred at approximately 90 cps and 60 g's. A new vibration-test adapter was fabricated for subsequent tests.

The wire failed at approximately 1/4 inch from the flexure tangency point in Tests 5 and 9 at g-levels of 50 and 60 respectively. The failure was on the vane end of the damper in Test 5 and on the adapter end of the damper in Test 9.

REFERENCES:

A-1 "Lot Qualification of Wire, Passive Hysteresis Damper Suspension", Specification PT-1-12, Revision C, Dated 24 November 1965.

A-2 "Failure of PHD Wire (ATS-D&E) During Wire Vibration Qualification Test Series", TRW Memo No. 65-9713.5-164, by D. H. Mitchell, dated 3 December 1965.

TABLE A-1. SINUSOIDAL VIBRATION LEVELS USED FOR PHD DESIGN QUALIFICATION THRUST (Z-Z) AXIS

Frequency (cps)	Acceleration (g, 0-pk)
10-36.5	0.5 inch d.a.
36.5-250	±34.5
250-500	±18.5
400-2000	± 7.5
Sweep rate, two octaves per minute.	

TABLE A-2. SWEEP SEQUENCES FOR VIBRATION OF 3-MIL PHD WIRES

(All Sweep Rates 2 Octaves/Minute)

Sequence A	
Sweep 1	Qualification Levels
2	Qualification Levels
3	Qualification Levels
Sequence B	
Sweep 1	Qualification Levels
2	Qualification Levels
3	Qualification Levels
4	250 to 2000 cps - 20 g
5	250 to 2000 cps - 30 g
6	40 to 250 cps - 40 g, 250 - 2000 cps - 20 g
7	50 to 250 cps - 50 g, 250 - 2000 cps - 20 g
8	60 to 250 cps - 60 g, 250 - 2000 cps - 20 g
Sequence C	
Sweep 1	Qualification Levels
2	Qualification Levels
3	Qualification Levels
4	40 to 250 cps - 40 g, 250 to 2000 cps - 20 g
5	50 to 250 cps - 50 g, 250 to 2000 cps - 20 g
6	60 to 250 cps - 60 g, 250 to 2000 cps - 20 g

Note: The wire was inspected for damage after each sweep. The sweep was then continued until either the wire failed or the sequence was completed.

TABLE A-3. SUMMARY OF VIBRATION TESTS PERFORMED PHD 3 - MIL WIRE

Test No.	Date	Wire Sample Number	Vibration Sequence (See Tables A-1 & A-2)	Wire Tension (Pounds)	Results
1	11/8/65	34	A	0.55	No failures
2	11/15/65	36	A	0.55	The wire broke during the second sweep approximately 1/4 inch from the flexure tangency point. A detailed discussion is given in 65-9713.5-164. Failure occurred in the 10-400 cps region.
3	12/6/65	84	A	0.6	No failures
4	12/8/65	5	B	0.6	The special vibration test clutch adapter broke during sweep 8 at approximately 90 cps. No wire failures.
5	12/10/65	11	C	0.6	The wire broke during sweep 5 approximately 1/4 inch from the tangency point. Failure occured in the 10-400 cps region.
6	12/13/65	77	C	0.6	No failures
7	12/15/65	14	C	0.6	No failures
8	12/16/65	78	C	0.6	No failures
9	12/20/65	12	C	0.6	The wire broke during sweep 6, approximately 1/4 inch from the tangency point. Failure occurred in the 10-400 cps region.

TABLE A-4. RESULTS OF PHD 3-MIL WIRE QUALIFICATION FATIGUE TESTS

Test No.	Wire Sample No.	Wire Tension (Pounds)	Cycle Excursion (Degrees)	No. of Cycles	Results
1	34	0.55	±52	140,787	No failure
2	87	0.55	±52	125,073	No failure
3	84	0.6	±52	809,812	No failure

GENERAL ELECTRIC

SPACE DIVISION

SPACE SYSTEMS ORGANIZATION